Dissertation zur Erlangung des Doktorgrades

der Fakultät für Chemie und Pharmazie

der Ludwig-Maximilians-Universität München

Development of chemoresistance and formation of metastases: New aspects of two major obstacles in breast cancer treatment.

Ann-Katrin Sommer

aus

München, Deutschland

2021

Erklärung

Diese Dissertation wurde im Sinne von § 7 der Promotionsordnung vom 28. November 2011 von Herrn Prof. Dr. Ernst Wagner betreut.

Eidesstattliche Versicherung

Diese Dissertation wurde eigenständig und ohne unerlaubte Hilfe erarbeitet.

München, 23.05.2021

Ann-Katrin Sommer

Dissertation eingereicht am: 17.03.2021

1. Gutachter: Prof. Dr. Ernst Wagner

2. Gutachter: Prof. Dr. Stefan Zahler

Mündliche Prüfung am: 20.05.2021

„Zwei Dinge sind zu unserer Arbeit nötig: Unermüdliche Ausdauer und die Bereitschaft, etwas, in das man viel Zeit und Arbeit gesteckt hat, wieder wegzuwerfen.“

Albert Einstein

gewidmet

meiner Familie

TABLE OF CONTENTS

1. INTRODUCTION

1.1 BREAST CANCER INCIDENCE, CLASSIFICATION AND THERAPEUTIC OPTIONS

1.1.1 INCIDENCE AND MORTALITY OF BREAST CANCER WORLDWIDE AND IN EUROPE

According to the Global Cancer Observatory 18,078,957 new cancer cases occurred worldwide in 2018 of which 2,088,849 cases were breast cancer (Ferlay et al., 2019; IARC, 2018). Therefore, breast cancer is the second most common cancer type after lung cancer.

In women, breast cancer has the highest incidence with 24.2% and is the leading cause of cancer deaths with 626,679 cases in 2018 (Fig.1).

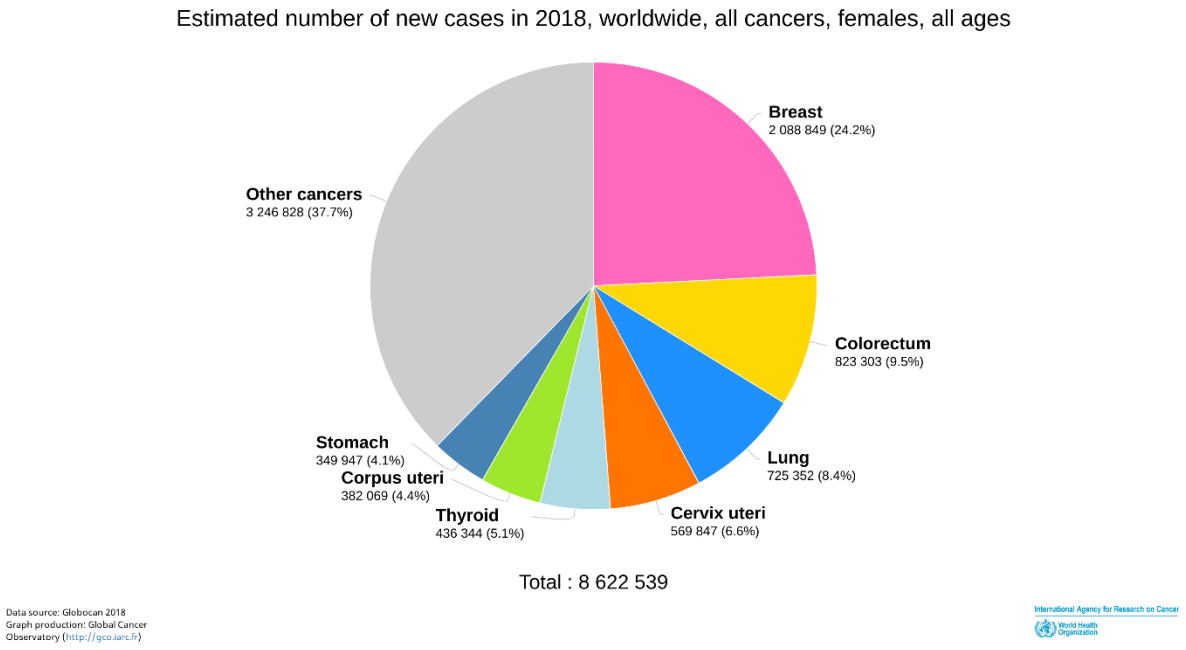

Figure 1. Estimated number of new cases of cancer in women worldwide in 2018 according to Globocan 2018, World Health Organization

In Europe 74.4 of 100,000 women develop breast cancer of whom 14.9 die due to this disease (Fig.2).

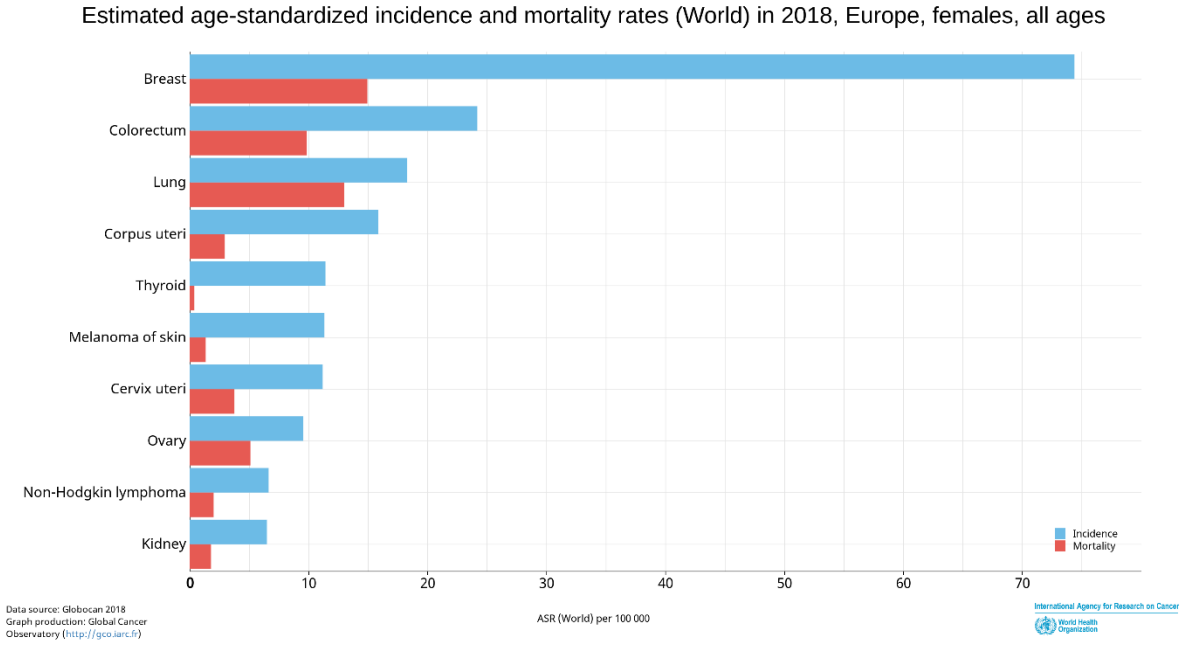

Figure 2. Estimated incidence and mortality rates in Europe of different cancer types in women in 2018 according to Globocan 2018, World Health Organization.

These statistics clearly show, that breast cancer is still a huge threat for women worldwide, especially in developed countries.

1.1.2 DIFFERENT SUBTYPES OF BREAST CANCER AND THERAPEUTIC OPTIONS

Even though breast cancer is a serious disease in general, it is important to differentiate between breast cancer subtypes for prognostic and therapeutic reasons.

In general, breast cancer can be classified according to histological and molecular characteristics. Here, the differentiation of molecular subtypes was of special interest. Nowadays, four different breast cancer subtypes are known: Luminal A, Luminal B, Her2+ and basal like/triple-negative breast cancer (TNBC) (American-Cancer-Society, 2019; Cardoso et al., 2019; Harbeck et al., 2014; Li et al., 2015; Prat et al., 2015; Sorlie, 2016; Sorlie et al., 2001; Vuong et al., 2014).

1.1.2.1 LUMINAL A BREAST CANCER

The subtype Luminal A is the most common one with approximately 73% of all mamma carcinoma, and the molecular phenotype is characterized by high expression levels of the hormone receptors estrogen receptor (ER) and progesterone receptor (PR) (American-Cancer-Society, 2019; Prat et al., 2015). However, the human epidermal growth factor 2 (Her2) is not expressed in this molecular subtype. The Luminal A breast cancer subtype is known to be less aggressive and has therefore the most favorable prognosis. Usually, this phenotype is well treatable with anti-hormonal therapy like selective estrogen receptor modulators (SERMs) e.g. tamoxifen, selective estrogen receptor degraders (SERDs) e.g. fulvestrant or aromatase inhibitors (AIs) e.g. letrozol (Cardoso et al., 2019). Chemotherapy can be considered as addition to endocrine therapy in cases of high tumor burden.

1.1.2.2 LUMINAL B BREAST CANCER

Similar to Luminal A breast cancer, this breast cancer subtype expresses high levels of estrogen receptor. Additionally, Luminal B breast cancer is defined by the expression of Ki67, leading to exaggerated cell proliferation and thus increased aggressiveness compared to Luminal A breast cancer (American-Cancer-Society, 2019; Cardoso et al., 2019). Her2 can also be overexpressed in this breast cancer subtype, however this is not a mandatory characteristic. According to the European Society for Medical Oncology (ESMO) guidelines these tumors should be treated with endocrine therapy like SERMs, SERDs or AIs and chemotherapy. Depending on the Her2 status trastuzumab can also be added to the therapeutic regimen (Cardoso et al., 2019). In the US this phenotype is present in approximately 11% of all breast cancer patients and causes depending on the invasiveness a poor prognosis (American-Cancer-Society, 2019).

1.1.2.3 HER2 OVEREXPRESSING (HER2+) BREAST CANCER

In contrast to the Luminal breast cancer subtypes described above, this phenotype is expressing neither estrogen, nor progesterone receptor and is therefore hormone receptor negative. Instead, in this subtype Her2, a receptor tyrosine kinase, is overexpressed causing increased cell proliferation and hence tumor growth as well as aggressiveness. Therefore, this breast cancer subtype had the worst prognosis in the past. With the development of targeted therapy like therapeutic antibodies e.g. trastuzumab and pertuzumab, small molecule inhibitors (SMIs) e.g. lapatinib and neratinib and antibody drug conjugates (ADCs) e.g. trastuzumab-emtansine (T-DM1) the patient outcome can be improved (Cardoso et al., 2019; Coates et al., 2015). According to the S3 guidelines, Her2+ tumors should moreover be treated with chemotherapy including taxanes e.g. paclitaxel and anthracyclines e.g. doxorubicin (Leitlinienprogramm-Onkologie (Deutsche Krebsgesellschaft, 2020).

In the US this tumor phenotype is prevalent in approximately 4% of all breast cancer patients, in Europe Her2+ breast cancer accounts for about 15% of all mamma carcinoma depending on the molecular test cut-offs (American-Cancer-Society, 2019; Cardoso et al., 2019; Leitlinienprogramm-Onkologie (Deutsche Krebsgesellschaft, 2020).

1.1.2.4 TRIPLE-NEGATIVE BREAST CANCER

This breast cancer subtype is characterized by the absence of estrogen, progesterone and Her2 receptor and is therefore called triple-negative breast cancer (TNBC). 75-80% of all TNBC tumors have a basal-like phenotype (American-Cancer-Society, 2019; Cardoso et al., 2019; Prat et al., 2013). Hence, the endocrine or Her2-targeted therapy is not effective in this tumor entity. The current standard of care in this breast cancer subtype is still chemotherapy including taxanes and anthracyclines (Coates et al., 2015).

Recent approvals of the Food and Drug Administration (FDA) and the European Medicines Agency (EMA) allow the treatment of special subcategories of TNBC with Poly(ADP-Ribose)-Polymerase (PARP) inhibitors e.g. olaparib for patients with BReast CAncer (BRCA) mutated, metastatic TNBC and immune checkpoint inhibitors e.g. atezolizumab for Programmed Cell Death Ligand 1 (PD-L1) positive, metastatic TNBC (Heimes and Schmidt, 2019; Le and Gelmon, 2018).

Nonetheless, this subtype has the worst prognosis of all breast cancer types, and approximately 11% of breast cancer patients suffer of TNBC (American-Cancer-Society, 2019). Therefore, the medical need for new therapeutic options is huge.

1.2 CHALLENGES IN BREAST CANCER TREATMENT

As mentioned above depending on the subtype of breast cancer there are several options for treatment. Nonetheless, many tumors are initially hard to treat or recur. Thereby, the development of resistance to therapies and the formation of metastases belong to the major obstacles in fighting breast cancer (Weigelt et al., 2005).

1.2.1 DEVELOPMENT OF CHEMORESISTANCE

Regarding chemoresistance one can discriminate between *de novo* and acquired resistance. Whereas *de novo* resistant tumors are per se refractory to the applied treatment, acquired resistance appears after initial response to therapies. The latter has two possible reasons: the existence of so-called cancer stem cells (CSCs) or clonal evolution (Li et al., 2008; Navin, 2014; Vogelstein et al., 1988).

1.2.1.1 CANCER STEM CELL MODEL

The cancer stem cell model is based on the assumption that solid tumors are heterogenous tissues consisting of different tumor cells like cancer stem cells (CSCs), fast proliferating progenitors and differentiated cancer cells. (Lawson et al., 2015; Meacham and Morrison, 2013).

CSCs are capable to self-renew indefinitely, give rise to a multitude of different cell clones and are per se refractory to chemotherapy. One reason is that CSCs are less proliferative compared to differentiated cancer cells and are therefore less harmed by chemo- and radiotherapy mainly targeting fast dividing cells, (Bao et al., 2006; Visvader and Lindeman, 2008). Furthermore, it was previously shown that CSCs express high levels of efflux pumps like ABC-transporters e.g., MDR1, BCRP1. These P-glycoproteins protect CSCs of cytotoxic agents by removing them from the intracellular space (Schatton et al., 2008). Therefore, these CSCs are able to survive cancer therapy and give rise to novel tumors (Bai et al., 2018; Carnero et al., 2016).

1.2.1.2 CLONAL EVOLUTION MODEL

The clonal evolution is based on the theorem "survival of the fittest". As chemotherapies represent a huge selection pressure on tumors, cancer cells are forced to adapt to these cytotoxic agents (Kim et al., 2018a; Navin, 2014). Here, one possible escape mechanism is the augmentation of somatic mutations which can be induced by several chemotherapies (Wang et al., 2014). This causes increased expression of efflux pumps like ABC-transporters e.g., MDR1, BCRP1, which leads to reduced drug concentrations in the cancer cells. Moreover, elevated expression of oncogenes like growth factors e.g., EGFR induce cell proliferation, differentiation and thus cell survival. Also, genomic alterations in DNA repair mechanisms, apoptosis as well as autophagy belong to chemoresistance mechanisms (Wein and Loi, 2017; Zheng, 2017). Cancer cells that are able to adapt to cytotoxic agents by the above-mentioned mechanisms will survive chemotherapy and give rise to novel chemoresistant tumors.

1.2.2 FORMATION OF METASTASES

Even though emerging novel treatment options for breast cancer have improved patient outcome, metastatic breast cancer is still an incurable disease (American-Cancer-Society, 2019; Scully et al., 2012) as one of the leading causes of breast cancer associated deaths is metastatic spread (Hosseini et al., 2016; Schwartz and Erban, 2017).

Especially, TNBC patients have a high risk to develop a metastatic disease with the highest metastatic burden in lung, liver, bone and brain (Eckhardt et al., 2012; Valastyan and Weinberg, 2011). The 5-year survival rate of patients with metastatic breast cancer is only 20% (Gennari et al., 2005). One reason therefore is the lack of therapeutic options. In contrast to early breast cancer where surgery is a major component of the therapy this is hardly possible in a metastatic disease situation (Harbeck and Gnant, 2017). Moreover, breast cancer is usually diagnosed for the first time in a non-metastatic stage. Hence, metastatic breast cancer patients often received at least one prior treatment. As the formation of metastases is thought to occur as an early dissemination step in cancer development, these cell clones giving rise to metastases survived at least one prior cancer treatment and are therefore resistant (Lambert et al., 2017). Moreover, cell clones that are able to disseminate from primary tumors and colonize in different tissues evolved several clonal evolution steps. This results in more robust as well as proliferative phenotypes compared to the primary tumor and finally to decreased response to chemotherapy (McGranahan and Swanton, 2017). Due to these reasons the unmet medical need is very high.

1.3 AIM OF THE THESIS

In this thesis, these two major challenges in breast cancer therapy, i.e., development of chemoresistance and formation of metastases, were addressed.

Concerning the development of chemoresistance our aim was to investigate whether this process is directed and therefore follows a certain, designated pattern. If the clonal evolution leading to resistance alters the protein expression in breast cancer cells always in the same way, this process might be manageable or even avoidable by targeting the key drivers therapeutically. To investigate this phenomenon in an *in vitro* setting, a so-called "molecular evolution assay" (MEA) was developed in our laboratory. Here, breast cancer cells are treated sequentially with recovering periods in between mimicking several cycles of chemotherapy in a clinical setting. A subsequent proteomic analysis was intended to reveal the alterations of the proteome during chemotherapy compared to the parental cell line.

As the formation of metastases is another huge challenge in the treatment of breast cancer, the investigation of cancer cell migration was the aim in the second part of the thesis. As it was previously shown that the G protein-coupled receptor kinase GRK5 regulates cell migration in prostate cancer cells, its role in breast cancer should be investigated in this study. Therefore, the expression of GRK5 in different breast cancer cell lines as well as the influence of GRK5 knock-down on cancer cell migration and invasion were to be examined. Moreover, a comprehensive proteomics approach was intended to reveal signaling pathways regulated by GRK5. To evaluate the clinical relevance of GRK5 the impact of this kinase on distant-metastasis free survival in TNBC patients was to be examined using the Kaplan-Meier-Plotter. Finally, the therapeutic implication of GRK5 should be assessed by treating breast cancer cells with the multi-kinase inhibitor sunitinib, which was previously shown to inhibit GRK5 amongst others.

To sum up this thesis addresses two major obstacles in the treatment of breast cancer thus increasing the knowledge about development of chemoresistance and metastases. This may give rise to research in new medical entities for breast cancer therapy.

2. PROTEOMICS ANALYSIS OF CHEMORESISTANCE DEVELOPMENT

This chapter was adapted from the original publication, which was finally published as Sommer et al., International Journal of Molecular Medicine, 2018; *42*, 1987-1997. Sections may have been moved for consistency.

(Sommer et al., 2018)

A proteomic analysis of chemoresistance development via sequential treatment with doxorubicin reveals novel players in MCF-7 breast cancer cells

Ann-Katrin Sommer[1], Adam Hermawan[1], Bojan Ljepoja[1], Thomas Fröhlich[2], Georg J. Arnold[2], Ernst Wagner[1], and Andreas Roidl[1]

[1] Pharmaceutical Biotechnology, Department of Pharmacy, Ludwig-Maximilians-Universität, München, D-81377 Munich, Germany

[2] Laboratory for Functional Genome Analysis (LAFUGA), Gene Center, Ludwig-Maximilians-Universität München, D-81377 Munich, Germany

Contributions

AS analyzed the proteomics data, performed the pathway analysis and wrote the manuscript. AH preformed cell culture experiments and sample preparations for proteomics. BL provided support in presenting and discussing the data. TF conducted the LC-MS experiments and assisted with data analysis. EW and GJA provided conceptual advice. AR conceived the study and wrote the manuscript. All authors commented on the final manuscript and conclusions of this work.

2.1 ABSTRACT

Breast cancer exhibits the highest incidence of all cancer types and is the 2nd leading cause of cancer mortality in women. Up to 82% of breast cancer patients receive a chemotherapy-containing treatment regimen. However, numerous breast tumors recur within ten years following an initial response and are frequently resistant to previous therapeutic agents. Thus, to analyze the crucial factors, and whether the development of resistance in tumor cells follows certain patterns, is of great importance. In the present study, the clinical treatment schedule of the frequently used chemotherapeutic drug doxorubicin was applied in an in vitro model, the Molecular Evolution Assay (MEA), leading to resistance formation. By investigating the alterations in protein expression in MCF-7 breast cancer cells with three biological replicates, it was observed that the development of resistance to doxorubicin is a multi-directed process. The number and composition of the differentially expressed proteins varied, in addition to the pathways involved in chemoresistance, leading to only a small number of proteins and pathways being commonly regulated in all the MEAs. The proteins 60S ribosomal export protein NMD3 and 4F2 cell-surface antigen heavy chain (SLC3A2) were identified to be the most promising differentially expressed targets; the gene ontology term 'apoptotic signaling pathway' was reduced and 'cell redox homeostasis' was upregulated. Based on the present findings in vitro, it may be hypothesized that the development of resistance in patients is an even more complex process, emphasizing the need for further investigations of resistance development in the clinic to eventually improve patient outcomes.

2.2 INTRODUCTION

According to the American Cancer Society and the International Agency for Research on Cancer, breast cancer has the highest incidence of all cancers in women worldwide (American Cancer Society, 2018; Globocan, 2012). Furthermore, breast cancer is the second-leading cause of cancer deaths in the United States, where, 38% to 82% of breast cancer patients, depending on the stage, receive chemotherapy in adjuvant and neoadjuvant treatment regimen (Miller et al., 2016).

One of the most frequently used chemotherapeutics in breast cancer therapy is doxorubicin (DXR). This drug belongs to the anthracycline antibiotic family and was isolated from the *Streptomyces peucetius* (Arcamone et al., 1969). It acts by binding topoisomerase II (Tewey et al., 1984), via DNA intercalation (Chen et al., 2012) and by generating free radicals (Mizutani et al., 2005) resulting in DNA damage (Benchekroun et al., 1993; Gewirtz, 1999; Hilmer et al., 2004; Minotti et al., 2004; Tacar et al., 2013). A major obstacle in the treatment of breast cancer is the recurrence of the tumor. According to the Early Breast Cancer Trialists' Collaborative Group (EBCTCG) 39.4% of breast tumors previously treated with anthracyclines recur within ten years (Early Breast Cancer Trialists' Collaborative et al., 2012). A majority of relapses are resistant to the previous chemotherapeutic drugs resulting in a poor prognosis for breast cancer patients. In general, there are two hypotheses explaining the development of chemoresistance: the cancer stem cell (CSC) model and the clonal evolution model (Cairns, 1975; Greaves and Maley, 2012; Kopp et al., 2014; Meacham and Morrison, 2013; Nowell, 1976; Shackleton et al., 2009). The CSC model is based on the hypothesis that solid tumor cells are hierarchically organized with CSC at the apex, followed by fast proliferating progenitors and finally differentiated cancer cells. CSCs are capable of indefinite self-renewal, give rise to aberrant differentiated cells and are intrinsically resistant to chemotherapy (Meacham and Morrison, 2013). The clonal evolution model, on the other hand, states that tumor cells are stochastically organized and that tumor progression is driven by the fittest clone and not by CSC (Greaves and Maley, 2012). Since genomic instability is one hallmark of cancer (Hanahan and Weinberg, 2011), mutations in the tumor cells occur spontaneously. A subsequent selection pressure or a biological advantage leads to the propagation of certain cell clones (Greaves and Maley, 2012). One example of a strong selection pressures are chemotherapeutic drugs, including DXR which kill the majority of cancer cells, although certain resistant clones survive, giving rise to a new tumor cell population that is insensitive to the drug used previously (Bedard et al., 2013; Turner and Reis-Filho, 2012).

Previous studies demonstrated that DXR resistant cancer cells exhibit activated DNA damage repair mechanisms (Bankusli et al., 1989), alterations in topoisomerase II expression (de Jong et al., 1990), overexpression of drug metabolizing enzymes (Gehrmann et al., 2004; Wang et al., 2015), mutations in cellular tumor antigen p53 (Aas et al., 1996) and, particularly, enhanced drug efflux mediated by transporters belonging to the ATP-binding cassette superfamily (Gottesman, 2002; Hermawan et al., 2016). However, all of the *in vitro* studies dealing with DXR resistance have analyzed resistant cells which were permanently maintained in DXR-containing media. In the clinical setting however, chemotherapy with DXR is usually applied in four cycles of 60 mg/m^2 every third week in combination with cyclophosphamide (Early Breast Cancer Trialists' Collaborative et al., 2012). Recovery phases up to two weeks in between are an important part of the therapy to allow the patient to cope with the toxic drugs.

Therefore, the aim of the present study was to investigate the development of resistance by treating breast cancer cells for five rounds with DXR, and including treatment-free periods in between, thus mimicking the clinical therapy regimen of patients. This assay was termed the Molecular Evolution Assay (MEA), as it was possible to observe alterations in the protein expression upon a selection pressure (in this case, DXR) over time. This assay may reflect the development of acquired resistance in a more realistic way compared with constant high-dose drug treatments. Three independent MEAs (A, B and C) were performed in the breast cancer cell line MCF-7 to address the question of whether resistance formation follows similar patterns upon the same selection pressure, and to identify its crucial factors. Thus, the present study analyzed different biological replicates under the same conditions. In order to investigate the alterations in protein expression during resistance formation, a proteomics approach using liquid chromatography-mass spectrometry (LC-MS) was performed. This technique revealed differentially expressed proteins by comparing untreated cells with cells treated three and five times, thus elucidating important mechanisms of resistance formation.

2.3 RESULTS

2.3.1 MEA MIMICS RESISTANCE DEVELOPMENT

Chemoresistance remains one of the primary obstacles to treating cancer. Thus, an *in vitro* model that mimics sequential treatment in the clinic was established to investigate the development of resistance to DXR. In the present study, the breast cancer cell line MCF-7 was treated with 50 nM doxorubicin for five rounds. Generally, each round consisted of a treatment phase (72 h; 50 nM DXR) and a recovery phase. The next round was initiated when cells had recovered, indicated by attaining 80% confluency. At the beginning of the MEA (R0) and subsequent to the recovery phases of R3 and R5, cells were seeded for cell viability assays and proteomic analyses. A total of three independent biological replicates were performed to investigate the process of resistance formation. These replicates were termed MEA A, B and C (Fig. 3A). Different passage numbers of the parental cells (R0) were chosen (passage 5 for MEA A, passage 7 for MEA B and passage 8 for MEA C) to compensate for possible clonal effects or cell culture artefacts. R0, R3 and R5 of the three different MEAs (A, B and C) were further analyzed. Every proteomics sample was analyzed three times and are measurement replicates in the following sections.

2.3.2 DEVELOPMENT OF RESISTANCE UPON DOXORUBICIN TREATMENT DIFFERS IN MEA A, B AND C

To examine the sensitivity of the cells to 1 µM DXR, the untreated MCF-7 cells (R0), and R3 and R5 of the MEAs A, B and C, were analyzed by a cell viability assay. It was observed that resistance to DXR developed differently in each MEA (Fig. 3B). In the MEA A R3, a 1.3-fold decreased sensitivity to DXR was noted, whereas R5 displayed almost the same sensitivity to DXR as the untreated MCF-7 cells. R3 of MEA B was also 1.3-fold more resistant to treatment with DXR compared with the parental cells (R0), and the resistance was maintained in R5.

MEA C, on the other hand, exhibited no resistance increase in R3, although R5 exhibited the highest increase in resistance to DXR compared with all other MEAs. These data indicated that the development of resistance to DXR in the different MEAs was neither constantly increasing nor occurring in a consistent manner.

2.3.3 PROTEOMIC ANALYSIS OF THE TREATMENT ROUNDS REVEALS NO INCREASE IN DIFFERENTIAL PROTEIN EXPRESSION IN LATER ROUNDS

Alterations in protein expression during resistance formation were analyzed using a label-free proteomics approach. Herein, ~3,000 proteins were identified in each measurement.

To visualize the expression alterations between R0, R3 and R5 of MEA A, B and C, a scatter blot analysis was performed (Fig. 3C). In the left scatter blots, depicting the parental MCF-7 cells at different passage numbers, the spots are very close to the bisecting line of an angle, indicating that the protein expression of the untreated cells in MEA A, B and C hardly differed. The Pearson correlation value of 0.94 emphasizes these results. The scatter blots in the middle panel illustrate that the spots of R3A compared with R3B, and R3A compared with R3C, diverge more from the bisector. Likewise, the Pearson correlation indices decreased. Thus, the protein expression in R3 of MEA A, B and C differed more amongst each other compared with that of the untreated cells (R0). The right panel displays the comparison of the different R5s and illustrates that the perturbation of protein expression in general was not further increased by additional treatments with DXR. Thus, it was identified that the parental cells (R0) were similar in protein expression and that a considerable perturbation was induced by three treatment rounds with DXR. A total of five treatment rounds with DXR, however, did not lead to a further increase in the difference in protein expression.

A

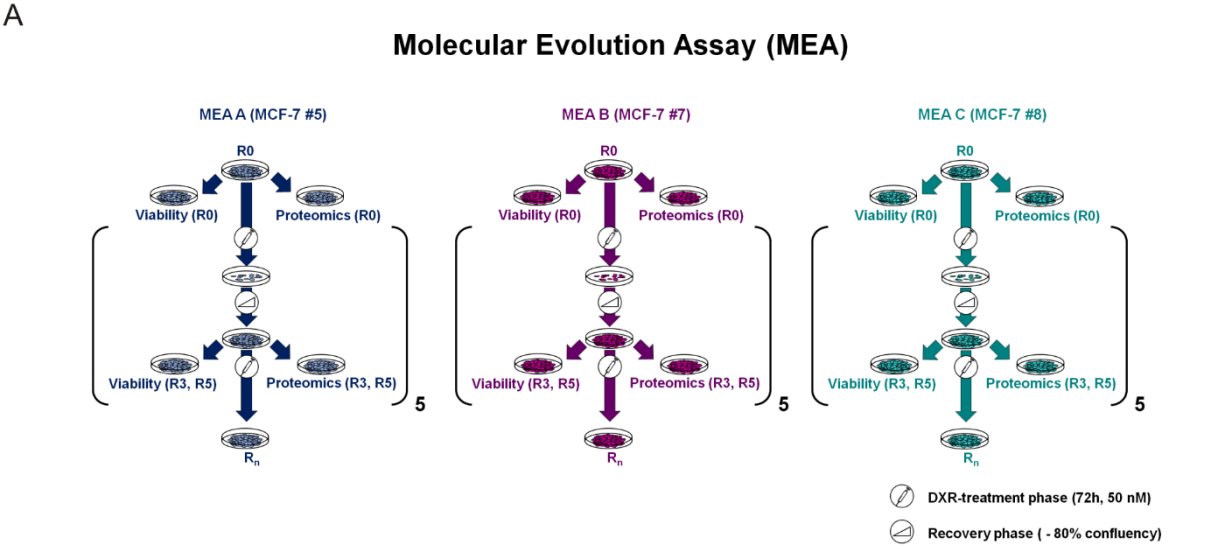

B

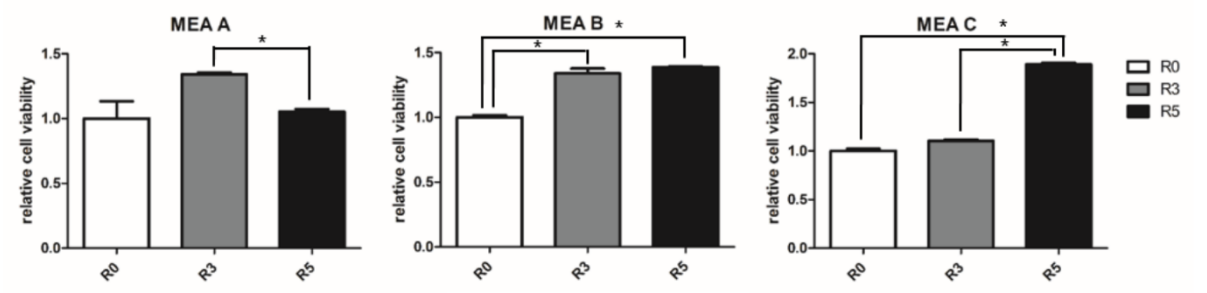

C

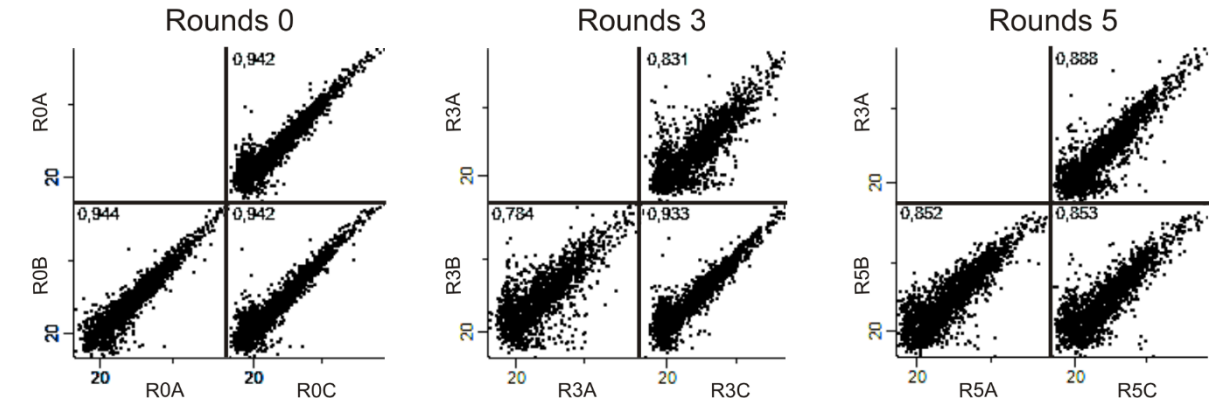

Figure 3. Introduction of the MEA. (A) Schematic representation of the MEA. MCF-7 cells were treated by Dr. Adam Hermawan in five rounds (R1-R5) with 50 nM DXR for 72 h. In between the treatment rounds, the cells were allowed to recover until they reached a confluence of 80%. Three independent biological replicates were performed with cells at passage number 5, 7 and 8 (MEA A, B, C). R0, R3 and R5 were used for further analysis. Proteomics analysis were performed by Dr. Thomas Fröhlich and Dr. Georg J. Arnold, Laboratory for Functional Genome Analysis (LAFUGA), Gene Center, LMU (B) Analysis of resistance formation in MCF-7 cells. To evaluate the resistance formation to DXR, the MCF-7 cells of R0, R3 and R5 in MEA A, MEA B and MEA C were seeded in triplicate, treated with 1 µM doxorubicin for 72 h and subsequently analyzed by applying a CellTiter-Glo Luminescent cell viability assay. Results are presented as the mean + standard deviation. A two-tailed paired Student's t-test was performed to evaluate significance. *P<0.05.

(C) Multiscatter analysis. To evaluate the similarity of the different rounds, a multiscatter analysis was performed. The median of three measurement replicates was calculated and R0, R3 and R5 of MEA A, B and C were compared with each other. A Pearson correlation index close to 1 indicates high similarity. MEA, Molecular Evolution Assay; R, round; DXR, doxorubicin.

2.3.4 GSEA REVEALS SIGNALING PATHWAYS INVOLVED IN THE DEVELOPMENT OF RESISTANCE TO DXR

To investigate the alterations in signaling pathways involved in the development of chemoresistance in the different MEAs, a GSEA (Mootha et al., 2003; Subramanian et al., 2005) was performed. The global ES histogram in Fig. 4A gives an overview of up- and downregulated proteins and illustrates that in R3 the majority of proteins were downregulated. This effect was even more marked in R5 compared with R0. For a more detailed analysis, the MEAs were examined separately. The differences in enriched gene sets are visible in the global ES histograms (Supplementary Figure S1). Furthermore, the results were screened for GO terms and pathways known to be relevant for resistance formation (Shibue and Weinberg, 2017). The normalized ES of the selected pathways exhibit alterations occurring between R0, R3 and R5 (Supplementary Figure S2). Proteins assigned to the GO pathway 'apoptotic signaling pathway' were reduced following three and five treatment cycles with DXR in all MEAs (Fig.4B). On the other hand, 'cell redox homeostasis' was generally upregulated in the DXR-treatment rounds (R3 and R5) and all MEA replicates (Fig. 4C). All other analyzed pathways, including 'locomotion', 'cell cycle', 'autophagy', 'cell motility', 'cell division', 'detoxification', 'response to toxic substance' and 'glutathione metabolic process', differed between MEA A, B and C (Supplementary Figure S2). Therefore, all cells in this setting escaped the chemotherapeutic selection pressure of DXR, primarily by reducing the expression of proteins belonging to the GO pathway 'apoptotic signaling pathway' and increasing the expression of the members of 'cell redox homeostasis'.

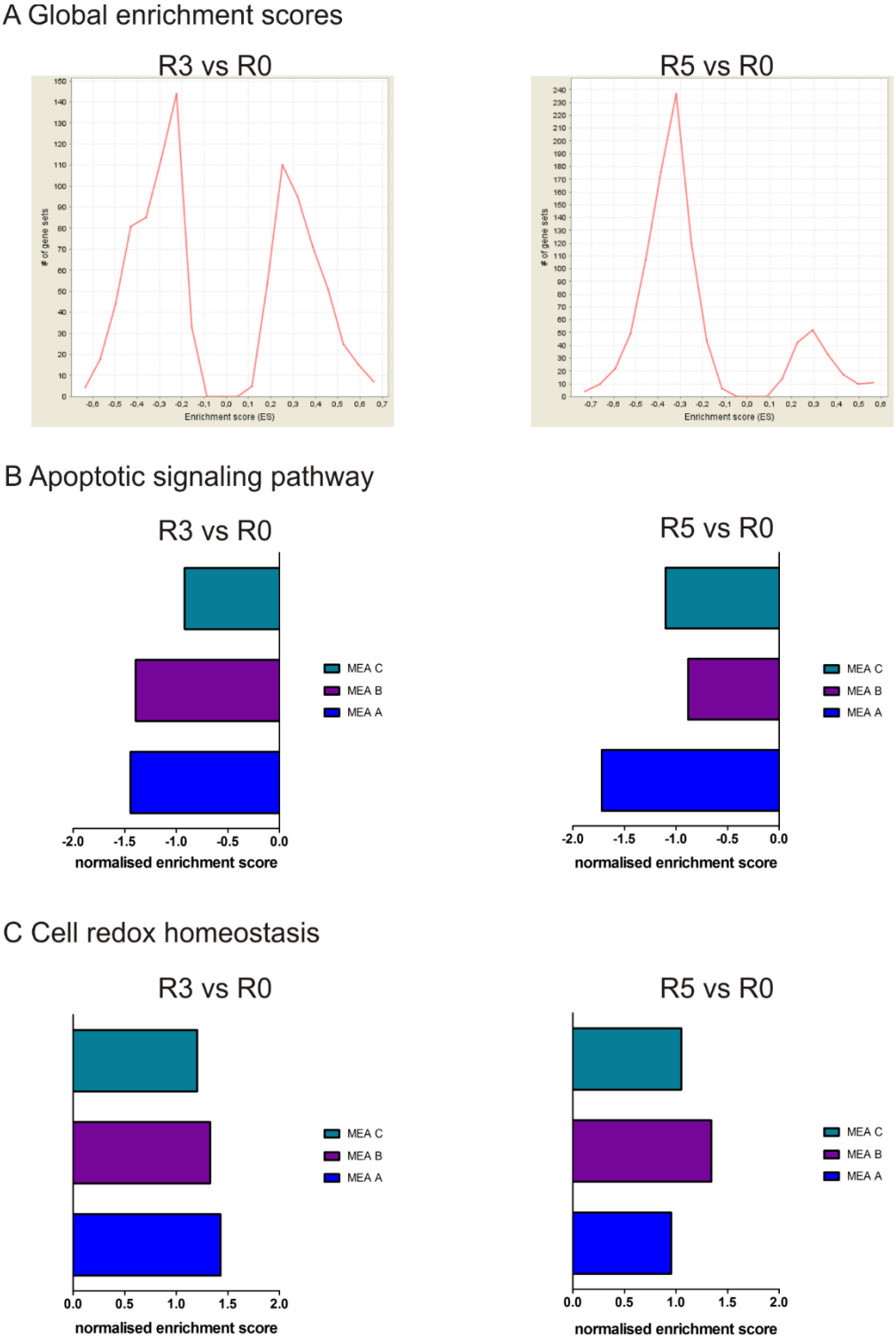

Figure 4. GSEA. GSEA was performed using gsea2-2.2.3 from the Broad Institute. (A) Global enrichment score histogram. The global enrichment score histograms are depicted to illustrate an overview of the amount of upregulated and downregulated gene sets in all the MEAs, comparing R3 and R5 with R0. (B) Apoptotic signaling pathway. The normalized enrichment score was used to facilitate the comparison of different MEAs. (C) Cell redox homeostasis. The normalized enrichment score was used to facilitate the comparison of different MEAs. GSEA, gene set enrichment analysis; R, round; MEA, Molecular Evolution Assay.

2.3.5 COMPARING THE DIFFERENT MEAS REVEALS 111 PROTEINS WITH DECREASED AND 42 PROTEINS WITH INCREASED EXPRESSION IN ALL CONDITIONS

Subsequently, the three biological replicates (MEA A, B and C) were analyzed separately for up- and downregulated proteins. A total of ~1,000 proteins exhibited decreased or increased expression between R3 and R0 or R5 and R0 in each of the MEAs (Fig. 5). However, the amount of differentially expressed proteins was not consistent among the individual MEAs. To identify proteins which were commonly up- or downregulated in all MEAs, a Venn analysis was performed. Fig. 5A illustrates the number of proteins with reduced expression upon treatment with DXR. Following three treatment cycles with DXR, 360 proteins out of all the downregulated proteins were identical in all three MEAs (R3 vs. R0). Furthermore, 317 proteins were commonly downregulated in all MEAs following five treatment cycles with DXR (R5 vs. R0). Subsequently, these 360 proteins, which were downregulated in all MEAs following three treatment rounds with DXR, and the 317 proteins that were reduced following five treatment rounds, were compared in a further Venn diagram to determine the proteins exhibiting decreased expression in R3 and R5 compared with R0. A total of 111 proteins were commonly downregulated in all MEAs upon three and five treatment rounds with DXR. The same analysis was performed for proteins with increased expression (Fig. 5B). A total of 160 proteins were commonly upregulated in all MEAs, comparing R3 with R0. The analysis of R5 compared with R0 revealed 162 proteins with increased expression in all MEAs. The obtained proteins of R3 compared with R0 and R5 compared with R0 were further compared, and 42 proteins were detected as commonly upregulated. These up- and downregulated proteins are presented in tables in the Supplements. Taken together, the analysis of the protein abundance of the different MEAs revealed only a few commonly regulated proteins.

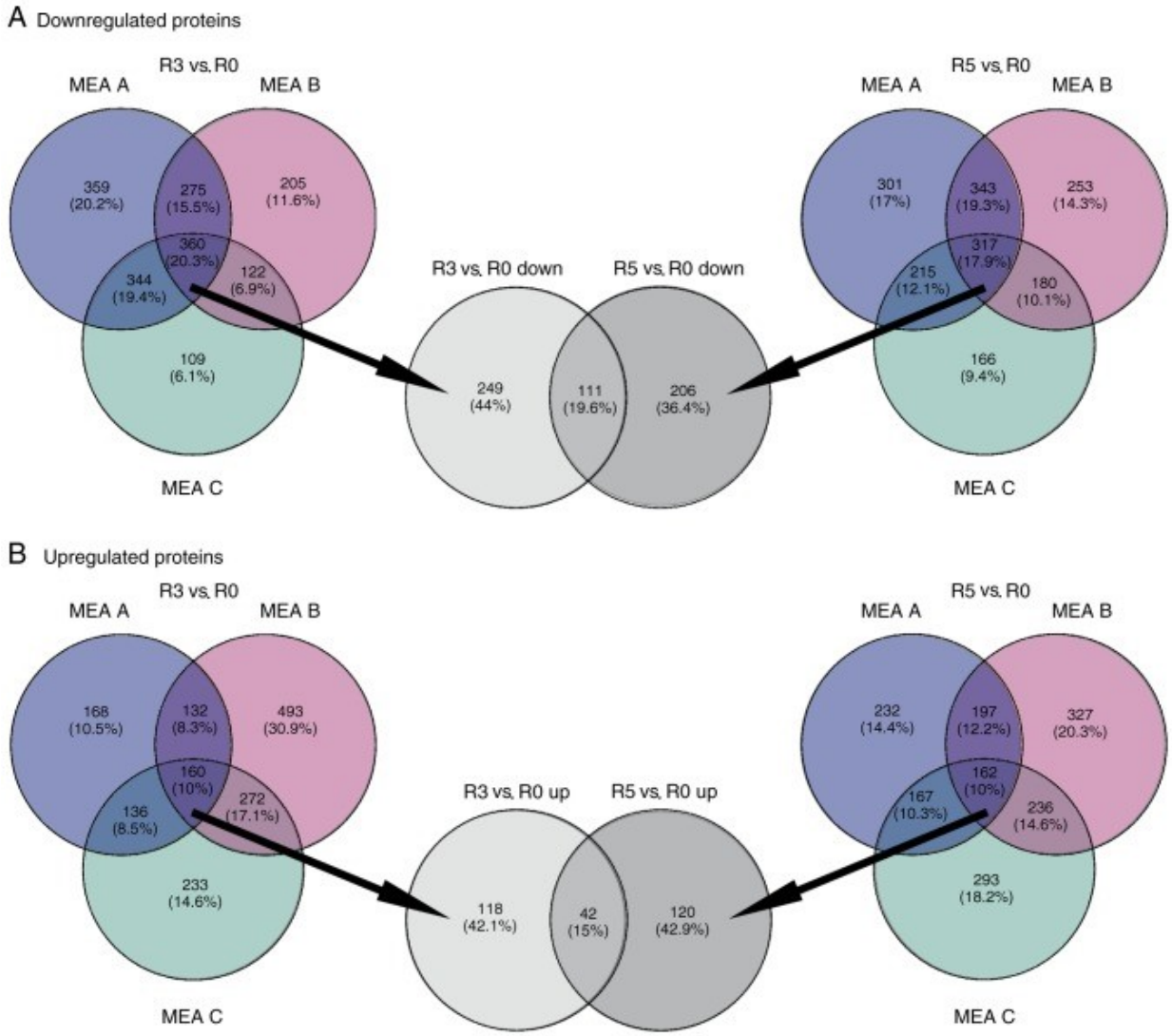

Figure 5. Comparison of MEA A, B and C. In order to compare MEA A, B and C, proteins that were identified twice in at least one group were analyzed. Missing values were replaced from a normal distribution (width, 0.3; down shift, 1.8) and a Student's t-test was performed to evaluate alterations in protein expression upon treatment with doxorubicin. Subsequently, proteins were sorted according to their t-test difference (<0, downregulated; >0, upregulated). (A) Venn diagram of downregulated proteins. To investigate the number of commonly regulated proteins between MEA A, B and C, a Venn analysis was performed. The downregulated proteins of R3 (left) and R5 (right) compared with R0 were analyzed. Proteins exhibiting decreased expression in R3 and R5 across all MEAs were again compared to elucidate which proteins were downregulated between R0 and R3 and between R0 and R5. (B) Venn diagram of upregulated proteins. The Venn diagrams illustrate the amount of commonly upregulated proteins in MEA A, B and C. Left, upregulated proteins in R3 compared with R0. Right, upregulated proteins in R5 compared with R0. Proteins with increased expression in all MEAs were compared to determine the number of continuously upregulated proteins. MEA, Molecular Evolution Assay; R, round.

2.3.6 ANALYSIS OF DIFFERENTIALLY EXPRESSED PROTEINS REVEALS THE 20 PROTEINS WITH THE HIGHEST OVERALL EXPRESSION ALTERATION

Subsequently, the three MEAs were analyzed separately for differentially expressed proteins, with a threshold of a 1.5-fold change. This led numbers of downregulated proteins between R3 and R0 of 946 in MEA A, 212 in MEA B and 233 in MEA C. A smaller number of proteins were upregulated: 318 in MEA A, 307 in MEA B and 146 in MEA C. Regarding alterations in protein expression comparing R5 to R0, it was observed that 851 proteins in MEA A, 960 in MEA B and 435 in MEA C were differentially expressed. Only 4-7% of all identified and differentially expressed proteins were commonly regulated in all MEAs (Fig. 6A hatched area).

In Fig. 6B, the 20 proteins with the highest overall abundance alterations are depicted, displaying their relative expression and the respective P-values.

A 1.5 Fold differentially expressed proteins

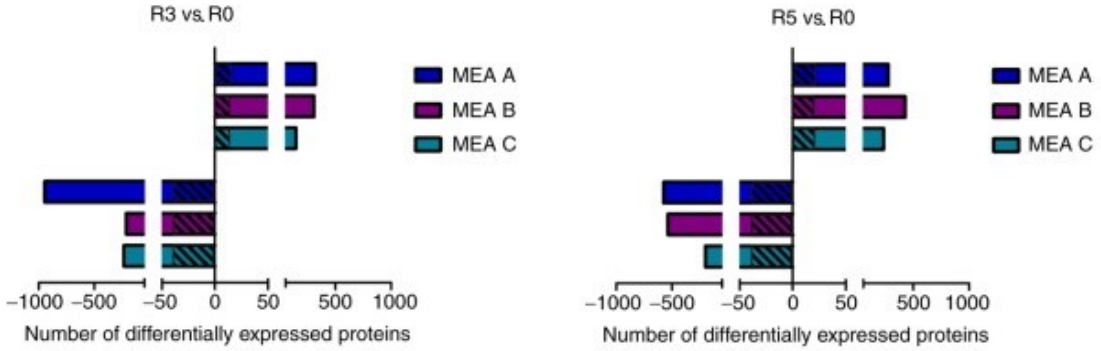

B Proteins with highest abundance alterations

Up	R3 vs. R0						R5 vs. R0					
Genename	MEA A		MEA B		MEA C		MEA A		MEA B		MEA C	
	RE	P-value	RE	P-value	RE	P-value	RE	P-value	RE	P-value	RE	P-value
SLC3A2	2.2x10^{1}	1.1x10^{-5}	1.7x10^{0}	1.5x10^{-1}	1.6x10^{0}	2.4x10^{-2}	2.6x10^{1}	6.2x10^{-6}	1.0x10^{1}	2.5x10^{-5}	1.2x10^{0}	1.6x10^{-2}
ASS	1.1x10^{1}	1.1x10^{-4}	2.1x10^{0}	9.0x10^{-4}	1.0x10^{0}	9.7x10^{-1}	5.0x10^{0}	4.5x10^{-4}	2.1x10^{1}	1.3x10^{-7}	6.5x10^{0}	1.3x10^{-2}
BCAS1	2.8x10^{1}	1.3x10^{-6}	1.6x10^{0}	6.5x10^{-2}	4.4x10^{0}	3.6x10^{-2}	2.6x10^{0}	4.4x10^{-2}	4.6x10^{0}	2.2x10^{-5}	2.1x10^{0}	1.4x10^{-1}
KTN1	2.6x10^{1}	3.0x10^{-5}	3.4x10^{0}	5.4x10^{-3}	1.2x10^{0}	8.0x10^{-1}	7.2x10^{0}	2.5x10^{-4}	2.9x10^{0}	8.6x10^{-2}	1.0x10^{0}	9.7x10^{-1}
TFF1	1.3x10^{1}	1.1x10^{-2}	2.2x10^{0}	1.4x10^{-1}	1.4x10^{0}	3.8x10^{-1}	1.9x10^{0}	2.6x10^{-1}	7.4x10^{0}	1.4x10^{-3}	4.5x10^{0}	1.6x10^{-2}
SLC7A5	5.8x10^{0}	2.0x10^{-2}	2.0x10^{0}	1.2x10^{-1}	1.5x10^{0}	9.6x10^{-2}	1.7x10^{0}	4.4x10^{-1}	1.1x10^{1}	1.7x10^{-3}	1.1x10^{0}	6.8x10^{-1}
S100P	3.9x10^{0}	6.4x10^{-2}	4.0x10^{0}	9.1x10^{-2}	2.4x10^{0}	1.1x10^{-1}	1.3x10^{0}	8.5x10^{-1}	4.9x10^{0}	4.9x10^{-2}	3.4x10^{0}	2.2x10^{-2}
ABHD11	4.4x10^{0}	9.7x10^{-3}	1.1x10^{0}	5.8x10^{-1}	1.9x10^{0}	1.6x10^{-1}	2.1x10^{0}	3.5x10^{-2}	2.5x10^{0}	1.1x10^{-3}	2.2x10^{0}	7.3x10^{-2}
LAD1	1.0x10^{0}	8.1x10^{-1}	1.6x10^{0}	3.4x10^{-2}	1.6x10^{0}	3.0x10^{-1}	1.9x10^{0}	1.1x10^{-2}	6.0x10^{0}	5.7x10^{-4}	1.7x10^{0}	4.1x10^{-1}
PLEC	5.1x10^{0}	1.3x10^{-7}	1.5x10^{0}	1.7x10^{-4}	1.7x10^{0}	1.5x10^{-3}	2.6x10^{0}	2.6x10^{-6}	1.3x10^{0}	8.6x10^{-3}	1.7x10^{0}	1.1x10^{-3}

Down	R3 vs. R0						R5 vs. R0					
Genename	MEA A		MEA B		MEA C		MEA A		MEA B		MEA C	
	RE	P-value	RE	P-value	RE	P-value	RE	P-value	RE	P-value	RE	P-value
GFRA1	2.0x10^{-1}	3.7x10^{-5}	6.0x10^{-1}	4.7x10^{-3}	5.0x10^{-1}	5.4x10^{-2}	1.2x10^{-1}	4.5x10^{-4}	1.1x10^{-1}	8.1x10^{-4}	1.9x10^{-1}	9.8x10^{-3}
TAX1BP3	1.5x10^{-1}	6.1x10^{-4}	2.1x10^{-1}	1.3x10^{-4}	2.3x10^{-1}	1.7x10^{-1}	1.1x10^{-1}	8.7x10^{-4}	3.1x10^{-1}	1.6x10^{-1}	9.1x10^{-1}	2.5x10^{-1}
PRKAR1A	1.9x10^{-1}	7.0x10^{-4}	6.2x10^{-1}	2.9x10^{-2}	3.2x10^{-1}	5.1x10^{-3}	3.1x10^{-1}	4.5x10^{-5}	1.7x10^{-1}	1.5x10^{-2}	4.2x10^{-1}	2.2x10^{-2}
CNBP	2.5x10^{-1}	3.7x10^{-2}	4.5x10^{-1}	3.2x10^{-2}	3.0x10^{-1}	2.8x10^{-2}	4.1x10^{-1}	7.8x10^{-2}	7.7x10^{-1}	4.0x10^{-1}	1.9x10^{-1}	6.4x10^{-2}
AGR3	3.1x10^{-1}	1.3x10^{-3}	3.7x10^{-1}	1.6x10^{-3}	7.7x10^{-1}	6.9x10^{-1}	2.7x10^{-1}	2.4x10^{-3}	1.3x10^{-1}	5.6x10^{-4}	6.6x10^{-1}	5.4x10^{-1}
CA2	1.5x10^{-2}	2.5x10^{-5}	9.3x10^{-1}	1.0x10^{-2}	7.7x10^{-1}	3.7x10^{-1}	9.5x10^{-3}	7.7x10^{-5}	1.1x10^{-2}	2.7x10^{-4}	7.7x10^{-1}	6.6x10^{-2}
CMBL	4.9x10^{-1}	5.6x10^{-2}	4.7x10^{-1}	5.7x10^{-3}	4.8x10^{-1}	6.0x10^{-2}	6.5x10^{-1}	1.5x10^{-3}	7.1x10^{-2}	7.4x10^{-5}	4.3x10^{-1}	3.6x10^{-2}
NMD3	1.3x10^{-1}	1.3x10^{-4}	7.2x10^{-1}	2.7x10^{-3}	4.9x10^{-1}	6.5x10^{-2}	4.4x10^{-1}	1.2x10^{-2}	2.5x10^{-1}	4.7x10^{-4}	5.7x10^{-1}	1.1x10^{-1}
PNPO	4.3x10^{-1}	2.1x10^{-2}	7.7x10^{-1}	2.3x10^{-1}	2.5x10^{-1}	6.2x10^{-2}	9.6x10^{-2}	9.4x10^{-5}	5.8x10^{-1}	1.7x10^{-1}	5.9x10^{-1}	4.3x10^{-4}
TPD52L2	2.8x10^{-1}	1.5x10^{-3}	7.9x10^{-1}	1.1x10^{-2}	3.9x10^{-1}	1.5x10^{-1}	2.3x10^{-1}	1.6x10^{-2}	9.3x10^{-1}	3.6x10^{-1}	3.6x10^{-1}	2.6x10^{-1}

Figure 6. Differentially expressed proteins. For a comparison of MEA A, B and C only proteins that were identified twice in at least one group were considered. Missing values were imputated (width, 0.3; down shift, 1.8). In order to determine the alterations in protein expression during resistance formation, a Student's t-test was performed and R3 vs. R0 and R5 vs. R0 were compared. Only proteins exhibiting a Student's t-test difference of at least |0.6| (1.5-fold) were further examined. The proteins with decreased expression levels are presented as negative values, and vice versa. (A) Number of differentially expressed proteins. The differentially expressed proteins of R3 (left) and R5 (right) compared with R0 were analyzed. The hatched area represents the commonly regulated proteins.

(B) Proteins with the highest abundance alterations. The depicted tables illustrate the proteins with the highest abundance alterations across all MEAs. In the upper table the 10 proteins with the largest overall increase in expression are presented. The lower table displays the 10 proteins with the greatest reduction in expression upon treatment with doxorubicin. A two-tailed student's t-test with a false discovery rate of 0.05 was used to compare R3 with R0 and R5 with R0. $P<0.05$ was considered to indicate a statistically significant difference. MEA, Molecular Evolution Assay; R, round; RE, relative expression.

2.3.7 COMMONLY REGULATED PROTEINS ARE LIKELY TO BE ASSOCIATED WITH CHEMORESISTANCE.

In order to identify the most promising targets in the development of chemoresistance, treated samples (R3 and R5) were compared with untreated samples (R0) across all three MEAs. The proteins which were present in all MEAs (A, B and C) were further analyzed, according to their differential expression. Finally, 15 proteins with the highest overall expression alterations are presented in a table in the Supplements. The majority of these proteins are known to be involved in crucial mechanisms and pathways, including tumorigenesis, the cell cycle and apoptosis. A total of two representative proteins are presented in Fig. 7. 60S ribosomal export protein NMD3 (NMD3) is a representative example of proteins which were downregulated upon treatment with DXR in every MEA and exhibited a decrease in protein expression. On the other hand, 4F2 cell-surface antigen heavy chain (SLC3A2) was upregulated 12.7-fold on average, and represents an example of increasing proteins expression levels (Fig. 7A). The detailed alteration in expression of these targets in the individual MEAs and rounds is displayed in Fig. 7B. The individual expression levels overall followed a similar trend throughout the MEAs: Reduced expression following treatment with DXR in the case of NMD3, and an increase in SLC3A2. This indicated the importance of these proteins in resistance development. To further evaluate the impact of these proteins on cancer progression, the RFS of a cohort of patients with breast cancer (luminal A tumors) was investigated *in silico* using a Kaplan-Meier analysis provided by Kaplan-Meier Plotter (Gyorffy et al., 2010). Breast tumors with low NMD3 expression levels recurred earlier [hazard ratio (HR) =0.7] compared with tumors exhibiting high NMD3 expression. In line with the present proteomic analysis, high expression levels of SLC3A2 led to shorter RFS periods in comparison with tumors with low SLC3A2 expression (HR =1.4) (Fig. 7C).

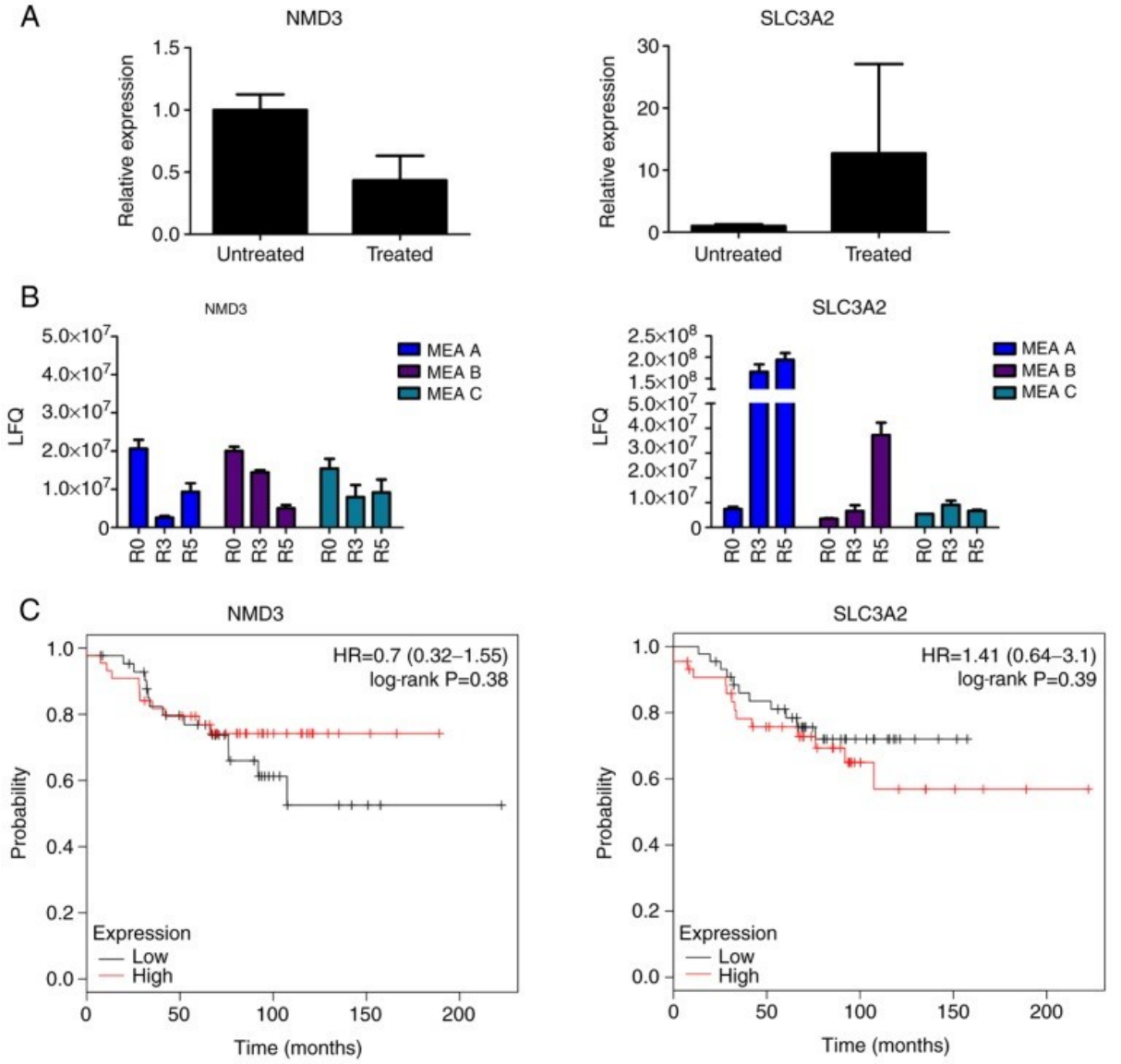

Figure 7. Potential common drivers of chemoresistance. Treated cells (R3 and R5) were compared with untreated cells (R0) to identify proteins that were commonly regulated during resistance formation across all MEAs. NMD3 and SLC3A2 are presented as representative examples. (A) Global comparison of treated and untreated cells. All values are depicted as relative expression values normalized to untreated cells, and are presented as the mean + standard deviation of all MEAs. (B) Detailed analysis of each MEA. The LFQ values of each round are depicted here as the mean + standard deviation of the measurement replicates. (C) Kaplan-Meier plots. The relapse-free survival of luminal A breast cancer patients was analyzed using the GSE21653 dataset. MEA, Molecular Evolution Assay; R, round; NMD3, 60S ribosomal export protein NMD3; SLC3A2, 4F2 cell-surface antigen heavy chain; LFQ, label free quantification.

2.4 DISCUSSION

Drug resistance remains one of the principal obstacles in the treatment of cancer and frequently correlates with tumor relapse, in addition to poor patient outcomes. In the present study, the development of chemoresistance was investigated using a proteomics approach, to acquire a comprehensive analysis of the fundamental factors, patterns and mechanisms.

To generate chemoresistance, other studies have maintained cells in DXR-containing medium, whereas in the present study, to the best of our knowledge for the first time, cells were treated in rounds with treatment-free periods and were subsequently analyzed with proteomics. Persistent treatment with DXR leads to a continuous up- or downregulation of proteins compensating for the permanent toxic stress, similar to multiple drug resistance mechanisms, including the upregulation of 5'-adenosine triphosphate-binding cassette transporters (Aas et al., 1996; Bankusli et al., 1989; de Jong et al., 1990; Gehrmann et al., 2004; Gottesman, 2002; Hermawan et al., 2016; Wang et al., 2015). In the present assay, the temporary absence of the selection pressure caused further perturbations in protein expression. This increased the complexity of the resistance model. The removal of DXR leads to regrowth of surviving cells in which the fittest clones with the highest proliferation rate have the highest impact on the composition of the recurrent tumor cell population. Therefore, it was hypothesized that the MEA was more reflective of the therapeutic regimen in the clinic. Analyzing resistance formation by MEA may thus lead to novel insights.

The development of chemoresistance in tumors may generally be explained by two hypotheses: The CSC model and the clonal evolution model (Cairns, 1975; Greaves and Maley, 2012; Kopp et al., 2014; Meacham and Morrison, 2013; Nowell, 1976; Shackleton et al., 2009). Choi *et al* (Choi et al., 2017) reported that only 1.2% of wild type MCF-7 cells exhibit a CSC-like phenotype. If only these CSCs had survived the treatment, a more homogenous protein pattern, in addition to an increase in stem cell markers, may have been detected in the present study.

Therefore, it may be hypothesized that CSCs have only a minor impact on the development of chemoresistance in the present setting, and the clonal evolution model may therefore be favored for the present *in vitro* resistance assay. There are numerous pathways involved in drug resistance (Aas et al., 1996; Bankusli et al., 1989; de Jong et al., 1990; Gehrmann et al., 2004; Gottesman, 2002; Wang et al., 2015) in which proteins were not observed to be altered in the present study. A possible reason may be conditions of this assay, for example with recovery phases and sequential treatment. Another reason may be the performed proteomic analysis. The analysis of differentially expressed proteins with the present method has a number of advantages compared with frequently used genomics methods. However, it is not possible to perform a comprehensive analysis due to limitations in detecting the entirety of human proteins. Furthermore, the applied proteomic analysis is not able to detect alterations in mRNA expression levels, which a number of publications have investigated (Aas et al., 1996; Gottesman, 2002). Furthermore, it has been reported that there is only a very weak correlation between mRNA expression levels and protein expression (Pertea, 2012). However, protein expression is responsible for the manifestation of biological phenotypes and, therefore, a proteomics approach may be the superior analysis for the evaluation of resistance formation. By applying the label-free LC-MS technique in the present study, 3,000 of the 30,057 human proteins (Kim et al., 2014) were identified, a notable improvement compared with previous studies (Holm et al., 2018; Koplev et al., 2018; Wang et al., 2015). Also, stringent cut-off criteria were chosen to minimize the detection of false positive results.

For an unbiased analysis, a GSEA was utilized. Common resistance mechanisms, including ‘apoptotic signaling pathway’ and ‘cell redox homeostasis’ were demonstrated to be altered. A reduction in apoptosis is a common mechanism through which to escape cell death, and has been reported in previous studies (Marin et al., 2016; Pfeffer and Singh, 2018). Particularly in the context of treatment with DXR, the increased expression of proteins regulating cell redox homeostasis is plausible. This pathway analysis further demonstrated that the development of resistance to DXR differed in each MEA.

By comparing treated (R3 and R5) with untreated cells (R0) of all MEAs, NMD3 and SLC3A2 were identified to be representative examples of downregulated or upregulated proteins, respectively. SLC3A2 is associated with cell survival, migration and tumor growth in renal cancer, and may thus be a promising resistance marker in breast cancer (Poettler et al., 2013; Prager et al., 2009). Additionally, NMD3 has a marked impact on RNA biosynthesis, particularly ribosomal RNA synthesis, and may therefore influence tumorigenesis in general (Bai et al., 2013); however, a direct role for this protein in chemoresistance remains to be elucidated.

The results of the present study demonstrated through the commonly up- or downregulated targets that the development of chemoresistance differed in each MEA. Thus, only a few general drivers of resistance formation were identified (4-7% of the identified proteins) and >90 % of the differentially expressed proteins were altered only in one of the assays. This phenomenon may be caused, on the one hand, by slightly heterogeneous initial protein expression due to pre-existing genomic instability and, on the other hand, by the treatment with DXR, which had the highest impact on the perturbation of differentially expressed proteins in MEA A, B and C. It was not possible to detect a dominant pattern of differential protein expression which was reproducibly present in all replicates. The assay conditions and analyses also did not allow for the drawing of conclusions as to whether resistance formation is a stochastic or, at least, a multi-directed process, as an increased number of replicates may identify patterns in resistance formation. Furthermore, it was observed that the sensitivity to DXR varied in each MEA during the five treatment rounds. Chemoresistance is defined as the insensitivity of tumor cells to chemotherapeutic drugs, leading to tumor progression during chemotherapy (Schwab, 2011). However, the underlying mechanisms are different. One such mechanism is intrinsic drug resistance; this means that tumor cells are resistant to the applied drug from the beginning of treatment. The other mechanism is acquired resistance, wherein tumor cells develop resistance to the applied drug following an initial response (Sommer et al., 2016). In the present study, it was observed that in MEA A, for example, five times-treated cells exhibited the same sensitivity to DXR as untreated cells. This indicated that five treatment rounds with DXR did not further increase resistance compared with three times-treated cells, and also that resistance may not be a persistent condition.

Furthermore, it was demonstrated that five treatment rounds altered protein expression while not necessarily increasing resistance to the applied drug. This observed effect may be due to clonal selection, which favors faster growing cell clones that then represent the majority of cells in the recovery phase. Thus, the present assay did not select for the most resistant clones; rather, for those that survived the treatment and were subsequently able to repopulate. This resembles the situation in the clinic more accurately than maintaining a constant selection pressure.

Additionally, the diversity in the development of resistance may be due to the heterogeneity of tumor cells. According to The Cancer Genome Atlas and the International Cancer Genome Consortium, estrogen receptor positive (ER^+) breast cancer exhibits the greatest diversity concerning gene expression, mutations, alterations in copy numbers and patient outcomes (Cancer Genome Atlas, 2012; Nik-Zainal et al., 2016; Parker et al., 2009). Thus, it may be hypothesized that the response to chemotherapy may differ in each patient. This may lead to varying selection of resistant clones, which give rise to metastases and recurrent tumors. It was previously reported that disseminating breast cancer cells exhibit a different gene expression pattern and an increased resistance to chemotherapeutics compared with the primary tumor (Goswami et al., 2009; Goswami et al., 2004; Patsialou et al., 2012; Wang et al., 2003; Wyckoff et al., 2000; Yates et al., 2017). Furthermore, Folgueira *et al* (Koike Folgueira et al., 2009) demonstrated, by comparing ER^+ breast tumor samples pre- and post-treatment with DXR and cyclophosphamide, that 389 genes were differentially expressed.

Another general reason for the heterogeneity of tumors is genomic instability, a hallmark of cancer (Hanahan and Weinberg, 2011). Tomasetti *et al* (Tomasetti et al., 2017) reported that the majority of mutations leading to tumorigenesis are random DNA replication errors, aside from hereditary and environmental mutations. This finding indicated that every patient with breast cancer may exhibit a different response to therapy, RFS and overall survival.

In conclusion, the present *in vitro* model indicated that the development of chemoresistance is a multi-directed or varying process. Due to the genomic instability in breast cancer, the response to chemotherapeutics, and thus the development of resistance by clonal selection, may be an event that rarely follows certain patterns.

Transferred to the clinical setting with even more perturbations in resistance formation, these results may explain why cancer remains difficult to treat and why the patient outcome is hard to predict. This furthers emphasizes the requirement for an individual diagnosis of resistance markers, in addition to patient-tailored therapy.

2.5 MATERIALS AND METHODS

2.5.1 CELL CULTURE

The breast cancer cell line MCF-7 was obtained from CLS Cell Lines Service GmbH (Eppelheim, Germany) and cultured in Dulbecco's modified Eagle's medium high glucose (Sigma-Aldrich; Merck KGaA, Darmstadt, Germany) containing 10% fetal calf serum (Gibco; Thermo Fisher Scientific, Inc., Waltham, MA, USA) at 37˚C and 5% CO_2. For the following experiments, cells were used at passage number 5 (MEA A), 7 (MEA B) and 8 (MEA C), respectively.

2.5.2 MOLECULAR EVOLUTION ASSAY

The MEA was performed by Dr. Adam Hermawan as described previously (Kopp et al., 2012). MCF-7 cells were treated with 50 nM DXR (Sigma-Aldrich; Merck KGaA) for 72 h. Subsequently, the drug was removed and the remaining cells were cultured until they reached a confluence of 80%. Finally, the cells were split and 4 days subsequently one dish was taken for the next treatment round, one for proteomics analysis and one for cell viability measurements. The rounds 0 (R0), 3 (R3) and 5 (R5) were used for proteomics analysis. This experiment was performed three times independently.

2.5.3 CELL VIABILITY ASSAY

To assess the resistance formation of R3 and R5 compared with R0, a CellTiter Glo Assay (Promega Corporation, Madison, WI, USA) was performed. Untreated cells, three times DXR-treated and five times DXR-treated cells were seeded in triplicates (3,000 cells/well), treated with 1 µM DXR for 72h and were analyzed subsequently using a luminometer (Berthold Technologies GmbH & Co. KG, Bad Wildbad, Germany), according to the manufacturer's protocol.

2.5.4 PROTEIN LYSIS

For protein lysis, cells were seeded at a density of 80%, washed three times with cold PBS and subsequently harvested using a protein lysis buffer containing 8 M urea and 400 mM ammonium bicarbonate. To improve cell lysis, ultrasound was used and samples were centrifuged through QIA-shredder devices (Qiagen GmbH, Hilden, Germany) at 2,800 x g for 1 min at room temperature. A total of 20 µg protein was used for subsequent reduction with 45 mM dithioerythritol (DTE) and for alkylation with 0.1 M iodoacetamide, both performed for 30 min at room temperature. Finally, samples were trypsinized at 37°C overnight using 400 ng porcine trypsin.

2.5.5 LIQUID-CHROMATOGRAPHY MASS SPECTROMETRY

LC-MS was performed by Dr. Thomas Fröhlich and Dr. Georg J. Arnold, Laboratory for Functional Genome Analysis (LAFUGA), Gene Center, LMU. Peptide separation and identification was performed on an EASY-nLC 1000 chromatography system (Thermo Fisher Scientific, Inc.) coupled to an Orbitrap XL instrument (Thermo Fisher Scientific, Inc.). A total of 2.5 µg peptides was diluted in 10 µl 0.1% formic acid and injected on a trap column (PepMap100 C18; 75 µm x2 cm; 3 µm particles; Thermo Fisher Scientific, Inc.).

Chromatography was performed at a flow rate of 200 nl/min at 40˚C (column, PepMap RSLC C18; 75 µm x50 cm; 2 µm particles; Thermo Fisher Scientific, Inc.) with a 260-min linear gradient of 5-25% solvent B (0.1% formic acid; 100% acetonitrile) and a subsequent 60-min gradient of 25-50 % solvent B.

MS spectra were acquired using a top five data dependent collision-induced dissociation method. Mass spectra were acquired in parallel mode performing the precursor mass scanning in the Orbitrap (60,000 full width at half maximum resolution at m/z 400; 300-2,000 m/z), and five data dependent collision-induced dissociation tandem MS scans (dynamic exclusion activated) in the LTQ ion trap at a collision energy of 35%.

2.5.6 BIOINFORMATICS

The mass spectrometry data were processed using MaxQuant 1.5.1.0 (Tyanova et al., 2015). To analyze the MS data, the Perseus module of the MaxQuant software was used (Tyanova et al., 2016). For the following investigations the label free quantification value of the identified proteins was used and proteins that were identified as potential contaminants or only identified by site were excluded. Subsequently, the values were transformed applying the logarithm to base 2.

For the multiscatter blot, the R0s of each MEA were compared with each other to identify the initial perturbation of protein expression at different passage numbers (5, 7 and 8) of MCF-7 cells. Therefore, two valid values in at least one MEA were required and the missing values were replaced from a normal distribution using the imputation feature of Perseus (width, 0.3; down-shift, 1.8). Subsequently, the median of each MEA was calculated and the R0s of the different MEAs were compared with each other applying a Pearson correlation analysis (Perseus module of the MaxQuant software). The same analysis was used to compare the different R3s and R5s.

A gene set enrichment analysis (GSEA) was performed to evaluate alterations in signaling pathways. All MEAs were grouped to investigate the overall abundance alterations in R3 and R5 compared with R0. Subsequently, each MEA was analyzed separately and the measurement replicates were grouped.

Only proteins that were identified twice in at least one group were further investigated. The missing values were replaced from a normal distribution. The resulting values were analyzed with gsea2-2.2.3 from the Broad Institute (Cambridge, MA, USA) (Mootha et al., 2003; Subramanian et al., 2005).

The gene set database gene ontology biological process (GO_BP) (Ashburner et al., 2000) was used, and as metric for ranking genes the t-test was chosen. The global enrichment score (ES) reflects the degree to which a defined set of genes is overrepresented at the top or the bottom of the entire ranked gene list, and it corresponds to a weighted Kolmogorov-Smirnov-like statistic.

Subsequently, the MEAs A, B and C were examined separately to evaluate the differentially expressed proteins. The three measurement replicates of R0, R3 and R5 were grouped and two valid values in at least one group were required for further investigation. The missing values were replaced applying the aforementioned imputation feature of Perseus to allow for statistical evaluation. In the present study, a two-tailed and paired Student's t-test with a false discovery rate of 0.05 was performed to compare R0 with R3 and R0 with R5 using the Perseus module of the MaxQuant software. To identify up- and downregulated proteins they were sorted according to their t-test difference, and values >0 were regarded as increased and <0 as decreased protein expression. Following this, Venn analysis was performed to determine the common regulated proteins in MEA A, B and C. Venny 2.1 was utilized (Oliveros, 2007-2015). Finally, the common regulated proteins were compared by Venn analysis to identify proteins which were up-or downregulated in R3 and R5 compared with R0 in all the MEAs.

For further analysis, only proteins with an abundance alteration of at least log2-fold were considered. The significance of the differential expression was evaluated also, and $P<0.05$ was considered to indicate a statistically significant difference. To identify the ten proteins with the highest increases or decreases in protein expression, the average of the relative expression values in R3 and R5 of MEA A, B and C was calculated and sorted by size. The proteins with the ten lowest and the ten highest overall relative expression values were listed in tables in the Supplements.

To identify the most important targets in resistance formation, MEA A, B and C were analyzed separately and all valid values were used for further evaluation. Those proteins that followed the criteria for validity in each MEA were further analyzed.

The measurement replicates of R0 were grouped (untreated) in addition to the measurement replicates of R3 and R5 (treated) and the means were compared with each other. The 15 proteins with the highest overall abundance alterations were selected. In order to evaluate the clinical relevance of these proteins, the Kaplan-Meier Plotter (Gyorffy et al., 2010) was used (release 2018/02/12). The relapse-free survival (RFS) in patients with luminal A breast cancer in the dataset GSE21653 was investigated.

2.6 SUPPLEMENTS

Supplementary figure 1 (S1): Global enrichment score histogram

A) R3 vs R0

MEA A

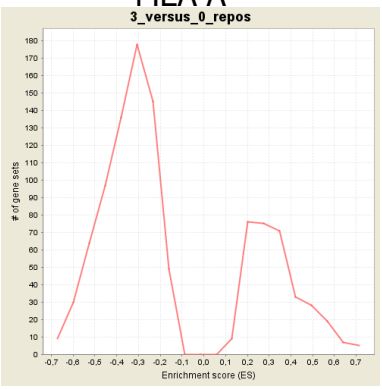

MEA B

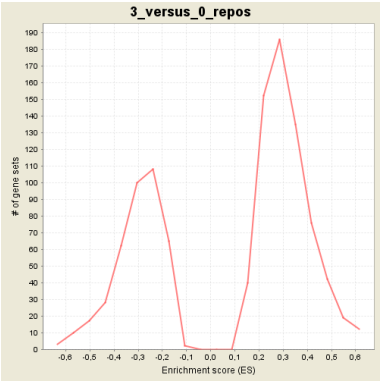

MEA C

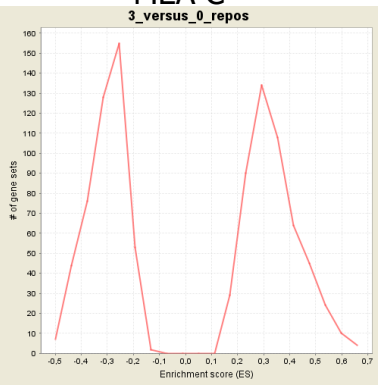

B) R5 vs R3

MEA A

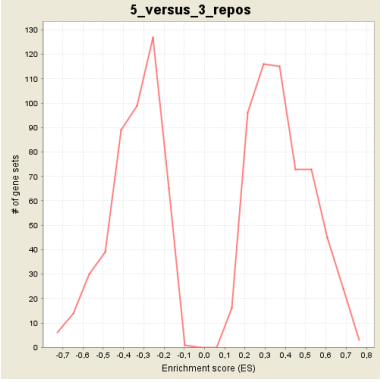

MEA B

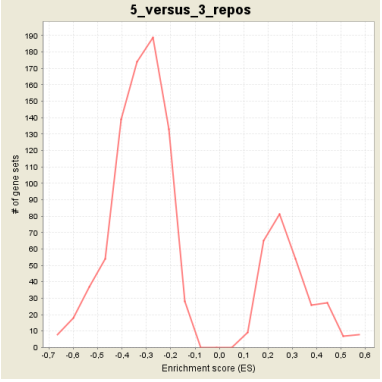

MEA C

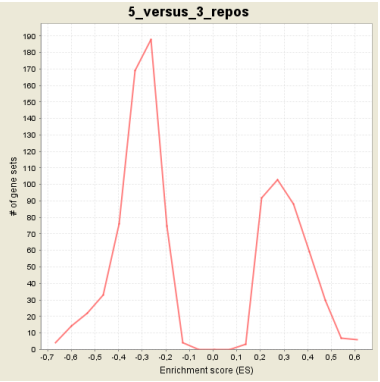

C) R5 vs R0

MEA A

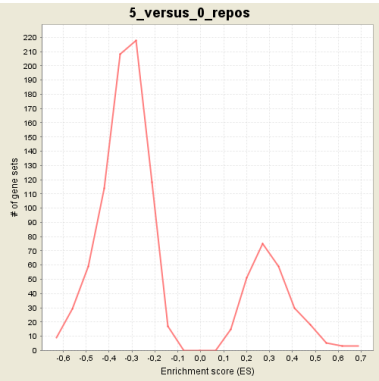

MEA B

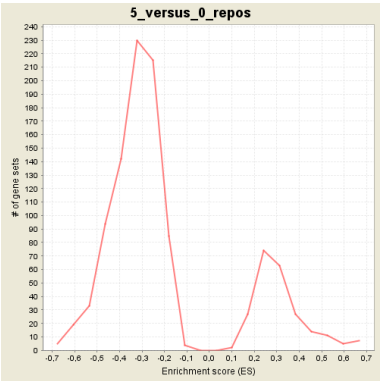

MEA C

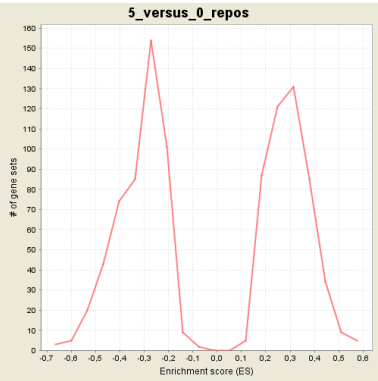

The global enrichment score histogram depicts the amount of up- (positive ES values) and down-regulated (negative ES values) gene sets.

Supplementary figure 2 (S2): Normalized enrichment scores of resistance related GO_BP pathways

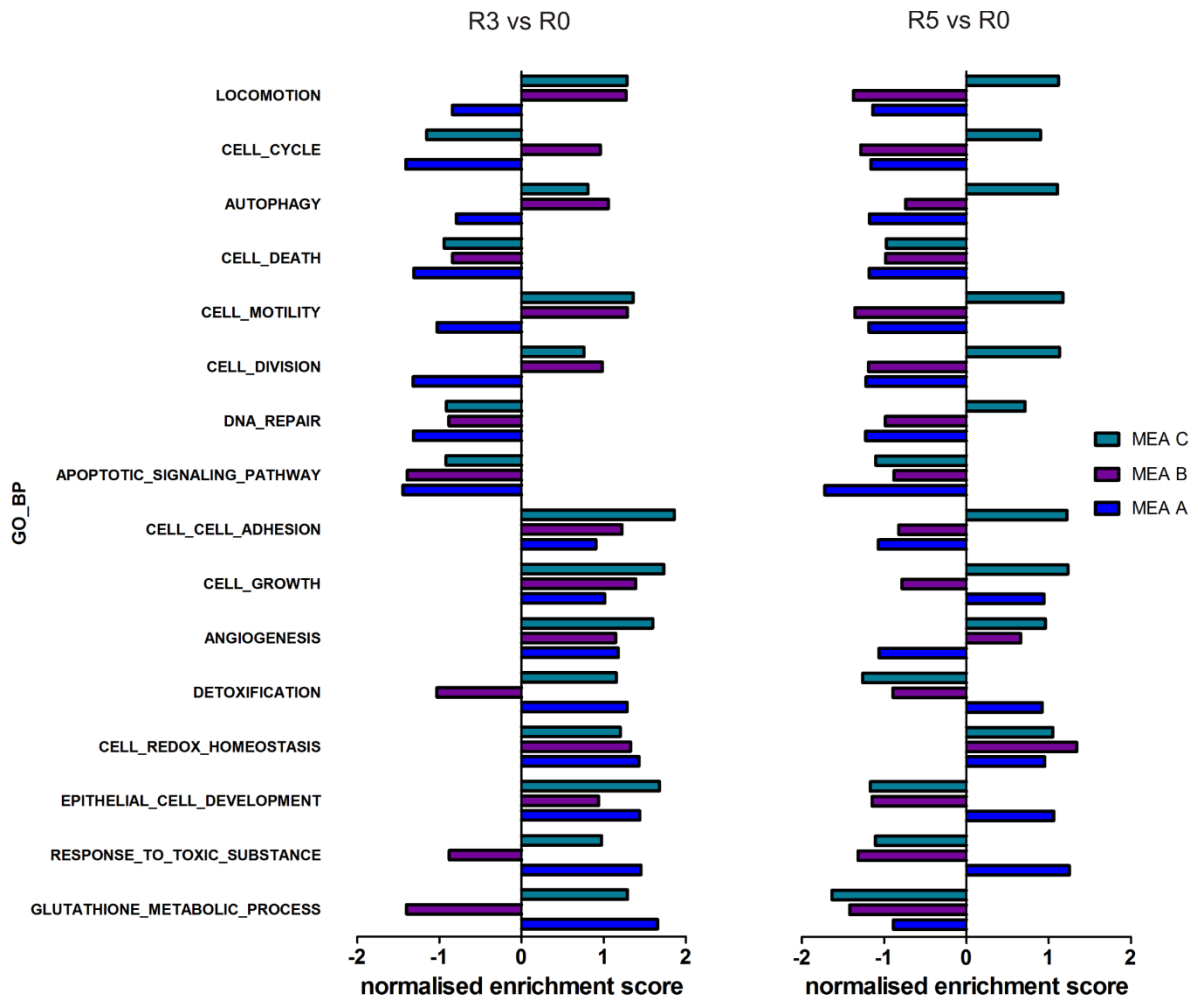

Gene set enrichment analysis of differentially expressed proteins. Resistance related Gene ontology biological processes (GO_BP) were selected and the normalized enrichment score is depicted to compare the different MEAs.

Supplementary table 1(ST1): Common down-regulated targets

down	MEA A				MEA B				MEA C			
Gene name	RE R3	p-value	RE R5	p-value	RE R3	p-value	RE R5	p-value	RE R3	p-value	RE R5	p-value
GFRA1	0,20	3,7E-05	0,12	4,5E-04	0,60	4,7E-03	0,11	8,1E-04	0,50	5,4E-02	0,19	9,8E-03
TAX1BP3	0,15	6,1E-04	0,11	8,7E-04	0,21	1,3E-04	0,31	1,6E-01	0,23	1,7E-01	0,91	2,5E-01
PRKAR1A	0,19	7,0E-04	0,31	4,5E-03	0,62	2,9E-02	0,17	1,5E-02	0,32	5,1E-03	0,42	2,2E-02
CNBP	0,25	3,7E-02	0,41	7,8E-02	0,45	3,2E-02	0,77	4,0E-01	0,30	2,8E-02	0,19	6,4E-02
AGR3	0,31	1,3E-03	0,27	2,4E-03	0,37	1,6E-03	0,13	5,6E-04	0,77	6,9E-01	0,66	5,4E-01
CA2	0,01	2,5E-05	0,01	7,7E-05	0,93	1,0E-02	0,01	2,7E-06	0,77	3,7E-01	0,77	6,6E-02
CMBL	0,49	5,6E-02	0,65	1,5E-03	0,47	5,7E-03	0,07	7,4E-05	0,48	6,0E-02	0,43	3,6E-02
NMD3	0,13	1,3E-04	0,44	1,2E-02	0,72	2,7E-03	0,25	4,7E-04	0,49	6,5E-02	0,57	1,1E-01
PNPO	0,43	2,1E-02	0,10	9,4E-05	0,77	2,3E-01	0,58	1,7E-01	0,25	6,2E-02	0,59	4,3E-04
TPD52L2	0,28	1,5E-03	0,23	1,6E-02	0,79	1,1E-02	0,93	3,6E-01	0,39	1,5E-01	0,36	2,6E-01
CLPB	0,34	4,0E-02	0,37	6,2E-02	0,86	4,7E-01	0,47	3,7E-02	0,57	2,6E-01	0,52	2,0E-01
PRPF6	0,30	9,6E-03	0,48	4,4E-02	0,62	4,1E-02	0,34	9,3E-04	0,76	3,1E-01	0,65	1,3E-01
STAU1	0,17	1,7E-05	0,23	7,4E-05	0,98	7,8E-01	0,32	1,0E-04	0,54	3,4E-03	0,93	3,6E-01
KYNU	0,07	3,6E-05	0,83	3,8E-01	0,54	3,4E-02	0,41	4,9E-03	0,74	2,1E-01	0,63	1,4E-02
HAT1	0,11	1,4E-05	0,50	5,3E-03	0,90	2,7E-01	0,20	4,3E-05	0,84	6,1E-01	0,67	2,9E-01
PHPT1	0,54	4,7E-02	0,30	1,2E-02	0,48	8,2E-03	0,81	4,5E-01	0,57	3,5E-01	0,54	1,2E-01
GBE1	0,41	4,4E-04	0,35	2,2E-02	0,91	7,3E-01	0,37	1,1E-02	0,74	3,0E-01	0,47	1,0E-01
RABGAP1	0,19	1,7E-02	0,63	1,0E-01	0,99	9,4E-01	0,41	1,8E-03	0,59	9,8E-03	0,47	2,1E-03
DTYMK	0,16	4,8E-03	0,38	1,8E-01	0,66	7,2E-02	0,79	1,3E-01	0,64	2,8E-02	0,66	1,2E-02
DYNLT3	0,77	6,7E-01	0,24	1,4E-02	0,81	3,2E-01	0,27	9,8E-04	0,71	6,1E-02	0,52	1,5E-01
SF3B5	0,23	5,7E-02	0,70	5,4E-01	0,58	1,6E-03	0,93	4,3E-01	0,58	3,2E-01	0,35	8,6E-02
ARPC1A	0,29	1,3E-03	0,38	1,1E-01	0,86	2,8E-02	0,35	9,5E-02	0,83	8,3E-01	0,70	6,7E-01
SULT2B1	0,30	8,7E-03	0,25	1,0E-02	0,97	8,8E-01	0,24	7,7E-03	0,99	9,8E-01	0,66	5,6E-01
ARPC5	0,68	3,7E-01	0,44	8,6E-03	0,73	6,0E-02	0,67	1,7E-02	0,53	1,5E-01	0,39	1,3E-01
DDX39A	0,18	1,6E-03	0,66	1,0E-02	0,88	2,2E-01	0,31	5,1E-02	0,62	6,5E-01	0,79	7,5E-01
BZW2	0,70	2,2E-03	0,28	1,5E-02	0,60	1,4E-01	0,52	9,3E-02	0,72	1,2E-01	0,65	2,7E-02
TPD52L1	0,63	3,8E-02	0,40	2,4E-03	0,48	1,3E-03	0,82	2,4E-01	0,47	5,8E-01	0,69	6,6E-01
SHMT1	0,30	4,3E-04	0,76	4,7E-01	0,84	2,1E-01	0,41	6,5E-04	0,57	2,0E-03	0,62	5,4E-02
CBX5	0,16	5,7E-05	0,70	1,0E-02	0,55	1,2E-02	0,82	8,2E-02	0,50	7,5E-02	0,80	1,6E-02
LRPAP1	0,59	1,1E-02	0,33	5,8E-04	0,77	9,1E-02	0,60	1,1E-03	0,72	4,8E-01	0,53	8,0E-02
SRSF2	0,26	1,1E-03	0,41	1,2E-03	0,76	6,7E-02	0,93	3,8E-01	0,46	3,3E-01	0,75	1,3E-01
ARFGAP1	0,34	1,1E-02	0,27	5,3E-02	0,85	2,0E-01	0,55	2,0E-01	0,75	5,8E-01	0,81	5,8E-01
FAM50A	0,19	1,7E-02	0,50	1,1E-02	0,68	4,1E-02	0,60	4,3E-03	0,86	2,3E-01	0,77	2,4E-02
RBM4	0,17	3,2E-03	0,37	1,8E-03	0,74	9,3E-02	0,55	8,1E-03	0,82	4,9E-01	0,94	6,5E-01
MAPT	0,58	2,9E-01	0,54	7,7E-03	0,44	8,0E-02	0,72	6,2E-01	0,69	3,2E-01	0,63	2,5E-01
DNAJC8	0,11	2,1E-03	0,33	3,5E-03	0,81	3,2E-01	0,92	7,5E-01	0,56	1,9E-01	0,90	6,9E-01
PPM1G	0,14	7,6E-03	0,57	3,1E-02	0,80	3,1E-03	0,45	1,6E-03	0,92	7,6E-01	0,78	8,5E-02
MAGED2	0,53	2,5E-01	0,78	2,2E-01	0,85	1,3E-01	0,14	1,8E-03	0,63	2,0E-01	0,77	1,7E-01
RMDN1	0,43	9,6E-04	0,28	3,2E-02	0,73	2,5E-02	0,58	3,1E-02	0,74	4,1E-01	0,94	6,0E-01
CACYBP	0,13	1,8E-05	0,40	2,6E-04	0,88	8,8E-02	0,53	1,3E-04	0,80	2,8E-01	0,95	8,1E-01
CBX1	0,22	9,9E-06	0,26	6,7E-05	0,69	4,2E-03	0,82	4,2E-01	0,91	6,1E-01	0,80	3,8E-02
DKFZp686A1765	0,17	1,8E-02	0,17	3,2E-06	0,84	1,6E-01	0,96	6,3E-01	0,87	6,3E-01	0,72	1,5E-01
PAFAH1B1	0,51	6,3E-02	0,62	2,2E-01	0,71	9,6E-03	0,50	5,7E-03	0,80	2,9E-01	0,58	9,6E-02
ADI1	0,55	2,9E-03	0,85	1,7E-02	0,62	4,4E-02	0,83	1,3E-02	0,54	3,0E-02	0,40	7,6E-02
ATOX1	0,69	7,0E-02	0,46	5,3E-03	0,55	1,8E-02	0,94	8,0E-01	0,78	7,3E-02	0,39	1,9E-01
EDF1	0,44	2,5E-02	0,31	1,1E-01	0,91	4,9E-01	0,81	8,3E-01	0,79	7,5E-01	0,60	5,4E-01
PRMT1	0,30	1,3E-05	0,60	5,7E-05	0,92	1,2E-01	0,52	8,1E-05	0,75	2,0E-01	0,78	8,0E-02
YWHAE	0,57	5,0E-03	0,50	4,9E-04	0,67	4,5E-03	0,54	4,3E-04	0,83	5,4E-01	0,76	2,3E-01
HNRNPH1	0,23	4,8E-05	0,66	3,0E-03	0,69	2,0E-02	0,70	3,7E-03	0,93	5,4E-01	0,66	1,9E-02
PIN1	0,79	1,9E-01	0,66	1,3E-01	0,79	1,6E-01	0,49	1,4E-01	0,57	4,9E-01	0,59	5,3E-01
PCNA	0,09	9,1E-04	0,92	5,4E-01	0,80	1,8E-01	0,59	2,3E-03	0,89	3,5E-01	0,61	5,4E-03
KNS2	0,44	4,1E-03	0,50	5,8E-02	0,96	6,7E-01	0,68	9,8E-03	0,48	1,6E-01	0,88	6,1E-01
RPA3	0,24	2,2E-02	0,68	4,2E-02	0,67	8,1E-02	0,55	1,7E-04	0,90	8,5E-01	0,91	7,6E-01
STMN1	0,08	3,7E-03	0,72	1,1E-02	0,79	6,0E-02	0,75	7,9E-03	0,90	3,4E-01	0,73	3,3E-03
SUCLA2	0,77	3,3E-02	0,58	2,5E-04	0,81	2,7E-02	0,66	1,7E-03	0,57	3,1E-01	0,60	2,9E-01
HRSP12	0,59	4,1E-03	0,47	6,0E-03	0,57	4,6E-03	0,84	1,2E-01	0,98	9,1E-01	0,55	2,6E-03
CBX3	0,24	4,5E-05	0,57	5,0E-04	0,85	8,0E-02	0,68	1,4E-03	0,90	7,2E-01	0,77	2,4E-01
TRMT112	0,10	4,3E-03	0,87	6,4E-01	0,83	9,1E-02	0,92	5,8E-01	0,49	3,4E-01	0,82	2,4E-01
GRB2	0,34	5,6E-04	0,42	2,3E-04	0,82	1,1E-01	0,80	1,3E-01	0,87	2,0E-01	0,81	4,5E-02
TSFM	0,57	1,8E-01	0,62	6,5E-03	0,86	4,2E-02	0,47	5,5E-04	0,86	6,9E-01	0,70	2,3E-01
RBM14	0,20	8,4E-03	0,80	1,5E-01	0,66	2,2E-02	0,79	1,8E-01	0,81	3,8E-01	0,81	1,4E-01
HGS	0,68	4,6E-01	0,67	4,0E-01	0,94	6,5E-01	0,64	3,1E-01	0,56	2,3E-01	0,61	3,9E-01
TACO1	0,40	3,7E-04	0,63	8,8E-03	0,89	1,1E-01	0,89	3,3E-01	0,77	1,9E-01	0,50	2,4E-02

NUMA1	0,14	1,2E-02	0,68	4,5E-05	0,83	4,5E-03	0,71	1,0E-03	0,82	4,0E-01	0,95	8,2E-01
PSMG1	0,50	1,4E-01	0,51	5,4E-02	0,85	4,0E-01	0,73	6,2E-02	0,97	9,2E-01	0,57	1,7E-01
TBCB	0,66	2,8E-02	0,47	2,2E-02	0,63	2,5E-02	0,83	1,2E-01	0,81	2,4E-01	0,73	1,2E-01
DDX19B	0,49	3,4E-03	0,77	1,1E-01	0,77	5,6E-02	0,72	1,0E-02	0,47	3,7E-01	0,91	6,8E-01
IDI1	0,71	1,0E-01	0,87	3,7E-01	0,88	3,1E-01	0,28	1,9E-04	0,86	6,1E-01	0,54	2,6E-02
SRP9	0,45	1,1E-04	0,71	1,8E-02	0,65	6,0E-04	0,85	5,7E-03	0,76	3,8E-01	0,76	1,4E-01
CPNE3	0,43	1,7E-05	0,67	5,2E-05	1,00	9,1E-01	0,27	2,0E-05	0,84	8,6E-02	0,97	5,1E-01
WDR5	0,23	4,8E-03	0,99	9,8E-01	0,92	6,6E-01	0,80	1,0E-01	0,40	2,3E-01	0,84	3,5E-01
GLOD4	0,63	1,1E-02	0,77	1,1E-02	0,83	9,9E-03	0,82	1,2E-01	0,70	5,5E-01	0,46	3,2E-01
CAPZB	0,66	1,7E-03	0,49	1,0E-03	0,82	3,4E-02	0,63	3,0E-04	0,79	4,4E-01	0,82	1,2E-01
DPM1	0,57	9,9E-03	0,61	1,0E-01	0,64	5,5E-02	0,59	5,2E-03	0,97	8,8E-01	0,84	4,2E-01
PAIP1	0,47	1,7E-02	0,40	5,9E-02	0,89	3,0E-01	0,92	2,0E-01	0,66	9,8E-02	0,88	2,6E-01
EIF3H	0,62	6,0E-02	0,56	3,2E-01	0,66	1,1E-02	0,79	3,3E-03	0,77	3,4E-01	0,84	2,7E-01
PIR	0,43	9,2E-02	0,49	1,3E-01	0,84	6,1E-01	0,87	6,2E-01	0,78	4,2E-01	0,83	5,7E-01
FH	0,48	8,9E-04	0,70	3,6E-04	0,68	6,6E-03	0,89	5,8E-02	0,89	6,3E-01	0,63	1,9E-02
RBBP7	0,36	4,8E-04	0,76	1,9E-02	0,91	2,6E-01	0,69	3,5E-02	0,84	4,5E-01	0,71	6,2E-02
PHF5A	0,47	1,2E-02	0,55	1,2E-01	0,71	8,8E-02	0,89	5,9E-01	0,82	7,7E-01	0,83	6,5E-01
GGCT	0,59	1,7E-02	0,51	2,8E-03	0,85	1,5E-02	0,92	1,1E-01	0,77	2,2E-02	0,65	2,4E-03
SLC9A3R1	0,61	2,0E-03	0,47	3,2E-04	0,91	1,1E-01	0,76	9,6E-03	0,83	2,4E-01	0,70	2,4E-03
GDI1	0,97	5,3E-01	0,44	6,7E-04	0,80	2,7E-03	0,39	1,3E-05	1,00	9,9E-01	0,70	3,4E-02
EIF3K	0,47	3,4E-03	0,94	5,7E-01	0,93	6,7E-01	0,71	3,0E-03	0,76	1,6E-01	0,51	2,9E-01
PRKRA	0,80	6,2E-01	0,93	8,7E-01	0,49	2,1E-01	0,75	6,3E-01	0,48	5,6E-02	0,89	4,4E-01
SMC1A	0,22	7,7E-02	0,94	4,5E-01	0,98	7,1E-01	0,76	3,1E-02	0,57	4,7E-01	0,92	3,5E-01
BLVRA	0,88	1,9E-01	0,62	1,5E-02	0,86	1,8E-01	0,50	2,1E-03	0,82	1,0E-01	0,69	2,6E-02
TOMM40	0,84	5,0E-01	0,70	3,7E-01	0,70	5,6E-01	0,47	1,0E-01	0,96	9,3E-01	0,72	6,5E-01
PPP2R5E	0,50	8,5E-02	0,83	3,6E-01	0,88	3,6E-01	0,52	2,8E-01	0,78	2,2E-01	0,90	6,1E-01
PSMB5	0,78	1,1E-01	0,94	5,3E-01	0,83	1,7E-01	0,76	1,5E-02	0,53	3,0E-01	0,58	1,7E-01
ADK	0,59	6,3E-02	0,60	1,3E-01	0,67	1,1E-01	0,83	2,5E-01	0,95	7,8E-01	0,80	1,3E-01
FKBP4	0,39	2,6E-05	0,64	2,7E-04	0,98	6,0E-01	0,65	1,7E-03	0,91	1,4E-01	0,87	8,3E-02
CTPS2	0,83	3,9E-01	0,78	3,9E-01	0,91	6,4E-01	0,47	8,1E-02	0,94	6,2E-01	0,53	2,0E-01
DCTPP1	0,40	2,2E-03	0,88	1,9E-01	0,74	1,3E-02	0,87	1,4E-01	0,89	7,3E-01	0,71	1,5E-01
PSMB1	0,48	3,8E-02	0,66	1,3E-02	0,84	1,1E-01	0,74	6,3E-03	0,95	8,3E-01	0,82	2,2E-01
C9orf78	0,46	2,0E-01	0,85	7,8E-01	0,64	2,4E-01	0,73	2,0E-01	0,85	5,6E-01	0,97	8,8E-01
PSMB7	0,68	1,4E-02	0,78	6,2E-02	0,57	9,3E-03	0,76	2,6E-01	0,88	4,0E-01	0,82	2,9E-01
PSMA1	0,55	1,1E-02	0,66	1,9E-03	0,85	1,8E-02	0,95	2,0E-01	0,78	4,9E-01	0,74	8,2E-02
WDR61	0,63	8,4E-04	0,90	4,6E-01	0,93	4,5E-01	0,62	2,7E-02	1,00	9,9E-01	0,51	3,7E-02
MYO6	0,99	9,5E-01	0,87	3,1E-01	0,73	5,8E-02	0,43	4,5E-04	0,93	1,1E-01	0,83	3,7E-02
CCT8	0,61	3,5E-03	1,00	8,9E-01	0,95	1,9E-01	0,67	1,3E-03	0,81	5,8E-02	0,74	1,2E-02
UBE2M	0,58	1,5E-03	0,74	8,6E-03	1,00	9,7E-01	0,67	2,3E-03	0,91	4,3E-01	0,99	9,1E-01
GDI2	0,78	3,5E-03	0,73	5,7E-04	0,85	8,8E-04	0,67	8,3E-05	0,87	3,2E-01	0,98	8,7E-01
MCTS1	0,69	2,4E-01	0,85	1,2E-01	1,00	9,9E-01	0,83	3,2E-01	0,65	2,1E-01	0,91	5,5E-01
ABCF1	0,65	1,6E-02	0,79	1,1E-01	0,95	3,0E-01	0,94	4,1E-01	0,78	2,6E-01	0,82	2,0E-01
SNX5	0,60	3,6E-02	0,86	7,3E-04	0,94	6,8E-01	0,98	9,1E-01	0,94	7,7E-01	0,64	2,5E-02
SRP72	0,63	3,1E-02	0,70	9,8E-02	1,00	1,0E+0	0,90	2,0E-01	0,89	7,0E-01	0,84	4,4E-01
TPT1	0,47	1,2E-03	0,79	1,1E-01	0,96	4,0E-01	0,93	2,6E-01	1,00	9,8E-01	0,82	1,8E-01
AP1M2	0,68	4,4E-01	0,96	8,6E-01	0,87	1,8E-01	0,90	2,7E-01	0,74	3,3E-02	0,83	1,1E-01
BUB3	0,52	1,5E-03	0,96	6,6E-01	0,90	2,6E-01	0,82	8,5E-03	0,90	6,1E-01	0,88	1,9E-01
CSK	0,95	6,9E-01	0,96	7,6E-01	0,96	6,9E-01	0,56	6,2E-03	0,69	3,4E-02	0,89	1,1E-01

Common down-regulated proteins. A student's t-test with a FDR of 0.05 was performed to compare R3 with R0 and R5 with R0. The relative expression (RE) was calculated according to the following equation: $2^{\text{t-test difference}}$. A p-value < 0.05 was considered significant.

Supplementary table 2 (ST2): Common up-regulated proteins

up	MEA A				MEA B				MEA C			
Gene name	RE R3	p-value	RE R5	p-value	RE R3	p-value	RE R5	p-value	RE R3	p-value	RE R5	p-value
SLC3A2	22,30	1,1E-05	26,11	6,2E-06	1,70	1,5E-01	10,27	2,5E-05	1,64	2,4E-02	1,22	1,6E-02
ASS	10,66	1,1E-04	4,95	4,5E-04	2,05	9,0E-04	20,60	1,3E-07	1,03	9,7E-01	6,47	1,3E-02
BCAS1	27,62	1,3E-06	2,56	4,4E-02	1,58	6,5E-02	4,57	2,2E-05	4,44	3,6E-02	2,05	1,4E-01
KTN1	26,14	3,0E-05	7,21	2,5E-04	3,36	5,4E-03	2,93	8,6E-02	1,16	8,0E-01	1,02	9,7E-01
TFF1	13,40	1,1E-02	1,95	2,6E-01	2,23	1,4E-01	7,41	1,4E-03	1,42	3,8E-01	4,52	1,6E-02
SLC7A5	5,80	2,0E-02	1,72	4,4E-01	2,03	1,2E-01	10,92	1,7E-03	1,55	9,6E-02	1,13	6,8E-01
S100P	3,86	6,4E-02	1,26	8,5E-01	3,96	9,1E-02	4,91	4,9E-02	2,38	1,1E-01	3,45	2,2E-02
ABHD11	4,45	9,7E-03	2,13	3,5E-02	1,11	5,8E-01	2,47	1,1E-03	1,85	1,6E-01	2,19	7,3E-02
LAD1	1,05	8,1E-01	1,90	1,1E-02	1,59	3,4E-02	6,02	5,7E-04	1,65	3,0E-01	1,65	4,1E-01
PLEC	5,12	1,3E-07	2,56	2,6E-05	1,46	1,7E-04	1,27	8,6E-03	1,70	1,5E-03	1,71	1,1E-03
CDK5	6,12	1,3E-02	2,34	8,0E-02	1,20	3,4E-01	1,18	5,3E-02	1,65	2,2E-01	1,04	8,6E-01
TSTA3	4,57	1,7E-04	1,37	2,5E-01	1,50	4,9E-02	2,58	3,1E-04	1,30	1,1E-01	1,44	8,3E-02
PKP3	1,34	1,2E-01	1,90	4,7E-02	1,44	4,6E-02	4,90	6,2E-04	1,92	2,8E-01	1,01	9,9E-01
LAMP1	4,44	7,4E-03	1,01	9,7E-01	2,25	2,1E-02	1,06	8,4E-01	1,23	5,6E-01	1,71	1,8E-01
ETHE1	3,67	7,9E-03	2,27	8,0E-03	1,52	3,7E-01	2,15	1,4E-01	1,03	9,2E-01	1,01	9,9E-01
TXNRD1	2,08	3,0E-03	1,63	9,5E-03	2,14	1,6E-03	3,06	1,3E-03	1,16	5,8E-01	1,57	8,0E-02
ANXA11	2,40	6,1E-05	2,67	4,1E-04	1,26	3,2E-03	1,43	1,9E-03	1,65	1,8E-02	1,85	2,3E-04
CNN2	4,50	1,0E-02	2,10	5,6E-02	1,05	9,1E-01	1,33	5,2E-01	1,20	7,2E-01	1,02	9,6E-01
EIF4A2	3,56	9,4E-02	1,07	8,4E-01	1,44	3,3E-01	2,16	3,6E-01	1,74	1,9E-01	1,09	7,8E-01
ABAT	1,56	6,7E-02	1,51	3,2E-02	2,17	1,9E-02	1,93	7,5E-04	1,69	5,5E-02	2,00	1,4E-02
SEC31A	2,81	5,4E-04	1,67	3,6E-03	1,46	1,1E-03	1,07	3,6E-01	1,09	6,8E-01	2,14	1,9E-04
APEH	2,68	7,5E-05	1,93	1,8E-03	1,32	6,0E-03	1,08	4,0E-01	1,32	1,7E-01	1,65	3,6E-02
NAMPT	1,93	1,1E-02	2,24	4,4E-03	1,13	1,6E-01	2,22	3,9E-03	1,16	5,9E-01	1,22	2,8E-01
TRMT10C	1,21	1,6E-01	2,23	1,9E-04	1,57	1,4E-02	1,70	1,6E-04	1,14	8,5E-01	1,78	3,0E-01
ITGB1	2,91	3,2E-03	1,31	2,0E-01	1,64	4,0E-02	1,27	6,8E-01	1,01	9,6E-01	1,47	1,5E-01
C9orf142	1,27	4,5E-01	1,01	9,7E-01	1,48	1,8E-01	1,15	8,1E-01	1,95	7,7E-02	2,59	6,0E-03
PDIA3	2,42	1,5E-05	1,15	1,0E-02	1,04	6,4E-01	2,05	5,1E-04	1,36	9,7E-02	1,41	4,7E-02
LDHA	3,11	3,3E-04	0,97	7,4E-01	1,21	7,6E-02	1,41	2,3E-03	1,16	4,6E-01	1,52	1,4E-01
CDC42	1,23	5,9E-01	1,55	1,9E-02	2,77	1,4E-01	1,46	5,4E-01	1,14	8,0E-01	1,12	8,3E-01
ERO1L	3,06	1,4E-04	1,11	1,1E-01	1,23	3,6E-02	1,22	3,2E-02	1,30	1,8E-01	1,32	1,5E-01
MDH2	2,32	2,4E-04	1,65	2,0E-03	1,02	6,3E-01	1,56	1,1E-03	1,27	2,5E-01	1,16	3,9E-01
TXNDC5	2,14	1,6E-03	1,42	3,0E-03	1,58	6,7E-05	1,36	1,1E-01	1,29	6,6E-02	1,15	5,9E-01
CAT	1,80	2,0E-02	1,72	2,1E-03	1,37	3,3E-02	1,52	4,6E-02	1,49	5,5E-02	1,02	8,4E-01
EPS8L2	1,78	1,7E-02	1,25	3,1E-01	1,78	7,7E-03	1,24	1,6E-01	1,35	2,0E-01	1,32	3,6E-01
HPRT1	1,42	4,9E-02	1,97	3,0E-03	1,02	8,0E-01	2,00	2,4E-04	1,11	6,1E-01	1,14	3,9E-01
GANAB	2,36	2,9E-04	1,49	1,4E-02	1,08	1,6E-01	1,24	1,2E-02	1,05	7,9E-01	1,23	2,0E-01
PES1	1,10	8,6E-01	1,48	4,8E-01	1,13	7,0E-01	1,53	2,4E-01	1,60	4,3E-01	1,42	5,7E-01
UQCRC1	1,74	1,3E-03	1,26	4,1E-02	1,40	1,8E-03	1,02	7,4E-01	1,36	1,5E-01	1,37	1,8E-02
PDIA6	1,77	2,1E-03	1,05	6,4E-01	1,05	6,8E-01	1,59	1,2E-02	1,19	6,0E-01	1,13	7,0E-01
VPS35	1,37	1,3E-02	1,52	1,2E-03	1,29	3,8E-02	1,04	5,9E-01	1,46	1,2E-02	1,05	4,9E-01
VARS	1,22	3,5E-01	1,63	7,9E-03	1,10	2,0E-01	1,26	1,8E-02	1,02	7,8E-01	1,43	5,6E-03
UQCRC2	1,73	1,2E-03	1,08	4,9E-01	1,21	4,3E-03	1,13	5,2E-03	1,02	9,2E-01	1,23	1,4E-02

Common up-regulated proteins. A student's t-test with a FDR of 0.05 was performed to compare R3 with R0 and R5 with R0. The relative expression (RE) was calculated according to the following equation: $2^{\text{t-test difference}}$. A p-value < 0.05 was considered significant.

Supplementary table 3 (ST3): Potential common drivers of chemoresistance

Down	relative expression	SD	Biological process
NMD3	0.43	0.20	RNA biosynthesis
STAU1	0.48	0.25	cellular response to oxidative stress
PRPF6	0.54	0.17	RNA splicing
UGDH	0.55	0.40	metabolism
TMSB4X	0.57	0.24	TNF-signaling, chemotaxis. actin filament organization
RBM4	0.57	0.19	cell differentiation, RNA splicing
BZW2	0.58	0.19	cell differentiation
PHPT1	0.59	0.24	cell motility, actin filament organization
ISOC1	0.59	0.33	metabolism
LRPAP1	0.59	0.15	receptor mediated endocytosis
SHMT1	0.60	0.21	folic acid metabolic process
CBX5	0.61	0.30	transcription
PARP1	0.61	0.21	DNA repair, cellular response to oxidative stress
CSE1L	0.63	0.35	apoptosis, cell proliferation
PCNA	0.65	0.28	cell proliferation, cell differentiation. cell cycle

Up	relative expression	SD	Biological process
SLC3A2	12.72	14.36	cell growth, metabolism. glucose transport
ASS	8.83	9.21	metabolism
PHGDH	3.82	4.85	metabolism, G1 to G0 transition
PPL	2.71	1.44	cytoskeleton organization
PCK2	2.48	1.60	metabolism, cellular response to TNF
ABHD11	2.38	1.25	hydrolase
PLEC	2.23	1.13	RNA binding
TSTA3	2.17	1.18	metabolism, oxidation reduction process
TXNRD1	1.84	0.63	cell redox homeostasis
ANXA11	1.79	0.18	cell cycle, cell division
ABAT	1.79	0.17	cellular response to drug
TFRC	1.91	1.32	cellular response to drug
RAB7A	1.80	0.73	endocytosis
APEH	1.60	0.31	proteolysis
SEC31A	1.61	0.40	protein transport

Treated cells (R3 and R5) were compared with untreated cells (R0) and the relative expression values normalized to R0 are depicted as mean and SD of all MEAs.

3. GRK5 REGULATES BREAST CANCER CELL MIGRATION

This chapter was directly adapted from the original publication, which was finally published as Sommer et al., Scientific Reports, 2019; *9*, 15548. Sections may have been moved for consistency.

(Sommer et al., 2019)

Downregulation of GRK5 hampers the migration of breast cancer cells

Ann-Katrin Sommer[1], Mathias Falcenberg[2], Bojan Ljepoja[1], Thomas Fröhlich[3], Georg J. Arnold[3], Ernst Wagner[1], and Andreas Roidl[1]

[1] Pharmaceutical Biotechnology, Department of Pharmacy, Ludwig-Maximilians-Universität, München, D-81377 Munich, Germany

[2] Department of Molecular Biology, Max-Planck-Institute of Biochemistry, D-82152 Planegg, Germany

[3] Laboratory for Functional Genome Analysis (LAFUGA), Gene Center, Ludwig-Maximilians-Universität München, D-81377 Munich, Germany

Contribution

Conceptualization: AR and AS; Methodology: AS and AR; Data Curation: AS; Investigation: AS; Writing-Original Draft Preparation: AS and AR; Writing-Review & Editing: BL, MF, TF, GJA and EW; Supervision: AR, MF and EW; Cell line generation: BL; Proteomics measurement: TF and GJA

3.1 ABSTRACT

Sunitinib is a multispecific kinase inhibitor and one of its targets is the kinase GRK5, which is regulating a multitude of G protein-coupled receptors (GPCRs). In this study we demonstrate that a decreased GRK5 expression induced by knock-down experiments or sunitinib treatment hampers the migration of cancer cell lines. A proteomic analysis revealed many pathways related to cell migration which were down regulated upon the GRK5 knock-down. Furthermore, we found in MDA-MB-231 breast cancer cells that the inhibition of migration is mediated by the GPCR gastrin releasing peptide receptor (GRPR) leading to a reduced expression of migration regulating downstream targets like CDC42 and ROCK1. An *in-silico* Kaplan Meier analysis revealed that GRK5 and GRPR overexpression reduces the distant metastasis free survival in triple-negative breast cancer (TNBC) patients. Thus, we suggest a novel anti-migratory effect of impaired GRK5 expression which induces a negative feedback loop on GRPR signaling.

3.2 INTRODUCTION

G protein-coupled receptors (GPCRs) are the largest group of cell surface receptors in humans and comprise of more than 800 members (Pierce et al., 2002). They are also known as seven-transmembrane receptors and are involved in many physiological processes like neurotransmission, metabolism, immune response, regulation of blood pressure and cardiac activity (Dorsam and Gutkind, 2007). Therefore, a tight regulation of these signaling cascades is of great importance to avoid disease formation.

One regulatory protein class are the AGC kinases to which the G protein-coupled receptor kinase (GRK) family belongs. These seven serine-threonine kinases can be categorized according to their structural properties into three subgroups: the visual subfamily (GRK1, GRK7), the GRK2 subfamily (GRK2, GRK3) and the GRK4 subfamily (GRK4, GRK5, and GRK6) (Premont et al., 1995; Siderovski et al., 1996). In general, all GRKs regulate the GPCR signaling by phosphorylating agonist-activated GPCRs in the third cytoplasmic loop and/or the C-terminal tail.

This leads to the recruitment of β-arrestins and subsequently to the uncoupling of the G proteins. This process is termed GPCR desensitization (Gurevich et al., 2012; Komolov and Benovic, 2018). β-arrestins are also known to function as scaffold proteins that facilitate the internalization of GPCRs thus resulting in the recycling or lysosomal degradation of the receptor (Shenoy and Lefkowitz, 2011). Due to the fact that the seven GRKs regulate more than 800 GPCRs it is obvious that GRKs affect the signal transduction of complex signaling cascades which comprise of more than one GPCR. Therefore, aberrant expression of these kinases leads to malfunction of several GPCRs and consequently to diseases like diabetes, hypertension, cardiac dysfunction, Alzheimer's disease and cancer (Gurevich et al., 2012; Pierce et al., 2002). Tumorigenesis was shown to be influenced mainly by GRK2 and GRK5 (Gambardella et al., 2016; Nogues et al., 2018; Yu et al., 2018). These kinases often function as oncogenes in glioblastoma (Kaur et al., 2013), prostate (Chakraborty et al., 2014; Gambardella et al., 2016), pancreas (Buchholz et al., 2015), non-small-cell lung (Jiang et al., 2018) and breast cancer (Nogues et al., 2016).

According to the Human Protein Atlas, 50% of the analyzed breast cancer patients possessed elevated GRK2 or GRK5 expression (Uhlen et al., 2005; Uhlen et al., 2017), whereas the latter was shown to result in even worse prognosis concerning the 5-years survival rate. Nevertheless, the role of GRK5 in breast cancer has not been studied and the mechanism of action remains rather unclear. Breast cancer affects one of eight women during their lifetime and is estimated to be the second leading cause of cancer deaths in women in the United States in 2018 (American Cancer Society, 2018). Therefore, it is of great importance to identify novel predictive biomarkers and druggable targets associated with this disease.

Therefore, the aim of this study was to elucidate the function of GRK5 in breast cancer and investigate whether the targeting of GRK5 could have a beneficial effect on cancer treatment. Sunitinib is the most potent, approved small-molecule inhibitor (SMI) targeting GRK5 (Anastassiadis et al., 2011; Gao et al., 2013). Since 2006 sunitinib is approved by the FDA for the treatment of gastrointestinal stromal tumors, which are refractory or intolerant to imatinib treatment, and for advanced, metastatic renal cell carcinoma (mRCC) (Goodman et al., 2007; Rock et al., 2007).

This multispecific kinase inhibitor was shown to mainly inhibit the receptor tyrosine kinases (RTKs) vascular endothelial growth factor receptor (VEGFR) and platelet derived growth factor receptor (PDGFR) (Polyzos, 2008) thereby blocking the angiogenesis of tumors. Thus, we additionally investigated the effect of sunitinib on GRK5 and breast cancer cells *in vitro*.

3.3 RESULTS

3.3.1 ANALYSIS OF DIFFERENT BREAST CANCER CELL LINES REVEALS INCREASED GRK5 EXPRESSION IN MESENCHYMAL CELLS

To evaluate the expression level of GRK5 in breast cancer, a qPCR analysis was performed. The cell lines were grouped according to their morphology. Spindle-like cell lines were regarded as mesenchymal (MDA-MB-415, BT-549, MDA-MB-435s, HS-578T, MDA-MB-231) and cobblestone-like growing cells were considered as epithelial cells (MCF-7, BT-474, ZR-75, SKBR-3, MDA-MB-361).

We observed that GRK5 is significantly higher expressed in mesenchymal-like breast cancer cells and that MDA-MB-231 cells, a metastatic, triple-negative breast cancer cell line, showed the highest GRK5 expression level of all analyzed cell lines (Fig. 8A). A similar expression pattern was observed by western blot analysis in an additional panel of cancer cell lines (Supplementary Fig. S3). Therefore, MDA-MB-231 was chosen as model for further experiments. The expression levels of the other GRK4-family members, GRK4 and GRK6, were analyzed in MDA-MB-231 cells. Here, GRK6 is equally highly expressed as GRK5, whereas GRK4 shows a very low expression level (Fig. 8B).

3.3.2 *CHARACTERIZATION OF AN INDUCIBLE SHGRK5 KNOCKDOWN IN MDA-MB-231 ELUCIDATES THE IMPACT OF GRK5 ON CELL VIABILITY, APOPTOSIS, MIGRATION AND INVASION IN BREAST CANCER*

In order to further investigate the function of GRK5 in triple-negative breast cancer (TNBC), MDA-MB-231 cells stably expressing a doxycycline inducible shGRK5 were generated (termed MDA-MB-231 TRIPZ-shGRK5 in the following). As a gene coding for RFP is localized downstream of the doxycycline (DOX) inducible promotor, a fluorescence signal indicates shGRK5 expression upon DOX induction (Fig. 8C). Subsequently, we investigated the mRNA expression level of GRK5 in MDA-MB-231 TRIPZ-shGRK5 and MDA-MB-231 wild-type (wt) cells 72 h after inducing with DOX to determine the knockdown (KD) efficiency (Fig. 8C).

Moreover, possible compensatory effects of GRK4-family members were investigated in a time-dependent manner after DOX treatment and could be excluded as the mRNA expression levels of GRK4 and GRK6 remain similar after the GRK5 KD (Fig. 8D).

To elucidate the physiological impact of GRK5 KD in TNBC development and progression, cell viability and apoptosis induction were measured 90 h after DOX stimulation in MDA-MB-231 TRIPZ-shGRK5 cells. We observed that the GRK5 KD neither reduces the cell viability nor increases the apoptosis rate (Supplementary Fig. S4).

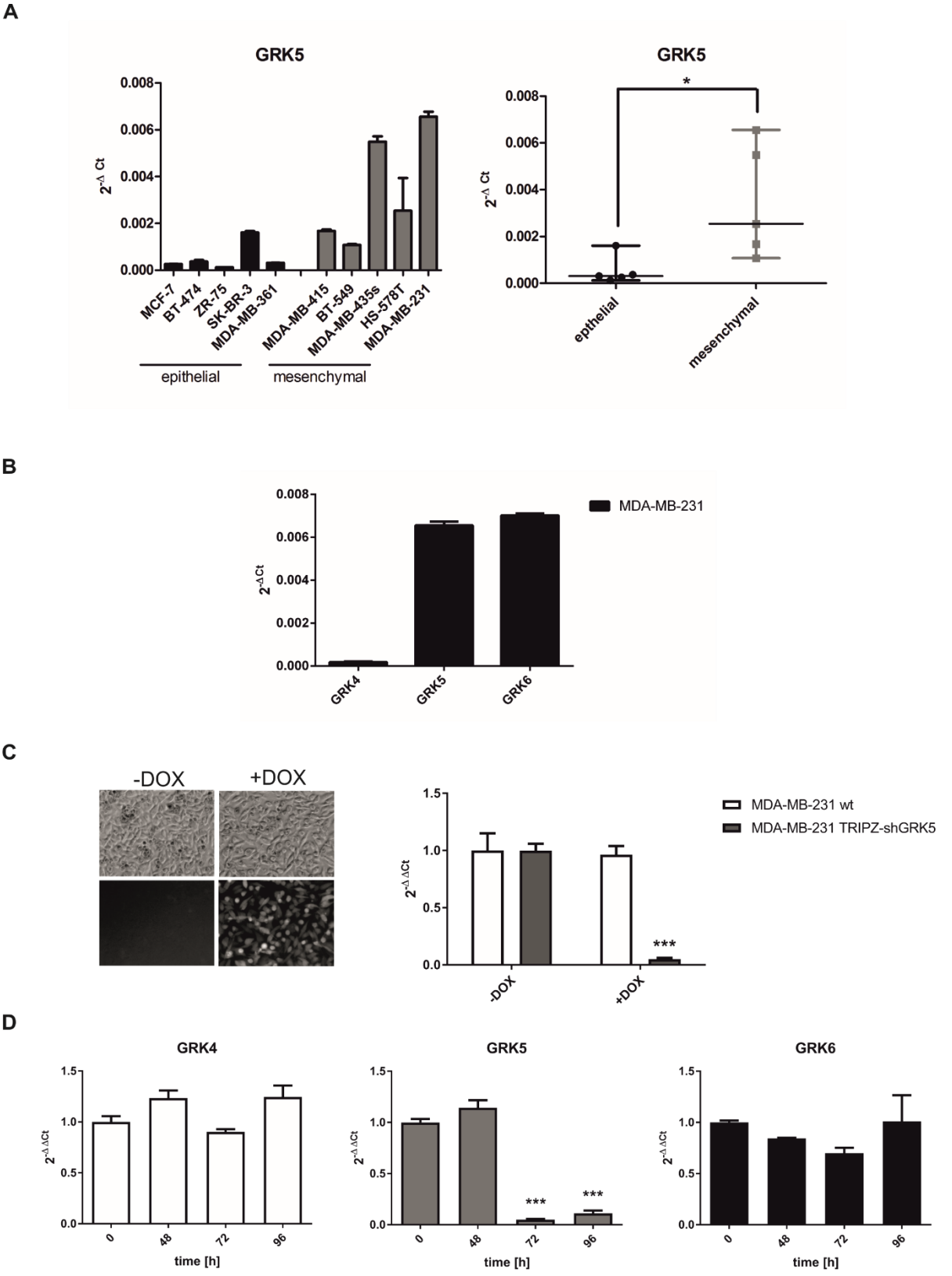

Figure 8. Expression analysis of GRK5 and characterization of MDA-MB-231 TRIPZ-shGRK5 which were generated by Dr. Bojan Ljepoja. (A) Expression analysis of GRK5 in different breast cancer cell lines utilizing qPCR. The values are depicted as mean + SD in the left panel and as median + range in the right panel. Student's t-test was used for statistical evaluation. (B) Expression analysis of GRK4 family members in MDA-MB-231 wild-type cells.

(C) Characterization of MDA-MB-231 TRIPZ-shGRK5. GRK5 expression analysis and fluorescence microscopy pictures upon induction with 5 µg/ml doxycycline for 72 h. This cell line was generated by Bojan Ljepoja. (D) Expression analysis of GRK4 family members at the indicated time points upon induction with 5 µg/ml doxycycline. N = 3, * $p < 0.05$, ** $p < 0.01$, *** $p < 0.001$

3.3.3 PROTEOMIC ANALYSIS AND BOYDEN CHAMBER EXPERIMENTS REVEAL IMPACT OF GRK5 ON CANCER CELL MIGRATION

To investigate whether GRK5 influences breast cancer development and progression in general, a proteomics approach utilizing LC-MS was performed. Therefore, MDA-MB-231 TRIPZ-shGRK5 were seeded in quintuples, twice induced with doxycycline and harvested after 90 h (Fig. 9A). The subsequent proteomic analysis revealed 2220 proteins that were identified at least three times in induced and not-induced samples. The following gene set enrichment analysis (GSEA) utilizing Gene Ontology Biological Process (GO_BP) elucidated up and down regulated signaling pathways upon GRK5 KD. By clustering the resulting pathways in signaling cascades important for tumorigenesis it was observed that a decrease in GRK5 expression primarily leads to a down regulation of cell motility pathways (Fig. 9B).

To validate the effect of GRK5 on cancer cell migration, boyden chamber experiments with and without matrigel coating were performed. Thereby, we showed that GRK5 KD significantly hampers both migration and invasion in TNBC cells (Fig. 9C and D). Additionally, a KD by a pool of GRK5 siRNAs was performed in another breast cancer (HS-578T) and two prostate cancer cell lines (DU-145, PC-3) (Fig. 9E) and its effect on cancer cell migration was confirmed (Fig. 9F).

A

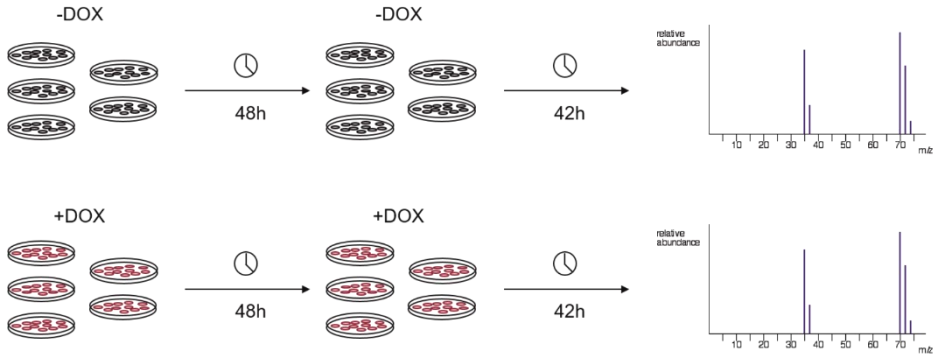
-DOX
48h
-DOX
42h
relative abundance
m/z
+DOX
48h
+DOX
42h
relative abundance
m/z

B

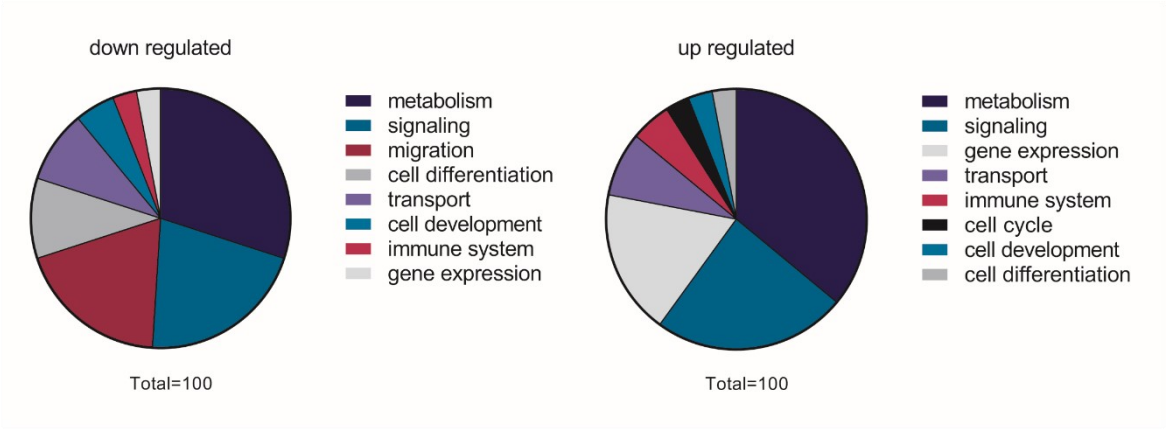
down regulated
metabolism
signaling
migration
cell differentiation
transport
cell development
immune system
gene expression
Total=100
up regulated
metabolism
signaling
gene expression
transport
immune system
cell cycle
cell development
cell differentiation
Total=100

C

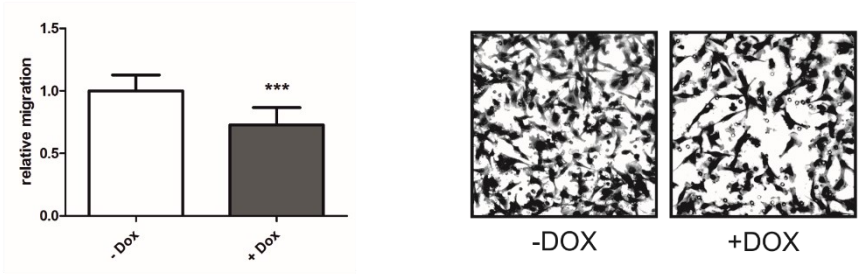
relative migration
1.5
1.0
0.5
0.0
***
- Dox
+ Dox
-DOX
+DOX

D

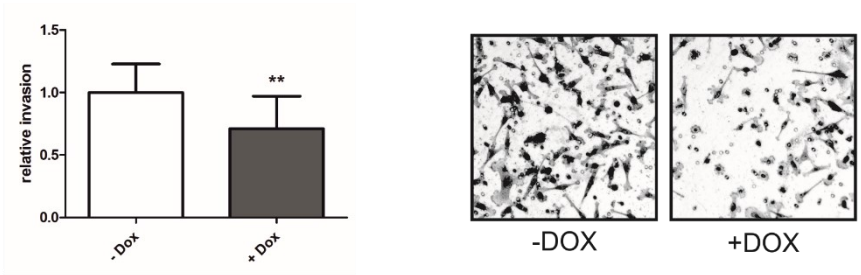
relative invasion
1.5
1.0
0.5
0.0
**
- Dox
+ Dox
-DOX
+DOX

E

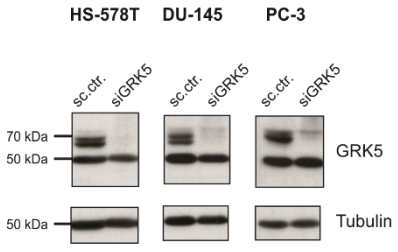
HS-578T
DU-145
PC-3
sc.ctr.
siGRK5
70 kDa
50 kDa
GRK5
50 kDa
Tubulin

F

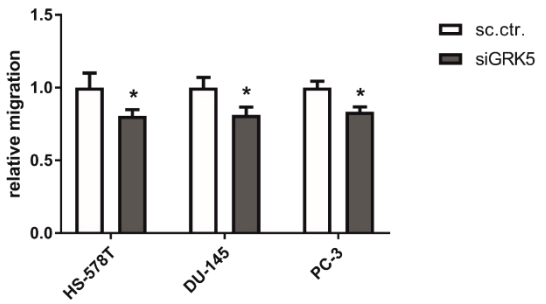
relative migration
1.5
1.0
0.5
0.0
*
HS-578T
DU-145
PC-3
sc.ctr.
siGRK5

Figure 9. Proteomics, migration and invasion analysis of MDA-MB-231 TRIPZ-shGRK5. (A) Scheme of proteomics analysis. Cells were seeded in quintuples and stimulated with 5 µg/ml doxycycline or control every 48 h for 90 h. Subsequently a proteomic analysis utilizing LC-MS was performed by Dr. Thomas Fröhlich and Dr. Georg J. Arnold, Laboratory for Functional Genome Analysis (LAFUGA), Gene Center, LMU. (B) Overview of up and down regulated pathways revealed by GSEA. Gene ontology biological process was utilized as dataset. (C) Migration analysis of MDA-MB-231 TRIPZ-shGRK5 90 h upon stimulation with doxycycline or control using a boyden chamber migration assay. Representative pictures are shown. (D) Invasion analysis utilizing matrigel coated boyden chambers 90 h after stimulation 5 µg/ml doxycycline or control. (E) Western blot analysis of HS-578T, DU-145 and PC-3 72h upon siGRK5 KD. The presented blots were cropped (F) Migration analysis of HS-578T, DU-145 and PC-3 90 h upon transfection with sc.ctr. or siGRK5. Relative migration or invasion is shown as mean + SD normalized to not induced or sc.ctr. transfected samples (N = 3). A two-tailed Student's t-test was performed. * $p < 0.05$, ** $p < 0.01$, *** $p < 0.001$

3.3.4 GRK5 KD HAMPERS CHEMOTAXIS OF MDA-MB-231 CELLS TOWARDS BOMBESIN

To identify the underlying signaling pathways, different chemoattractants were analyzed in a boyden chamber experiment with respect to their pro-migratory activity on MDA-MB-231 cells. Moreover, it was investigated whether this effect can be blocked or reduced by a siGRK5 KD. We demonstrate that only bombesin, bradykinin and insulin increased the migratory behavior of MDA-MB-231 cells, which can be significantly decreased by a GRK5 KD in the case of bradykinin and bombesin (Fig. 10A and B). As bombesin shows the most significant change in migratory behavior this ligand was analyzed further.

The impact of bombesin on the migration of TNBC cells was also examined in MDA-MB-231 TRIPZ-shGRK5 cells to exclude transfection artefacts, as transfection agents could influence cancer cell migration. Here, the chemotactic effect of bombesin was also reduced by shGRK5 (Fig. 10C). Furthermore, the influence of GRK5 and bombesin on the invasiveness of MDA-MB-231 TRIPZ-shGRK5 cells was investigated. As depicted in Fig. 10D, a reduction of GRK5 expression leads to a decreased invasion of TNBC cells towards a bombesin gradient.

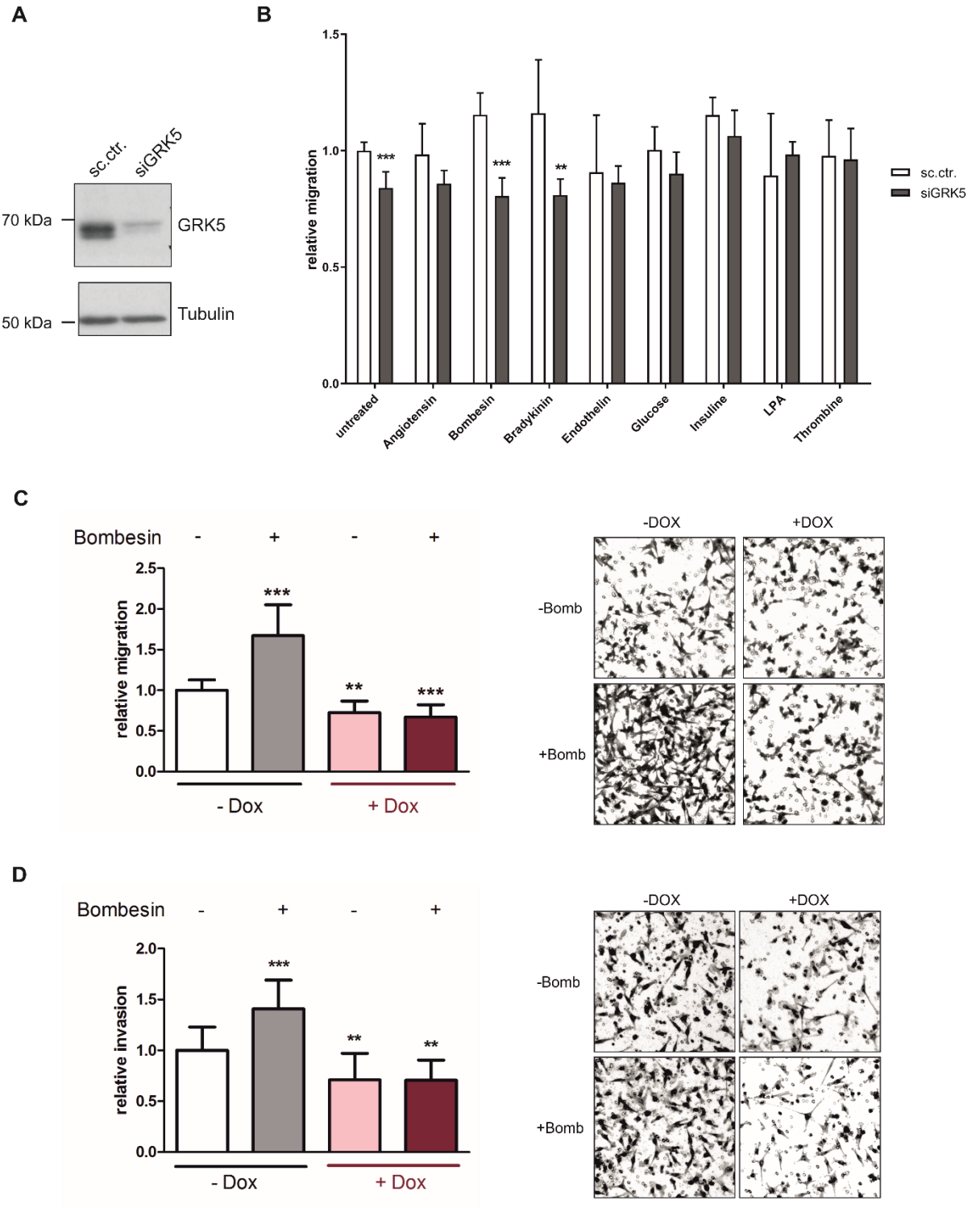

Figure 10. Evaluation of chemoattractants with regard to their migration stimulating capabilities in MDA-MB-231 cells and the blockage thereof by GRK5 KD. (A) Western blot analysis of MDA-MB-231 72h upon siGRK5 KD. The presented blots were cropped. (B) Screening of different chemoattractants. The indicated ligands were added in the lower well at the following concentrations: Angiotensin 100 nM, Bombesin 200 nM, Bradykinin 5 µM, Endothelin 100 nM, Glucose 4.5 g/ml, Insulin 10 µg/ml, LPA 10µM. Relative migration values are depicted as mean + SD and are normalized to untreated, sc.ctr. transfected cells (N = 3). (C) Analysis of migratory behavior of MDA-MB-231 TRIPZ-shGRK5 cells 90 h upon induction with 5 µg/ml doxycycline or control with or without stimulation with 200 nM bombesin. Cells were stained with crystal violet and representative pictures are shown (N = 3).

(D) Invasion analysis of MDA-MB-231 TRIPZ-shGRK5 90 h upon induction with 5 µg/ml doxycycline or control with or without stimulation with 200 nM bombesin. Cells were stained with crystal violet and representative pictures are shown. Values are depicted as mean + SD and are normalized to not induced, not stimulated samples (N = 3). One-way ANOVA with Dunnett's Multiple Comparison Test and multiple t-tests utilizing two-stage linear step-up procedure of Benjamini, Krieger and Yekutieli was used for statistical analysis. * $p < 0.05$, ** $p < 0.01$, *** $p < 0.001$

3.3.5 REDUCTION IN GRPR EXPRESSION BY GRK5 KD DECREASES CHEMOTAXIS OF MDA-MB-231 TOWARDS BOMBESIN

The gastrin releasing peptide receptor (GRPR) is the cellular receptor of bombesin and therefore, its expression levels were analyzed in different breast cancer cells to confirm its impact on migration. Fig. 11A shows that GRPR is significantly higher expressed in mesenchymal-like breast cancer cells. Subsequently, the influence of the GRK5 KD on the GRPR signaling pathway was investigated. Here, we observed that the autocrine activation loop of the GRPR signaling is hampered upon GRK5 KD since the mRNA level of GRPR as well as that of its natural ligand GRP was reduced (Fig. 11B). A GRPR KD on the other hand had no impact on the GRK5 expression (Supplementary Fig. S5). Next, the impact of GRPR on cell migration of TNBC was examined. We detected that GRPR KD reduces the migratory behavior of MDA-MB-231 to a similar extent as a GRK5 KD (Fig. 11C). In order to determine whether GRPR is the only GPCR that is regulated by GRK5 and thus is responsible for the reduced chemotaxis towards bombesin, cells were transfected with both siGRK5 and siGRPR. As depicted in Fig. 4D this double-KD is not further reducing the migration of MDA-MB-231 cells indicating that GRPR is the main player in the chemotactic process which is regulated by GRK5.

By comparing the measured migration data, we observed a constant reduction in the migratory behavior of 25-30 % upon GRK5 KD, GRPR KD and the double KD of GRK5 and GRPR emphasizing the key role of GRPR in GRK5 mediated migration.

A

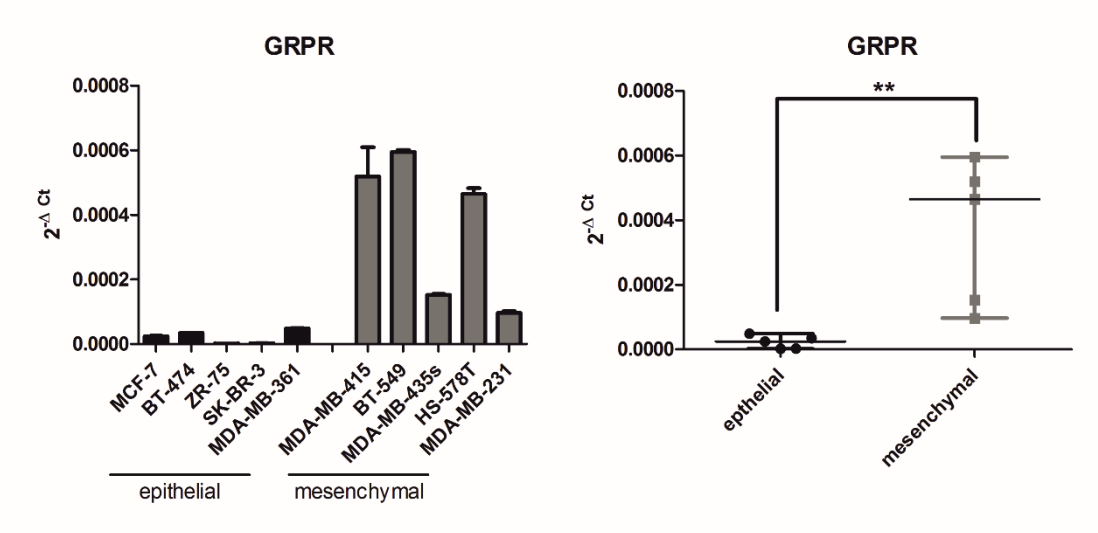
GRPR
0.0008
0.0006
0.0004
0.0002
0.0000
2^-Δ Ct
MCF-7
BT-474
ZR-75
SK-BR-3
MDA-MB-361
MDA-MB-415
BT-549
MDA-MB-435s
HS-578T
MDA-MB-231
epithelial
mesenchymal
GRPR
**
epithelial
mesenchymal

B

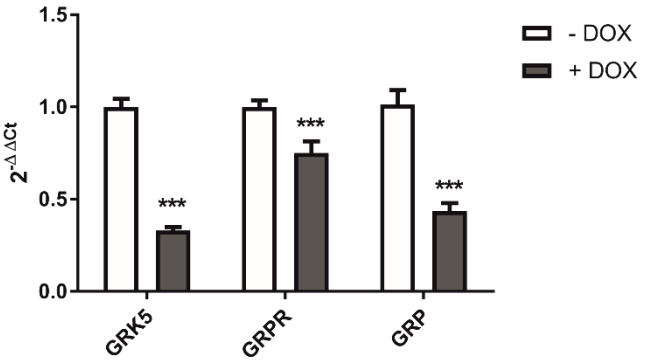
1.5
1.0
0.5
0.0
2^-ΔΔCt
- DOX
+ DOX
***
GRK5
GRPR
GRP

C

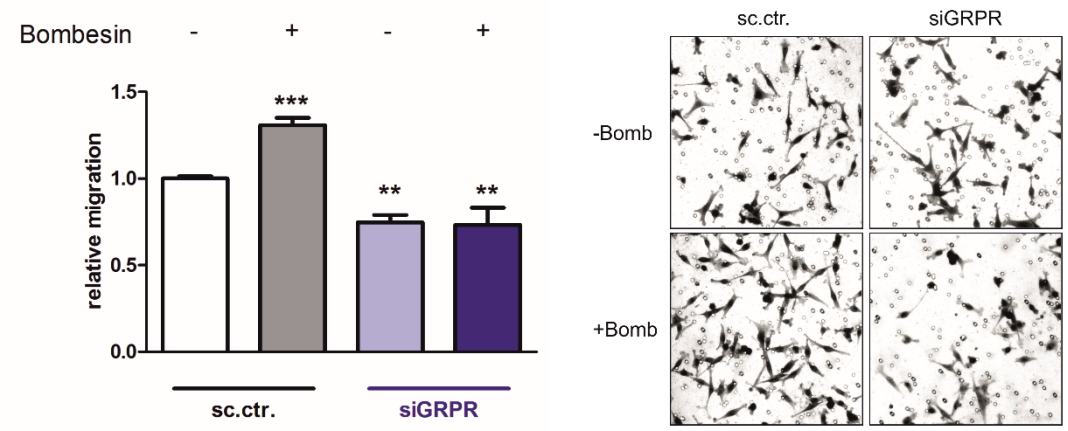
Bombesin
-
+
-
+
relative migration
1.5
1.0
0.5
0.0
***
**
sc.ctr.
siGRPR
sc.ctr.
siGRPR
-Bomb
+Bomb

D

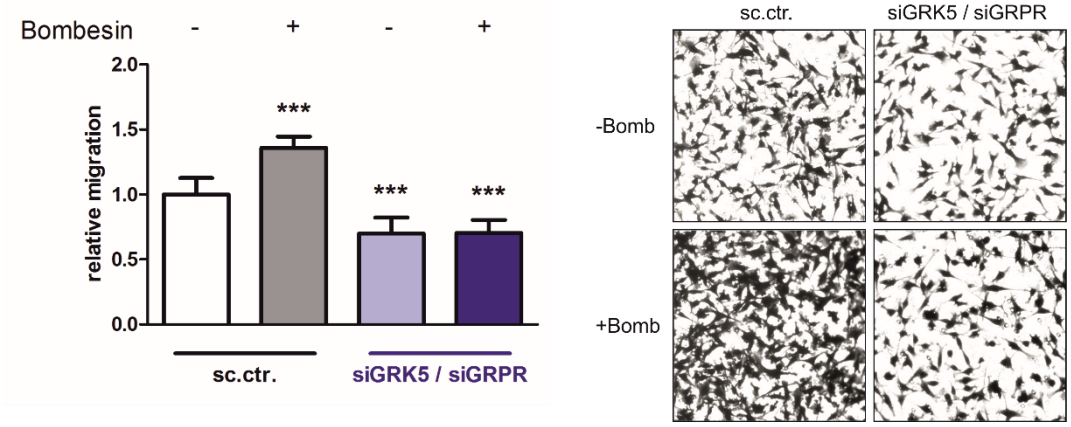
Bombesin
-
+
-
+
relative migration
2.0
1.5
1.0
0.5
0.0
***
sc.ctr.
siGRK5 / siGRPR
sc.ctr.
siGRK5 / siGRPR
-Bomb
+Bomb

Figure 11. Correlation of GRK5 and GRPR and their impact on migration. (A) Expression analysis of GRPR in different breast cancer cell lines utilizing qPCR. The values are depicted as mean + SD in the left panel and as median + range in the right panel. Student's t-test was used for statistical evaluation. (B) Expression analysis of GRK5, GRPR and GRP 90 h upon induction with 5 µg/ml doxycycline utilizing qPCR. Values are depicted as mean + SD. Two-tailed Student's t-test was utilized for statistical evaluation. (C) Migration analysis of MDA-MB-231 cells 90 h upon transfection with sc.ctr. or siGRPR with and without stimulation with 200 nM bombesin. Representative pictures of the crystal violet staining are shown at the right panel. Relative migration values are depicted as mean + SD and normalized to sc.ctr. transfected, not stimulated samples. (N = 3). (D) Migration analysis of MDA-MB-231 cells 90 h after transfection with sc. ctr. or siGRK5 and siGRPR, with or without bombesin stimulation using a boyden chamber assay. Representative pictures of the crystal violet staining are shown. The relative migration values are normalized to sc.ctr. transfected, not stimulated samples and depicted as mean + SD (N = 3). For statistical evaluation one-way ANOVA with Dunnett's Multiple Comparison Test was used. * $p < 0.05$, ** $p < 0.01$, *** $p < 0.001$

3.3.6 SUNITINIB TREATMENT HAMPERS CELL MIGRATION BY REDUCING THE EXPRESSION OF GRK5 AND GRPR

Sunitinib is the most potent, approved GRK5 inhibitor (Anastassiadis et al., 2011; Gao et al., 2013). To evaluate the clinical relevance of our findings MDA-MB-231 cells were treated with this SMI and its effect on cell viability, migration, GRK5 and GRPR expression as well as GRPR signaling was investigated. Fig. 12A shows that 5 µM sunitinib treatment reduces the cell viability of TNBC cells. Therefore, only lower, non-toxic concentrations were utilized for the cell migration analysis. Here, we demonstrated that 1 µM sunitinib treatment significantly reduces the migration of breast cancer cells. A similar effect was detected for the GRK5 KD. The impact of sunitinib treatment on the expression of GRK4-family members was investigated. Sunitinib significantly reduces the expression only of GRK5 - no significant expression changes were observed for GRK4 and GRK6 (Fig. 12B). Additionally, sunitinib significantly decreases the expression of GRPR and down-stream targets like CDC42 and ROCK1 (Fig. 12C). To investigate whether the GRK5 inhibition, which leads to impaired GRPR signaling and eventually reduced migration, has an impact on patient survival, we analyzed patient data *in silico*. The Kaplan-Meier Plotter (Gyorffy et al., 2010) revealed that GRK5 and GRPR overexpression shows a tendency to reduce the distant metastasis free survival (DMFS) in TNBC patients (Fig. 12D). Therefore, we hypothesize that sunitinib treatment of TNBC prolongs DMFS and thus could improve the patient outcome (Fig. 13).

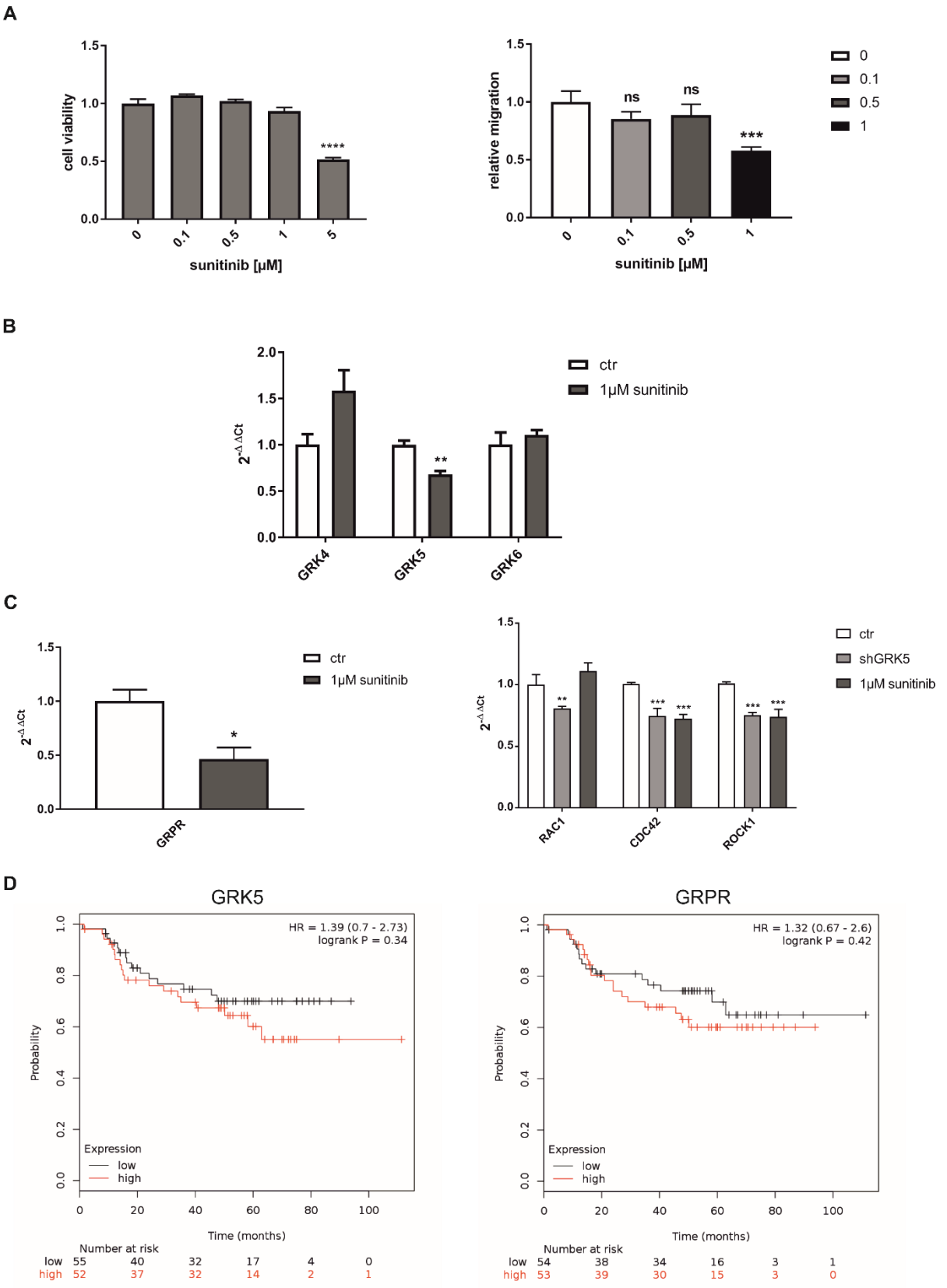

Figure 12. Analysis of clinical impact. (A) MDA-MB-231 cells were treated for 90 h with the indicated concentrations of sunitinib. Left panel: Cell viability measurement by CellTiter-Glo luminescent cell viability assay. Right panel: Migration analysis by boyden chamber. Values are presented as mean + SD and are normalized to untreated cells. For statistical evaluation one-way ANOVA with Dunnett's Multiple Comparison Test was used (N = 3).

(B) Gene expression analysis of GRK4-family members. Values are presented as mean + SD and are normalized to untreated cells. For statistical evaluation multiple t-tests utilizing two-stage linear step-up procedure of Benjamini, Krieger and Yekutieli, were used (N = 3). (C) Gene expression of GRPR and GRPR down-stream signaling components. Values are presented as mean + SD and are normalized to untreated cells. For statistical evaluation student's t-test (left panel) and multiple t-tests (right panel) utilizing two-stage linear step-up procedure of Benjamini, Krieger and Yekutieli, were used. (D) Kaplan Meier analysis (Gyorffy et al., 2010) of GRK5 and GRPR overexpression. The influence on distant metastasis free survival (DMFS) in breast cancer patients with basal like tumors is depicted. * $p < 0.05$, ** $p < 0.01$, *** $p < 0.001$

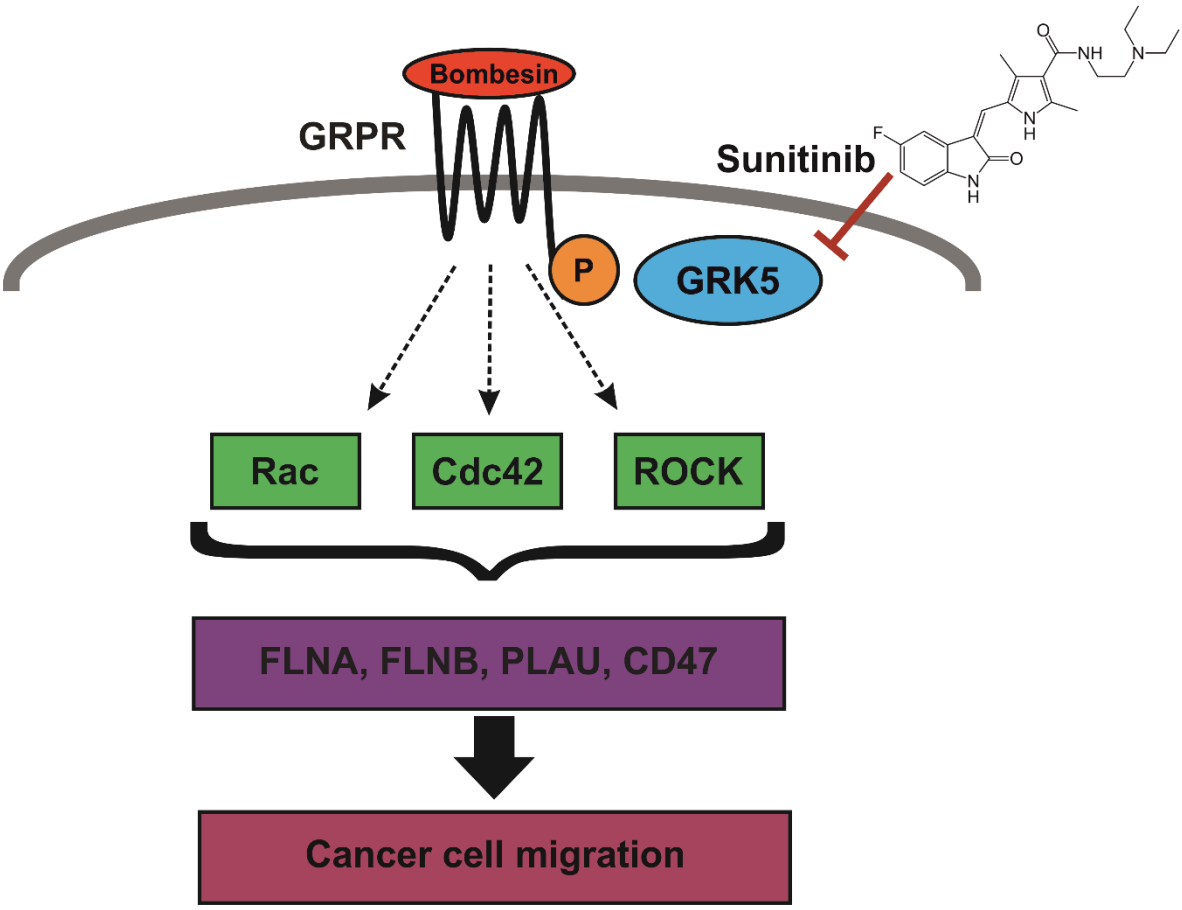

Figure 13. Supposed mechanism. GRK5 phosphorylates the GRPR upon bombesin binding. This leads to the activation of GRPR down-stream signaling and subsequently to the transcription of proteins like FLNA, PLAU and CD47. The final consequence is the maintenance of cell polarity and tension enabling cell migration which could be therapeutically exploited by inhibiting this pathway with sunitinib treatment.

3.4 DISCUSSION

Previous studies have shown that GRK5 affects the migration of prostate cancer via moesin (Chakraborty et al., 2014) and of non-small cell lung cancer cells via vinculin (Jiang et al., 2018). However, the function of GRK5 in breast cancer and the involved GPCRs remain unclear. In this study, a breast cancer cell line screen revealed that GRK5 is mainly expressed in TNBC cell lines, which possess a mesenchymal like phenotype and are able to migrate. Accordingly, the GRK5 KD by a pool of siRNAs and the inducible shRNA in MDA-MB-231 cells reduced cell migration and invasion as well as the expression of proteins involved in cell migration pathways. In order to uncover the responsible GPCRs different ligands were used as chemoattractants. Here, bombesin stimulation, amongst others, resulted in significantly increased cell migration which can be blocked by the GRK5 KD, mediated by both, the siRNA and shRNA approach. This finding led to the assumption that GRK5 interferes with the GRPR signaling pathway, as bombesin, an artificial ligand, binds and activates the GRPR (Gonzalez et al., 2008; Moreno et al., 2016; Ramos-Alvarez et al., 2015). GRPR is an important receptor in breast cancer and is overexpressed in up to 96 % of breast cancer patients (Dalm et al., 2015). An elevated GRPR expression in breast cancer tissue worsens the prognosis (Uhlen et al., 2005; Uhlen et al., 2017). Our expression analysis in different breast cancer cell lines revealed that GRPR is significantly higher expressed in mesenchymal like breast cancer cell lines and correlates with the GRK5 expression. The subsequent qPCR analysis of GRPR and its natural ligand GRP upon GRK5 KD displayed decreased GRPR and GRP expression. Vice versa the KD of GRPR had no influence on the GRK5 expression. Thus, the GRK5 KD hampers the autocrine signaling mechanism by inhibiting the expression of both the endogenous ligand as well as that of the corresponding receptor. GRPR is the sole receptor involved in the chemotaxis of cancer cells towards the ligands GRP/bombesin (Chao et al., 2009; Jaeger et al., 2017). The decrease in its expression by GRK5 KD therefore directly impacts the migration of cancer cells. It was previously shown that the increase in GRPR signaling leads to enhanced cancer cell migration and invasion in various cancer types (Nagakawa et al., 2001; Tell et al., 2011).

However, there are many more GPCRs involved in migration like the bradykinin receptor (Seifert and Sontheimer, 2014), angiotensin receptor (Kim et al., 2018b), endothelin receptor (Shi et al., 2017) and thrombin receptor (Vianello et al., 2016).Our ligand screen however revealed, that only bradykinin and bombesin stimulated migration was hampered by the GRK5 KD and are thus the crucial pathways influenced by GRK5. Moreover, we performed a KD with siRNAs against GRPR and a double KD with siRNAs against GRK5 and GRPR, and investigated the effect on migration. It was shown that all analyzed KD experiments with siGRK5, shGRK5, siGRPR and the double KD of GRK5/GRPR, had the same impact on cell migration. We therefore conclude, that the GRPR signaling pathway is an important migratory mechanism which is regulated by GRK5. The knock-down of GRK5 activates a negative feedback loop by attenuating the expression of GRP and GRPR, finally leading to reduced migration in our *in vitro* system.

To evaluate the clinical significance of our findings, TNBC cells were treated with sunitinib, the most potent, FDA approved GRK5 inhibitor (Anastassiadis et al., 2011; Gao et al., 2013). We observed that sunitinib hampers the migration of MDA-MB-231 cells at non-toxic doses. Previously, it was already shown that sunitinib hampers cell migration in different cancer subtypes but only at toxic doses (Andrae et al., 2012; Chinchar et al., 2014). Thus, these studies hardly allow a clear discrimination between cytotoxicity and migration. Furthermore, we performed an expression analysis of all GRK4-family members, GRPR and GRPR down-stream signaling components to elucidate whether the effect of sunitinib on cancer cell migration is based on the GRK5-GRPR signaling cascade. As sunitinib is a multispecific kinase inhibitor this SMI inhibits besides GRK5 e.g. VEGFR and PDGFR (Anastassiadis et al., 2011; Andrae et al., 2012; Bender and Ullrich, 2012; Gao et al., 2013). Our results show, that sunitinib treatment not only inhibits GRK5 but also significantly reduces its expression whereas GRK4 and GRK6 expression remains stable. Additionally, we observed that sunitinib treatment reduced the expression of GRPR and down-stream signaling components. As GRPR is no reported target gene of sunitinib, it is likely that sunitinib decreases the expression of GRK5 thus indirectly leading to the downregulation of GRPR and its downstream targets RAC1, CDC42 and ROCK1.

The latter three proteins belong to the Rho GTPase family and are crucial players in cell migration (Friedl et al., 2014; Zegers and Friedl, 2014). Previous studies have shown that increased CDC42 and ROCK1 expression directly correlates with elevated actomyosin contractility, actin turnover and actin polymerization and eventually facilitate the migration of cancer cells (Bray et al., 2013). Thus, sunitinib treatment of TNBC cells might reduce their ability to migrate by down regulating GRK5 resulting in the decreased expression of GRP, GRPR, CDC42 and ROCK1. Moreover, this finding might mechanistically explain the prolonged survival of mRCC patients upon sunitinib treatment (Tannir et al., 2017). Here, this therapy not only reduces the metastatic burden but also avoids the development of new metastases and thus leads to an improved patient outcome.

Taken together, this study shows that GRK5 KD hampers the chemotaxis of MDA-MB-231 cells towards bombesin by down regulating the GRPR. Furthermore, we observed that treatment with the multispecific kinase inhibitor sunitinib decreases the cancer cell migration by reducing the GRK5 expression levels resulting in attenuated GRPR signaling, depicting a novel mechanism of action of a well-known drug. We therefore encourage further studies on this mechanism and speculate, that the implementation of sunitinib in TNBC treatment regimen could be a promising option to reduce the formation of metastases which is still one of the major obstacles in the treatment of TNBC.

3.5 MATERIAL AND METHODS

3.5.1 REAGENTS

Doxycycline hyclate was purchased from Sigma-Aldrich (St. Louis, Missouri, USA) (cat.nr. D9891). Bombesin acetate salt hydrate (cat.nr. B4272), Bradykinin acetate salt (cat.nr. B3259), human angiotensin II (cat.nr. A9525), endothelin I (cat.nr. E7764), lysophosphatidic acid sodium salt (cat.nr. L7260), human thrombin (cat.nr. T4393), glucose (cat.nr. D7021) and human insulin (cat.nr. I3536) were purchased from Sigma-Aldrich. Sunitinib malate was purchased from Sigma-Aldrich (cat.nr. PZ0012). Lipofectamine 3000 was purchased from ThermoFisher Scientific (Waltham, Massachusetts, USA) (cat.nr. L3000008).

3.5.2 cDNA OF DIFFERENT BREAST CANCER CELL LINES

The cDNA of the different breast cancer cell lines was a kind gift of Axel Ullrich's lab.

3.5.3 CELL CULTURE

MDA-MB-231 cells were obtained from DSMZ (Braunschweig, Germany) MDA-MB-231 TRIPZ-shGRK5 were generated in our lab and both were cultured in DMEM high glucose supplemented with 10% fetal calf serum (FCS, Gibco) at 37°C and 5% CO_2. HS-578T, DU-145 and PC-3 were obtained from ATCC (Manassas, Virginia, USA) and cultured according to manufacturer's instructions. All cells were authenticated according to ANSI/ATCC standard ASN-0002 and routinely tested and confirmed as mycoplasm free.

3.5.4 GENERATION OF STABLE MDA-MB-231 TRIPZ-SHGRK5

MDA-MB-231 cells were transduced by Dr. Bojan Ljepoja with the doxycycline-inducible TRIPZ-shGRK5 [Clone-ID: V3THS_312367; Sequence: TCGTGAGCAGCATCTTGCA (Dharmacon)] construct utilizing a 2nd generation lentiviral system generated with the plasmids pCMV-dR8.2 dvpr (Addgene plasmid # 8455) and pCMV-VSV-G (Addgene plasmid # 8454) , which were a gift from Bob Weinberg (Stewart et al., 2003). After transduction, a 48 h selection with 5 µg/ml puromycin was performed.

Stimulation of the cells with doxycycline was performed in a concentration of 5 µg/ml in DMEM high glucose + 10% FCS for 90 h for mRNA, protein, migration and invasion analysis. Medium was replaced with fresh, doxycycline containing medium every 48 h to compensate for doxycycline degradation.

3.5.5 SIRNA TRANSFECTION

For siRNA transfection 300 000 cells/well were seeded in a 6-well plate and transfected at the same time with 5 µl Lipofectamine 3000 and 12.5 pmol siRNA per well.

siGRK5: SMARTpool: ON-TARGETplus Human GRK5 siRNA (L-004626-02, Dharmacon, Lafayette, Colorado, USA)

scramble control: ON-TARGETplus Non-targeting Pool (D-001810-10, Dharmacon)

siGRPR: Silencer Select siGRPR s6230 (4392420, Thermo Fisher)

3.5.6 RNA-LYSIS AND PURIFICATION

90 h prior to RNA lysis cells were seeded at a confluence of 50% and either transfected with siRNA or stimulated with doxycycline. Subsequently cells were harvested using RNeasy Mini Kit (Qiagen, Venlo, Netherlands) following the manufacturer's protocol.

3.5.7 cDNA SYNTHESIS

Upon RNA purification 1000 ng RNA were taken to synthesize cDNA according to manufacturer's protocol using qScript cDNA Synthesis Kit (Quantabio, Beverly. Massachusetts, USA).

3.5.8 QUANTITATIVE POLYMERASE CHAIN REACTION (QPCR)

To analyze the mRNA expression a qPCR was performed using the LightCycler 480 (Roche, Basel, Switzerland), the Universal Probe Library (UPL, Roche) and LighCycler 480 Probes Master (Roche). The examined mixture contained 10 µl Probes Master, 4.4 µl nuclease free water, 0.2 µl left primer (20 µM), 0.2 µl right primer (20 µM), 0.2 µl probe and 5 µl cDNA per well. The utilized primer probe pairs are listed below.

	left primer	**right primer**	**probe**
GRK5	aagtccatctgcaagatgctg	ggggtgtctcttgacctctg	# 26
GRPR	cccgtggaagggaatataca	gcggtacaggtagatgacatga	# 36
GRP	cagccacctcaacccaag	tggagcagagagtctaccaactt	# 61
ROCK1	gatcccaaatcggaagtgaa	caaatcatataccaaagcatccaa	# 42
CDC42	tggagtgttctgcacttacaca	ggctcttcttcggttctgg	# 37
RAC1	ctgatgcaggccatcaagt	caggaaatgcattggttgtg	# 77
GAPDH	tccactggcgtcttcacc	ggcagagatgatgacccttttt	# 45

For quantification the $2^{-\Delta Ct}$ or the $2^{-\Delta\Delta Ct}$ method was applied and GAPDH was used as an internal standard.

3.5.9 PROTEIN LYSIS AND WESTERN BLOT

Cells were lyzed at 80% confluence or 72h after siRNA transfection with RIPA buffer containing 1% Triton X. 30µg protein were separated using a SDS-PAGE and subsequently transferred to a nitrocellulose membrane. After one hour blocking with TRIS-buffered saline with Tween20 (TBST) containing 3% nonfat dry milk, the blots were incubated overnight at 4°C with GRK5-antibody (Millipore, Burlington, Massachusetts, USA, cat.nr. 05-466) solution in TBST containing 3% nonfat dry milk, followed by several washing steps. Afterwards, membranes were incubated for one hour in horseradish peroxidase conjugated anti-mouse (goat anti-mouse-hrp, Sigma Aldrich) secondary antibody at room temperature. After additional washing steps, detection was performed using enhanced chemiluminscence (ECL, GE Healthcare, Chicago, Illinois, USA) on X-ray films (Amersham Hyperfilm ECL, GE Healthcare). The α-Tubulin antibody (Sigma Aldrich, cat.nr. T9026) was used as loading control.

3.5.10 EVALUATION OF CELL VIABILITY AND APOPTOSIS INDUCTION

To determine the impact of doxycycline and the GRK5 KD on cell viability the CellTiter-Glo luminescent cell viability assay (Promega, Madison, Wisconsin, USA) was utilized. To assess the apoptosis induction upon doxycycline treatment and GRK5 KD the Caspase-Glo 3/7 Assay (Promega) was used. 90 h prior to both measurements 3 000 cells/well of MDA-MB-231 TRIPZ-shGRK5 cells were seeded in 96-well plates and treated with the indicated concentrations of doxycycline (N=3).

3.5.11 PROTEOMICS SAMPLE PREPARATION

For proteomics analysis 300 000 cells/well were seeded (N = 5) in a 6-well plate and stimulated every 48h with 5 µg/ml doxycycline for 90h. Subsequently, cells were washed three times with cold PBS and lysed with a buffer containing 8 M urea and 400 mM ammonium bicarbonate. Ultrasound was used to support cell lysis and finally the protein samples were purified using QIA-shredder devices (Qiagen).

For reduction, 30 µg of total protein was incubated for 30 min at a final concentration of 5 mM dithioerythritol (DTE). Cleaved bisulfide bonds were blocked using iodoacetamide (final concentration 15 mM) for 30 min in the dark. After dilution with water to a concentration of 1 M urea, proteins were first digested for 4 h with 300 ng LysC (FUJIFILM Wako Pure Chemicals, Osaka, Japan) and subsequently digested over night with 600 ng porcine trypsin (Promega, Madison, WI, USA) at 37°C. The following LC-MS was performed by Dr. Thomas Fröhlich and Dr. Georg J. Arnold. Peptides were separated and identified on an Ultimate 3000 (Thermo Scientific, Waltham, MA, USA) nano-chromatography system coupled to a QExavtive HF-X instrument (Thermo Scientific). 2.5 µg of peptides were dissolved in 15 µl solvent A (0.1 % formic acid in water) and transferred to a capillary trap column (PepMap 100 C18, 100 µm x 2 cm, 5 µM particles, Thermo Scientific). Separation was performed at 250 nL/min (Column: PepMap RSLC C18, 75 µm x 50 cm, 2 µm particles, Thermo Scientific) with a 160 min gradient from 5 % solvent A to 25 % solvent B (0.1% formic acid in acetonitrile) and a subsequent 10 min gradient from 25 % to 40 % solvent B. MS spectra were acquired using a top 15 data dependent CID method. Precursor spectra were acquired at a resolution 60,000 (mass-range: 350-1600) and MS/MS spectra at a resolution of 15,000.

3.5.12 MIGRATION AND INVASION ANALYSIS

For migration and invasion analysis cells were transfected with siRNA or stimulated with 5 µg/ml doxycycline 72 h prior to the experiment. Subsequently, 750 µl DMEM high glucose supplemented with 0.5% FCS and the indicated ligand was added to the lower well of the boyden chamber system Corning BioCoat Matrigel Invasion Chamber (Corning, Corning, New York, USA) in the case of invasion analysis and Falcon Cell Culture Inserts ([8 µm pores] Coring) in the case of migration analysis. The inserts (N = 3) were filled with 500 µl of a cell suspension containing 50 000 cells in DMEM high glucose supplemented with 0.5% FCS. 18 h later the cell suspension was removed and the inserts were put into 500 µl crystal violet solution containing 20% methanol for at least 10 min. Finally, the inserts were washed three times with demineralized water and kept overnight at room temperature.

To determine the amount of migrated / invaded cells five microscopic pictures (magnification 10x) of each insert were made (top, bottom, left, right, center) and afterwards analyzed using the ImageJ software.

3.5.13 SUNITINIB TREATMENT

For cell viability measurement 3 000 MDA-MB-231 cells/well were seeded in triplicates in a 96-well plate and treated with the indicated concentrations for 90 h. Afterwards the CellTiter-Glo luminescent cell viability assay (Promega) was utilized to measure cytotoxicity. To analyze the impact of sunitinib on migration 300 000 cells/well were seeded in a 6-well plate and pre-treated with sunitinib at the indicated concentrations for 72 h. Subsequently, sunitinib was added to the starvation medium (DMEM + 0.5% FCS) for the following boyden chamber experiment. Here, 50 000 cells/well were seeded in triplicates to the insert. For gene expression analysis 300 000 MDA-MB-231 cells/well were seeded in 6-well plates and treated with 1 µM sunitinib for 90 h.

3.5.14 BIOINFORMATICS

Statistical significance was calculated utilizing a two-tailed Student's t-test for the comparison of two samples and one-way ANOVA with Dunnett's Multiple Comparison Test or multiple t-tests utilizing two-stage linear step-up procedure of Benjamini, Krieger and Yekutieli, for the comparison of several samples with the control. * $p < 0.05$, ** $p < 0.01$, *** $p < 0.001$

To process the mass spectrometry (MS) data MaxQuant 1.5.1.0 was applied (Tyanova et al., 2015) and the Perseus module was used (Tyanova et al., 2016). For label free quantification (LFQ) values of the identified proteins were taken and proteins that were only identified by site or potential contaminants were excluded.

The doxycycline induced (+DOX) and the not induced (-DOX) samples were grouped and at least three valid values in each group were necessary to enter further analysis. The missing values were replaced from normal distribution using the imputation feature of Perseus (width, 0.3; down-shift, 1.8).

Subsequently, a gene set enrichment analysis (GSEA) was performed using gsea2-2.2.3 from the Broad Institute (Cambridge, MA, USA) (Mootha et al., 2003; Subramanian et al., 2005). As underlying gene set database, the gene ontology biological process (GO_BP) was used (Ashburner et al., 2000). The resulting, differentially expressed pathways were grouped in the following categories: metabolism, signaling, migration, cell differentiation, transport, cell development, immune system, gene expression and cell cycle to allow a comparison of up and down regulated signaling cascades.

In order to elucidate the clinical significance of GRK5 and GRPR in breast cancer patients the Kaplan-Meier-Plotter was utilized (Gyorffy et al., 2010) (released 2018/05/01). This web service allows the evaluation of more than 20,000 genes in about 1,800 breast cancer patients. MDA-MB-231 cells represent an example for a triple-negative breast cancer with a basal subtype according to its gene expression profile. Thus, patients with basal like tumors were analyzed and the filters were set accordingly. Distant metastasis free survival (DMFS) was chosen as endpoint as cancer cell migration and invasion were of special interest in this study.

3.6 SUPPLEMENTS

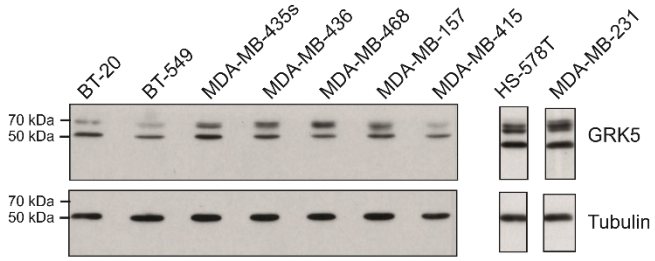

Supplementary figure S3. Western blot analysis of GRK5 protein expression in different breast cancer cell lines. Tubulin was used as loading control.

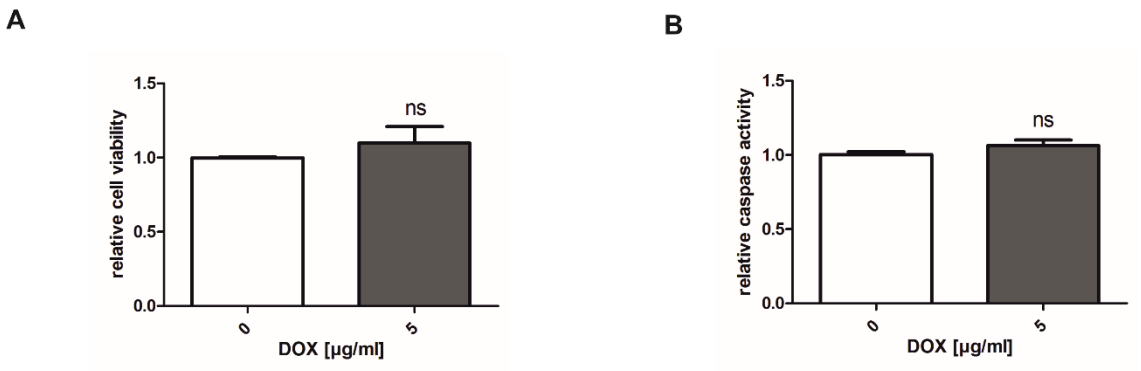

Supplementary figure S4. Cell viability and apoptosis measurement in MDA-MB-231 TRIPZ-shGRK5 (a) CellTiter-Glo Luminescent Cell Viability Assay 90h after treatment with 5 µg/ml DOX. (b) Caspase-Glo 3/7 Assay 90h after induction with 5µg/ml DOX.

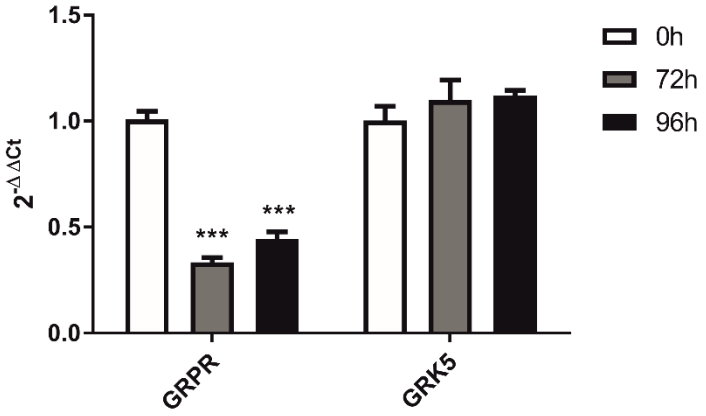

Supplementary Figure S5. qPCR analysis of GRPRP and GRK5. Examination of gene expression 72h and 96h after siGRPR transfection in MDA-MB-231 cells.

4. SUMMARY

In this thesis two major hurdles in treatment of breast cancer were investigated, namely the development of chemoresistance as well as the formation of metastases.

In the first part it was shown that the development of chemoresistance is a rather individual process without a predetermined pattern (Sommer et al., 2018). The sequential doxorubicin treatment in three independent experiments and the subsequent proteomics analysis revealed pathways being involved in resistance development namely downregulation of apoptotic signaling pathways and upregulation of cell redox homeostasis. Moreover, few proteins with altered expression were identified in all three experiments *i.e.,* downregulation of 60s ribosomal export protein NMD3 (NMD3) and upregulation of 4F2 cell-surface antigen heavy chain (SLC3A2). To further investigate the clinical implication of these two proteins the Kaplan-Meier Plotter was used. Thereby it was shown that both alterations negatively impact the relapse-free survival of luminal A breast cancer patients.

Albeit the transferability of *in vitro* data to clinical settings is limited, the result of this study clearly shows how complex the development of chemoresistance is and might be even more complex in breast cancer patients. These findings further underline that recurrent or persistent tumors might need a different treatment compared to the primary tumor and in case of targeted therapy require an additional biomarker test. As this procedure is not entirely adopted to the clinical praxis a comprehensive diagnosis of residual or recurrent tumor tissue may improve the treatment of breast cancer and thus patient outcome.

The second part of this thesis deals with the role of GRK5 in breast cancer metastases. Here, it was shown that GRK5 is mainly expressed in mesenchymal like, triple-negative breast cancer cells and that reduced GRK5 levels clearly hamper the migration and invasion of breast cancer cells (Sommer et al., 2019). Moreover, a comprehensive proteomics approach revealed that pathways being involved in cancer cell migration are mainly affected by down-regulation of GRK5. By stimulating the breast cancer cells with different GPCR ligands, Bombesin was identified as chemoattractant which loses its activity upon GRK5 knock-down.

Additional evaluation of the signaling pathway being regulated by GRK5 revealed that GRPR – the cellular receptor of Bombesin – is mainly expressed in TNBC cells. Furthermore, the mRNA level of GRPR and its endogenous ligand GRP decreases by GRK5 knock-down. Finally, it was observed that a knock-down of GRPR hampers the migration of breast cancer cells as well. To evaluate the clinical impact of these findings TNBC cells were treated with sunitinib – an approved multi-kinase inhibitor that is known to inhibit GRK5. Thereby, it was shown that sunitinib treatment reduces cancer cell migration as well as the mRNA levels of GRK5 and GRPR at a non-toxic concentration. Additionally, downstream molecules of GRPR – CDC42 and ROCK1 – were less expressed upon sunitinib treatment and GRK5 knock-down. By utilizing the Kaplan-Meier-Plotter we additionally figured out that the distant metastasis free survival decreases with overexpression of GRK5 and GRPR in breast cancer patients with basal like tumors.

With this study a novel signaling pathway that regulates the migration of breast cancer cells was identified. In addition to that the clinical impact of GRK5 and GRPR on the formation of metastases in basal like tumors was shown. Moreover, an approved drug – sunitinib – was found to be able to block this signaling cascade thereby reducing the migratory ability of breast cancer cells. Even though clinical trials would be necessary to prove the efficacy of sunitinib in TNBC this study gives a first hint how the formation of metastases can be overcome and may thus improve patient outcomes.

Breast cancer is one of the most prevalent and deadliest diseases in women worldwide. Therefore, it is very important to further investigate mamma carcinoma in clinical but also in pre-clinical settings. This thesis generated further knowledge on the development of chemoresistance and the formation of metastases *in vitro*. These two obstacles are still major challenges in the treatment of breast cancer patients and worsen their clinical outcome. Thus, each single piece contributing to a better understanding of breast cancer may improve future therapeutic options and treatment regimen.

5. REFERENCES AND INDICES

5.1 REFERENCES

Aas, T., Borresen, A.L., Geisler, S., Smith-Sorensen, B., Johnsen, H., Varhaug, J.E., Akslen, L.A., and Lonning, P.E. (1996). Specific P53 mutations are associated with de novo resistance to doxorubicin in breast cancer patients. Nat Med *2*, 811-814.

American-Cancer-Society (2019). Breast Cancer Fact & Figures 2019-2020. American Cancer Society, Inc.

American Cancer Society (2018). Cancer Facts & Figures 2018 (American Cancer Society).

Anastassiadis, T., Deacon, S.W., Devarajan, K., Ma, H., and Peterson, J.R. (2011). Comprehensive assay of kinase catalytic activity reveals features of kinase inhibitor selectivity. Nat Biotechnol *29*, 1039-1045.

Andrae, N., Kirches, E., Hartig, R., Haase, D., Keilhoff, G., Kalinski, T., and Mawrin, C. (2012). Sunitinib targets PDGF-receptor and Flt3 and reduces survival and migration of human meningioma cells. Eur J Cancer *48*, 1831-1841.

Arcamone, F., Cassinelli, G., Fantini, G., Grein, A., Orezzi, P., Pol, C., and Spalla, C. (1969). Adriamycin, 14-hydroxydaunomycin, a new antitumor antibiotic from S. peucetius var. caesius. Biotechnol Bioeng *11*, 1101-1110.

Ashburner, M., Ball, C.A., Blake, J.A., Botstein, D., Butler, H., Cherry, J.M., Davis, A.P., Dolinski, K., Dwight, S.S., Eppig, J.T.*, et al.* (2000). Gene ontology: tool for the unification of biology. The Gene Ontology Consortium. Nat Genet *25*, 25-29.

Bai, B., Moore, H.M., and Laiho, M. (2013). CRM1 and its ribosome export adaptor NMD3 localize to the nucleolus and affect rRNA synthesis. Nucleus *4*, 315-325.

Bai, X., Ni, J., Beretov, J., Graham, P., and Li, Y. (2018). Cancer stem cell in breast cancer therapeutic resistance. Cancer Treat Rev *69*, 152-163.

Bankusli, I., Yin, M.B., Mazzoni, A., Abdellah, A.J., and Rustum, Y.M. (1989). Enhancement of adriamycin-induced cytotoxicity by increasing retention and inhibition of DNA repair in DOX-resistant P388 cell lines with new calcium channel blocker, DMDP. Anticancer Res *9*, 567-574.

Bao, S., Wu, Q., McLendon, R.E., Hao, Y., Shi, Q., Hjelmeland, A.B., Dewhirst, M.W., Bigner, D.D., and Rich, J.N. (2006). Glioma stem cells promote radioresistance by preferential activation of the DNA damage response. Nature *444*, 756-760.

Bedard, P.L., Hansen, A.R., Ratain, M.J., and Siu, L.L. (2013). Tumour heterogeneity in the clinic. Nature *501*, 355-364.

Benchekroun, M.N., Sinha, B.K., and Robert, J. (1993). Doxorubicin-induced oxygen free radical formation in sensitive and doxorubicin-resistant variants of rat glioblastoma cell lines [corrected and republished erratum originally printed in FEBS Lett 1993 May 17;322(3):295-8]. FEBS Lett *326*, 302-305.

Bender, C., and Ullrich, A. (2012). PRKX, TTBK2 and RSK4 expression causes Sunitinib resistance in kidney carcinoma- and melanoma-cell lines. Int J Cancer *131*, E45-55.

Bray, K., Gillette, M., Young, J., Loughran, E., Hwang, M., Sears, J.C., and Vargo-Gogola, T. (2013). Cdc42 overexpression induces hyperbranching in the developing mammary gland by enhancing cell migration. Breast Cancer Res *15*, R91.

Buchholz, M., Honstein, T., Kirchhoff, S., Kreider, R., Schmidt, H., Sipos, B., and Gress, T.M. (2015). A multistep high-content screening approach to identify novel functionally relevant target genes in pancreatic cancer. PLoS One *10*, e0122946.

Cairns, J. (1975). Mutation selection and the natural history of cancer. Nature *255*, 197-200.

Cancer Genome Atlas, N. (2012). Comprehensive molecular portraits of human breast tumours. Nature *490*, 61-70.

Cardoso, F., Kyriakides, S., Ohno, S., Penault-Llorca, F., Poortmans, P., Rubio, I.T., Zackrisson, S., Senkus, E., and Committee, E.G. (2019). Early breast cancer: ESMO Clinical Practice Guidelines for diagnosis, treatment and follow-up. Ann Oncol *30*, 1674.

Carnero, A., Garcia-Mayea, Y., Mir, C., Lorente, J., Rubio, I.T., and ME, L.L. (2016). The cancer stem-cell signaling network and resistance to therapy. Cancer Treat Rev *49*, 25-36.

Chakraborty, P.K., Zhang, Y., Coomes, A.S., Kim, W.J., Stupay, R., Lynch, L.D., Atkinson, T., Kim, J.I., Nie, Z., and Daaka, Y. (2014). G protein-coupled receptor kinase GRK5 phosphorylates moesin and regulates metastasis in prostate cancer. Cancer Res *74*, 3489-3500.

Chao, C., Ives, K., Hellmich, H.L., Townsend, C.M., Jr., and Hellmich, M.R. (2009). Gastrin-releasing peptide receptor in breast cancer mediates cellular migration and interleukin-8 expression. J Surg Res *156*, 26-31.

Chen, N.T., Wu, C.Y., Chung, C.Y., Hwu, Y., Cheng, S.H., Mou, C.Y., and Lo, L.W. (2012). Probing the dynamics of doxorubicin-DNA intercalation during the initial activation of apoptosis by fluorescence lifetime imaging microscopy (FLIM). PLoS One *7*, e44947.

Chinchar, E., Makey, K.L., Gibson, J., Chen, F., Cole, S.A., Megason, G.C., Vijayakumar, S., Miele, L., and Gu, J.W. (2014). Sunitinib significantly suppresses the proliferation, migration, apoptosis resistance, tumor angiogenesis and growth of triple-negative breast cancers but increases breast cancer stem cells. Vasc Cell *6*, 12.

Choi, H.S., Kim, D.A., Chung, H., Park, I.H., Kim, B.H., Oh, E.S., and Kang, D.H. (2017). Screening of breast cancer stem cell inhibitors using a protein kinase inhibitor library. Cancer Cell Int *17*, 25.

Coates, A.S., Winer, E.P., Goldhirsch, A., Gelber, R.D., Gnant, M., Piccart-Gebhart, M., Thurlimann, B., Senn, H.J., and Panel, M. (2015). Tailoring therapies--improving the management of early breast cancer: St Gallen International Expert Consensus on the Primary Therapy of Early Breast Cancer 2015. Ann Oncol *26*, 1533-1546.

Dalm, S.U., Martens, J.W., Sieuwerts, A.M., van Deurzen, C.H., Koelewijn, S.J., de Blois, E., Maina, T., Nock, B.A., Brunel, L., Fehrentz, J.A.*, et al.* (2015). In vitro and in vivo application of radiolabeled gastrin-releasing peptide receptor ligands in breast cancer. J Nucl Med *56*, 752-757.

de Jong, S., Zijlstra, J.G., de Vries, E.G., and Mulder, N.H. (1990). Reduced DNA topoisomerase II activity and drug-induced DNA cleavage activity in an adriamycin-resistant human small cell lung carcinoma cell line. Cancer Res *50*, 304-309.

Dorsam, R.T., and Gutkind, J.S. (2007). G-protein-coupled receptors and cancer. Nat Rev Cancer *7*, 79-94.

Early Breast Cancer Trialists' Collaborative, G., Peto, R., Davies, C., Godwin, J., Gray, R., Pan, H.C., Clarke, M., Cutter, D., Darby, S., McGale, P.*, et al.* (2012). Comparisons between different polychemotherapy regimens for early breast cancer: meta-analyses of long-term outcome among 100,000 women in 123 randomised trials. Lancet *379*, 432-444.

Eckhardt, B.L., Francis, P.A., Parker, B.S., and Anderson, R.L. (2012). Strategies for the discovery and development of therapies for metastatic breast cancer. Nat Rev Drug Discov *11*, 479-497.

Ferlay, J., Colombet, M., Soerjomataram, I., Mathers, C., Parkin, D.M., Pineros, M., Znaor, A., and Bray, F. (2019). Estimating the global cancer incidence and mortality in 2018: GLOBOCAN sources and methods. Int J Cancer *144*, 1941-1953.

Friedl, P., Wolf, K., and Zegers, M.M. (2014). Rho-directed forces in collective migration. Nat Cell Biol *16*, 208-210.

Gambardella, J., Franco, A., Giudice, C.D., Fiordelisi, A., Cipolletta, E., Ciccarelli, M., Trimarco, B., Iaccarino, G., and Sorriento, D. (2016). Dual role of GRK5 in cancer development and progression. Transl Med UniSa *14*, 28-37.

Gao, Y., Davies, S.P., Augustin, M., Woodward, A., Patel, U.A., Kovelman, R., and Harvey, K.J. (2013). A broad activity screen in support of a chemogenomic map for kinase signalling research and drug discovery. Biochem J *451*, 313-328.

Gehrmann, M.L., Fenselau, C., and Hathout, Y. (2004). Highly altered protein expression profile in the adriamycin resistant MCF-7 cell line. J Proteome Res *3*, 403-409.

Gennari, A., Conte, P., Rosso, R., Orlandini, C., and Bruzzi, P. (2005). Survival of metastatic breast carcinoma patients over a 20-year period: a retrospective analysis based on individual patient data from six consecutive studies. Cancer *104*, 1742-1750.

Gewirtz, D.A. (1999). A critical evaluation of the mechanisms of action proposed for the antitumor effects of the anthracycline antibiotics adriamycin and daunorubicin. Biochem Pharmacol *57*, 727-741.

Globocan (2012). Cancer today (International Agency for Research on Cancer,).

Gonzalez, N., Moody, T.W., Igarashi, H., Ito, T., and Jensen, R.T. (2008). Bombesin-related peptides and their receptors: recent advances in their role in physiology and disease states. Curr Opin Endocrinol Diabetes Obes *15*, 58-64.

Goodman, V.L., Rock, E.P., Dagher, R., Ramchandani, R.P., Abraham, S., Gobburu, J.V., Booth, B.P., Verbois, S.L., Morse, D.E., Liang, C.Y.*, et al.* (2007). Approval summary: sunitinib for the treatment of imatinib refractory or intolerant gastrointestinal stromal tumors and advanced renal cell carcinoma. Clin Cancer Res *13*, 1367-1373.

Goswami, S., Philippar, U., Sun, D., Patsialou, A., Avraham, J., Wang, W., Di Modugno, F., Nistico, P., Gertler, F.B., and Condeelis, J.S. (2009). Identification of invasion specific splice variants of the cytoskeletal protein Mena present in mammary tumor cells during invasion in vivo. Clin Exp Metastasis *26*, 153-159.

Goswami, S., Wang, W., Wyckoff, J.B., and Condeelis, J.S. (2004). Breast cancer cells isolated by chemotaxis from primary tumors show increased survival and resistance to chemotherapy. Cancer Res *64*, 7664-7667.

Gottesman, M.M. (2002). Mechanisms of cancer drug resistance. Annu Rev Med *53*, 615-627.

Greaves, M., and Maley, C.C. (2012). Clonal evolution in cancer. Nature *481*, 306-313.

Gurevich, E.V., Tesmer, J.J., Mushegian, A., and Gurevich, V.V. (2012). G protein-coupled receptor kinases: more than just kinases and not only for GPCRs. Pharmacol Ther *133*, 40-69.

Gyorffy, B., Lanczky, A., Eklund, A.C., Denkert, C., Budczies, J., Li, Q., and Szallasi, Z. (2010). An online survival analysis tool to rapidly assess the effect of 22,277 genes on breast cancer prognosis using microarray data of 1,809 patients. Breast Cancer Res Treat *123*, 725-731.

Hanahan, D., and Weinberg, R.A. (2011). Hallmarks of cancer: the next generation. Cell *144*, 646-674.

Harbeck, N., and Gnant, M. (2017). Breast cancer. Lancet *389*, 1134-1150.

Harbeck, N., Sotlar, K., Wuerstlein, R., and Doisneau-Sixou, S. (2014). Molecular and protein markers for clinical decision making in breast cancer: today and tomorrow. Cancer Treat Rev *40*, 434-444.

Heimes, A.S., and Schmidt, M. (2019). Atezolizumab for the treatment of triple-negative breast cancer. Expert Opin Investig Drugs *28*, 1-5.

Hermawan, A., Wagner, E., and Roidl, A. (2016). Consecutive salinomycin treatment reduces doxorubicin resistance of breast tumor cells by diminishing drug efflux pump expression and activity. Oncol Rep *35*, 1732-1740.

Hilmer, S.N., Cogger, V.C., Muller, M., and Le Couteur, D.G. (2004). The hepatic pharmacokinetics of doxorubicin and liposomal doxorubicin. Drug Metab Dispos *32*, 794-799.

Holm, M., Saraswat, M., Joenvaara, S., Ristimaki, A., Haglund, C., and Renkonen, R. (2018). Colorectal cancer patients with different C-reactive protein levels and 5-year survival times can be differentiated with quantitative serum proteomics. PLoS One *13*, e0195354.

Hosseini, H., Obradovic, M.M.S., Hoffmann, M., Harper, K.L., Sosa, M.S., Werner-Klein, M., Nanduri, L.K., Werno, C., Ehrl, C., Maneck, M.*, et al.* (2016). Early dissemination seeds metastasis in breast cancer. Nature *540*, 552-558.

IARC (2018). Global Cancer Observatory (WHO).

Jaeger, N., Czepielewski, R.S., Bagatini, M., Porto, B.N., and Bonorino, C. (2017). Neuropeptide gastrin-releasing peptide induces PI3K/reactive oxygen species-dependent migration in lung adenocarcinoma cells. Tumour Biol *39*, 1010428317694321.

Jiang, L.P., Fan, S.Q., Xiong, Q.X., Zhou, Y.C., Yang, Z.Z., Li, G.F., Huang, Y.C., Wu, M.G., Shen, Q.S., Liu, K.*, et al.* (2018). GRK5 functions as an oncogenic factor in non-small-cell lung cancer. Cell Death Dis *9*, 295.

Kaur, G., Kim, J., Kaur, R., Tan, I., Bloch, O., Sun, M.Z., Safaee, M., Oh, M.C., Sughrue, M., Phillips, J.*, et al.* (2013). G-protein coupled receptor kinase (GRK)-5 regulates proliferation of glioblastoma-derived stem cells. J Clin Neurosci *20*, 1014-1018.

Kim, C., Gao, R., Sei, E., Brandt, R., Hartman, J., Hatschek, T., Crosetto, N., Foukakis, T., and Navin, N.E. (2018a). Chemoresistance Evolution in Triple-Negative Breast Cancer Delineated by Single-Cell Sequencing. Cell *173*, 879-893 e813.

Kim, D., Pattamatta, U., Kelly, E., Healey, P.R., Carnt, N., Zoellner, H., and White, A.J.R. (2018b). Inhibitory Effects of Angiotensin II Receptor Blockade on Human Tenon Fibroblast Migration and Reactive Oxygen Species Production in Cell Culture. Transl Vis Sci Technol *7*, 20.

Kim, M.S., Pinto, S.M., Getnet, D., Nirujogi, R.S., Manda, S.S., Chaerkady, R., Madugundu, A.K., Kelkar, D.S., Isserlin, R., Jain, S.*, et al.* (2014). A draft map of the human proteome. Nature *509*, 575-581.

Koike Folgueira, M.A., Brentani, H., Carraro, D.M., De Camargo Barros Filho, M., Hirata Katayama, M.L., Santana de Abreu, A.P., Mantovani Barbosa, E., De Oliveira, C.T., Patrao, D.F., Mota, L.D.*, et al.* (2009). Gene expression profile of residual breast cancer after doxorubicin and cyclophosphamide neoadjuvant chemotherapy. Oncol Rep *22*, 805-813.

Komolov, K.E., and Benovic, J.L. (2018). G protein-coupled receptor kinases: Past, present and future. Cell Signal *41*, 17-24.

Koplev, S., Lin, K., Dohlman, A.B., and Ma'ayan, A. (2018). Integration of pan-cancer transcriptomics with RPPA proteomics reveals mechanisms of epithelial-mesenchymal transition. PLoS Comput Biol *14*, e1005911.

Kopp, F., Hermawan, A., Oak, P.S., Ulaganathan, V.K., Herrmann, A., Elnikhely, N., Thakur, C., Xiao, Z., Knyazev, P., Ataseven, B.*, et al.* (2014). Sequential Salinomycin Treatment Results in Resistance Formation through Clonal Selection of Epithelial-Like Tumor Cells. Transl Oncol *7*, 702-711.

Kopp, F., Oak, P.S., Wagner, E., and Roidl, A. (2012). miR-200c sensitizes breast cancer cells to doxorubicin treatment by decreasing TrkB and Bmi1 expression. PLoS One *7*, e50469.

Lambert, A.W., Pattabiraman, D.R., and Weinberg, R.A. (2017). Emerging Biological Principles of Metastasis. Cell *168*, 670-691.

Lawson, D.A., Bhakta, N.R., Kessenbrock, K., Prummel, K.D., Yu, Y., Takai, K., Zhou, A., Eyob, H., Balakrishnan, S., Wang, C.Y.*, et al.* (2015). Single-cell analysis reveals a stem-cell program in human metastatic breast cancer cells. Nature *526*, 131-135.

Le, D., and Gelmon, K.A. (2018). Olaparib tablets for the treatment of germ line BRCA-mutated metastatic breast cancer. Expert Rev Clin Pharmacol *11*, 833-839.

Leitlinienprogramm-Onkologie (Deutsche Krebsgesellschaft, D.K., AWMF) (2020). S3-Leitlinie Früherkennung, Diagnose, Therapie und Nachsorge des Mammakarzinoms (Deutsche Krebsgesellschaft).

Li, J., Chen, Z., Su, K., and Zeng, J. (2015). Clinicopathological classification and traditional prognostic indicators of breast cancer. Int J Clin Exp Pathol *8*, 8500-8505.

Li, X., Lewis, M.T., Huang, J., Gutierrez, C., Osborne, C.K., Wu, M.F., Hilsenbeck, S.G., Pavlick, A., Zhang, X., Chamness, G.C.*, et al.* (2008). Intrinsic resistance of tumorigenic breast cancer cells to chemotherapy. J Natl Cancer Inst *100*, 672-679.

Marin, J.J., Al-Abdulla, R., Lozano, E., Briz, O., Bujanda, L., Banales, J.M., and Macias, R.I. (2016). Mechanisms of Resistance to Chemotherapy in Gastric Cancer. Anticancer Agents Med Chem *16*, 318-334.

McGranahan, N., and Swanton, C. (2017). Clonal Heterogeneity and Tumor Evolution: Past, Present, and the Future. Cell *168*, 613-628.

Meacham, C.E., and Morrison, S.J. (2013). Tumour heterogeneity and cancer cell plasticity. Nature *501*, 328-337.

Miller, K.D., Siegel, R.L., Lin, C.C., Mariotto, A.B., Kramer, J.L., Rowland, J.H., Stein, K.D., Alteri, R., and Jemal, A. (2016). Cancer treatment and survivorship statistics, 2016. CA Cancer J Clin *66*, 271-289.

Minotti, G., Menna, P., Salvatorelli, E., Cairo, G., and Gianni, L. (2004). Anthracyclines: molecular advances and pharmacologic developments in antitumor activity and cardiotoxicity. Pharmacol Rev *56*, 185-229.

Mizutani, H., Tada-Oikawa, S., Hiraku, Y., Kojima, M., and Kawanishi, S. (2005). Mechanism of apoptosis induced by doxorubicin through the generation of hydrogen peroxide. Life Sci *76*, 1439-1453.

Mootha, V.K., Lindgren, C.M., Eriksson, K.F., Subramanian, A., Sihag, S., Lehar, J., Puigserver, P., Carlsson, E., Ridderstrale, M., Laurila, E.*, et al.* (2003). PGC-1alpha-responsive genes involved in oxidative phosphorylation are coordinately downregulated in human diabetes. Nat Genet *34*, 267-273.

Moreno, P., Ramos-Alvarez, I., Moody, T.W., and Jensen, R.T. (2016). Bombesin related peptides/receptors and their promising therapeutic roles in cancer imaging, targeting and treatment. Expert Opin Ther Targets *20*, 1055-1073.

Nagakawa, O., Ogasawara, M., Murata, J., Fuse, H., and Saiki, I. (2001). Effect of prostatic neuropeptides on migration of prostate cancer cell lines. Int J Urol *8*, 65-70.

Navin, N.E. (2014). Tumor evolution in response to chemotherapy: phenotype versus genotype. Cell Rep *6*, 417-419.

Nik-Zainal, S., Davies, H., Staaf, J., Ramakrishna, M., Glodzik, D., Zou, X., Martincorena, I., Alexandrov, L.B., Martin, S., Wedge, D.C.*, et al.* (2016). Landscape of somatic mutations in 560 breast cancer whole-genome sequences. Nature *534*, 47-54.

Nogues, L., Palacios-Garcia, J., Reglero, C., Rivas, V., Neves, M., Ribas, C., Penela, P., and Mayor, F., Jr. (2018). G protein-coupled receptor kinases (GRKs) in tumorigenesis and cancer progression: GPCR regulators and signaling hubs. Semin Cancer Biol *48*, 78-90.

Nogues, L., Reglero, C., Rivas, V., Salcedo, A., Lafarga, V., Neves, M., Ramos, P., Mendiola, M., Berjon, A., Stamatakis, K.*, et al.* (2016). G Protein-coupled Receptor Kinase 2 (GRK2) Promotes Breast Tumorigenesis Through a HDAC6-Pin1 Axis. EBioMedicine *13*, 132-145.

Nowell, P.C. (1976). The clonal evolution of tumor cell populations. Science *194*, 23-28.

Oliveros, J.C. (2007-2015). Venny. An interactive tool for comparing lists with Venn's diagrams.

Parker, J.S., Mullins, M., Cheang, M.C., Leung, S., Voduc, D., Vickery, T., Davies, S., Fauron, C., He, X., Hu, Z.*, et al.* (2009). Supervised risk predictor of breast cancer based on intrinsic subtypes. J Clin Oncol *27*, 1160-1167.

Patsialou, A., Wang, Y., Lin, J., Whitney, K., Goswami, S., Kenny, P.A., and Condeelis, J.S. (2012). Selective gene-expression profiling of migratory tumor cells in vivo predicts clinical outcome in breast cancer patients. Breast Cancer Res *14*, R139.

Pertea, M. (2012). The human transcriptome: an unfinished story. Genes (Basel) *3*, 344-360.

Pfeffer, C.M., and Singh, A.T.K. (2018). Apoptosis: A Target for Anticancer Therapy. Int J Mol Sci *19*.

Pierce, K.L., Premont, R.T., and Lefkowitz, R.J. (2002). Seven-transmembrane receptors. Nat Rev Mol Cell Biol *3*, 639-650.

Poettler, M., Unseld, M., Braemswig, K., Haitel, A., Zielinski, C.C., and Prager, G.W. (2013). CD98hc (SLC3A2) drives integrin-dependent renal cancer cell behavior. Mol Cancer *12*, 169.

Polyzos, A. (2008). Activity of SU11248, a multitargeted inhibitor of vascular endothelial growth factor receptor and platelet-derived growth factor receptor, in patients with metastatic renal cell carcinoma and various other solid tumors. J Steroid Biochem Mol Biol *108*, 261-266.

Prager, G.W., Poettler, M., Schmidinger, M., Mazal, P.R., Susani, M., Zielinski, C.C., and Haitel, A. (2009). CD98hc (SLC3A2), a novel marker in renal cell cancer. Eur J Clin Invest *39*, 304-310.

Prat, A., Adamo, B., Cheang, M.C., Anders, C.K., Carey, L.A., and Perou, C.M. (2013). Molecular characterization of basal-like and non-basal-like triple-negative breast cancer. Oncologist *18*, 123-133.

Prat, A., Pineda, E., Adamo, B., Galvan, P., Fernandez, A., Gaba, L., Diez, M., Viladot, M., Arance, A., and Munoz, M. (2015). Clinical implications of the intrinsic molecular subtypes of breast cancer. Breast *24 Suppl 2*, S26-35.

Premont, R.T., Inglese, J., and Lefkowitz, R.J. (1995). Protein kinases that phosphorylate activated G protein-coupled receptors. FASEB J *9*, 175-182.

Ramos-Alvarez, I., Moreno, P., Mantey, S.A., Nakamura, T., Nuche-Berenguer, B., Moody, T.W., Coy, D.H., and Jensen, R.T. (2015). Insights into bombesin receptors and ligands: Highlighting recent advances. Peptides *72*, 128-144.

Rock, E.P., Goodman, V., Jiang, J.X., Mahjoob, K., Verbois, S.L., Morse, D., Dagher, R., Justice, R., and Pazdur, R. (2007). Food and Drug Administration drug approval summary: Sunitinib malate for the treatment of gastrointestinal stromal tumor and advanced renal cell carcinoma. Oncologist *12*, 107-113.

Schatton, T., Murphy, G.F., Frank, N.Y., Yamaura, K., Waaga-Gasser, A.M., Gasser, M., Zhan, Q., Jordan, S., Duncan, L.M., Weishaupt, C*., et al.* (2008). Identification of cells initiating human melanomas. Nature *451*, 345-349.

Schwab, M. (2011). Encyclopedia of cancer (Heidelberg: Springer).

Schwartz, R.S., and Erban, J.K. (2017). Timing of Metastasis in Breast Cancer. N Engl J Med *376*, 2486-2488.

Scully, O.J., Bay, B.H., Yip, G., and Yu, Y. (2012). Breast cancer metastasis. Cancer Genomics Proteomics *9*, 311-320.

Seifert, S., and Sontheimer, H. (2014). Bradykinin enhances invasion of malignant glioma into the brain parenchyma by inducing cells to undergo amoeboid migration. J Physiol *592*, 5109-5127.

Shackleton, M., Quintana, E., Fearon, E.R., and Morrison, S.J. (2009). Heterogeneity in cancer: cancer stem cells versus clonal evolution. Cell *138*, 822-829.

Shenoy, S.K., and Lefkowitz, R.J. (2011). beta-Arrestin-mediated receptor trafficking and signal transduction. Trends Pharmacol Sci *32*, 521-533.

Shi, L., Zhou, S.S., Chen, W.B., and Xu, L. (2017). Functions of endothelin-1 in apoptosis and migration in hepatocellular carcinoma. Exp Ther Med *13*, 3116-3122.

Shibue, T., and Weinberg, R.A. (2017). EMT, CSCs, and drug resistance: the mechanistic link and clinical implications. Nat Rev Clin Oncol.

Siderovski, D.P., Hessel, A., Chung, S., Mak, T.W., and Tyers, M. (1996). A new family of regulators of G-protein-coupled receptors? Curr Biol *6*, 211-212.

Sommer, A.K., Falcenberg, M., Ljepoja, B., Fröhlich, T., Arnold, G.J., Wagner, E., and Roidl, A. (2019). Downregulation of GRK5 hampers the migration of breast cancer cells. Sci Rep *9*, 15548.

Sommer, A.K., Hermawan, A., Ljepoja, B., Fröhlich, T., Arnold, G.J., Wagner, E., and Roidl, A. (2018). A proteomic analysis of chemoresistance development via sequential treatment with doxorubicin reveals novel players in MCF7 breast cancer cells. Int J Mol Med *42*, 1987-1997.

Sommer, A.K., Hermawan, A., Mickler, F.M., Ljepoja, B., Knyazev, P., Brauchle, C., Ullrich, A., Wagner, E., and Roidl, A. (2016). Salinomycin co-treatment enhances tamoxifen cytotoxicity in luminal A breast tumor cells by facilitating lysosomal degradation of receptor tyrosine kinases. Oncotarget *7*, 50461-50476.

Sorlie, T. (2016). The Impact of Gene Expression Patterns in Breast Cancer. Clin Chem *62*, 1150-1151.

Sorlie, T., Perou, C.M., Tibshirani, R., Aas, T., Geisler, S., Johnsen, H., Hastie, T., Eisen, M.B., van de Rijn, M., Jeffrey, S.S.*, et al.* (2001). Gene expression patterns of breast carcinomas distinguish tumor subclasses with clinical implications. Proc Natl Acad Sci U S A *98*, 10869-10874.

Stewart, S.A., Dykxhoorn, D.M., Palliser, D., Mizuno, H., Yu, E.Y., An, D.S., Sabatini, D.M., Chen, I.S., Hahn, W.C., Sharp, P.A.*, et al.* (2003). Lentivirus-delivered stable gene silencing by RNAi in primary cells. RNA *9*, 493-501.

Subramanian, A., Tamayo, P., Mootha, V.K., Mukherjee, S., Ebert, B.L., Gillette, M.A., Paulovich, A., Pomeroy, S.L., Golub, T.R., Lander, E.S.*, et al.* (2005). Gene set enrichment analysis: a knowledge-based approach for interpreting genome-wide expression profiles. Proc Natl Acad Sci U S A *102*, 15545-15550.

Tacar, O., Sriamornsak, P., and Dass, C.R. (2013). Doxorubicin: an update on anticancer molecular action, toxicity and novel drug delivery systems. J Pharm Pharmacol *65*, 157-170.

Tannir, N.M., Figlin, R.A., Gore, M.E., Michaelson, M.D., Motzer, R.J., Porta, C., Rini, B.I., Hoang, C., Lin, X., and Escudier, B. (2017). Long-Term Response to Sunitinib Treatment in Metastatic Renal Cell Carcinoma: A Pooled Analysis of Clinical Trials. Clin Genitourin Cancer.

Tell, R., Rivera, C.A., Eskra, J., Taglia, L.N., Blunier, A., Wang, Q.T., and Benya, R.V. (2011). Gastrin-releasing peptide signaling alters colon cancer invasiveness via heterochromatin protein 1Hsbeta. Am J Pathol *178*, 672-678.

Tewey, K.M., Rowe, T.C., Yang, L., Halligan, B.D., and Liu, L.F. (1984). Adriamycin-induced DNA damage mediated by mammalian DNA topoisomerase II. Science *226*, 466-468.

Tomasetti, C., Li, L., and Vogelstein, B. (2017). Stem cell divisions, somatic mutations, cancer etiology, and cancer prevention. Science *355*, 1330-1334.

Turner, N.C., and Reis-Filho, J.S. (2012). Genetic heterogeneity and cancer drug resistance. Lancet Oncol *13*, e178-185.

Tyanova, S., Temu, T., Carlson, A., Sinitcyn, P., Mann, M., and Cox, J. (2015). Visualization of LC-MS/MS proteomics data in MaxQuant. Proteomics *15*, 1453-1456.

Tyanova, S., Temu, T., Sinitcyn, P., Carlson, A., Hein, M.Y., Geiger, T., Mann, M., and Cox, J. (2016). The Perseus computational platform for comprehensive analysis of (prote)omics data. Nat Methods *13*, 731-740.

Uhlen, M., Bjorling, E., Agaton, C., Szigyarto, C.A., Amini, B., Andersen, E., Andersson, A.C., Angelidou, P., Asplund, A., Asplund, C.*, et al.* (2005). A human protein atlas for normal and cancer tissues based on antibody proteomics. Mol Cell Proteomics *4*, 1920-1932.

Uhlen, M., Zhang, C., Lee, S., Sjostedt, E., Fagerberg, L., Bidkhori, G., Benfeitas, R., Arif, M., Liu, Z., Edfors, F.*, et al.* (2017). A pathology atlas of the human cancer transcriptome. Science *357*.

Valastyan, S., and Weinberg, R.A. (2011). Tumor metastasis: molecular insights and evolving paradigms. Cell *147*, 275-292.

Vianello, F., Sambado, L., Goss, A., Fabris, F., and Prandoni, P. (2016). Dabigatran antagonizes growth, cell-cycle progression, migration, and endothelial tube formation induced by thrombin in breast and glioblastoma cell lines. Cancer Med *5*, 2886-2898.

Visvader, J.E., and Lindeman, G.J. (2008). Cancer stem cells in solid tumours: accumulating evidence and unresolved questions. Nat Rev Cancer *8*, 755-768.

Vogelstein, B., Fearon, E.R., Hamilton, S.R., Kern, S.E., Preisinger, A.C., Leppert, M., Nakamura, Y., White, R., Smits, A.M., and Bos, J.L. (1988). Genetic alterations during colorectal-tumor development. N Engl J Med *319*, 525-532.

Vuong, D., Simpson, P.T., Green, B., Cummings, M.C., and Lakhani, S.R. (2014). Molecular classification of breast cancer. Virchows Arch *465*, 1-14.

Wang, W., Wyckoff, J.B., Wang, Y., Bottinger, E.P., Segall, J.E., and Condeelis, J.S. (2003). Gene expression analysis on small numbers of invasive cells collected by chemotaxis from primary mammary tumors of the mouse. BMC Biotechnol *3*, 13.

Wang, Y., Waters, J., Leung, M.L., Unruh, A., Roh, W., Shi, X., Chen, K., Scheet, P., Vattathil, S., Liang, H.*, et al.* (2014). Clonal evolution in breast cancer revealed by single nucleus genome sequencing. Nature *512*, 155-160.

Wang, Z., Liang, S., Lian, X., Liu, L., Zhao, S., Xuan, Q., Guo, L., Liu, H., Yang, Y., Dong, T.*, et al.* (2015). Identification of proteins responsible for adriamycin resistance in breast cancer cells using proteomics analysis. Sci Rep *5*, 9301.

Weigelt, B., Peterse, J.L., and van 't Veer, L.J. (2005). Breast cancer metastasis: markers and models. Nat Rev Cancer *5*, 591-602.

Wein, L., and Loi, S. (2017). Mechanisms of resistance of chemotherapy in early-stage triple negative breast cancer (TNBC). Breast *34 Suppl 1*, S27-S30.

Wyckoff, J.B., Segall, J.E., and Condeelis, J.S. (2000). The collection of the motile population of cells from a living tumor. Cancer Res *60*, 5401-5404.

Yates, L.R., Knappskog, S., Wedge, D., Farmery, J.H.R., Gonzalez, S., Martincorena, I., Alexandrov, L.B., Van Loo, P., Haugland, H.K., Lilleng, P.K.*, et al.* (2017). Genomic Evolution of Breast Cancer Metastasis and Relapse. Cancer Cell *32*, 169-184 e167.

Yu, S., Sun, L., Jiao, Y., and Lee, L.T.O. (2018). The Role of G Protein-coupled Receptor Kinases in Cancer. Int J Biol Sci *14*, 189-203.

Zegers, M.M., and Friedl, P. (2014). Rho GTPases in collective cell migration. Small GTPases *5*, e28997.

Zheng, H.C. (2017). The molecular mechanisms of chemoresistance in cancers. Oncotarget *8*, 59950-59964.

5.2 INDEX OF FIGURES AND SUPPLEMENTS

5.2.1 INDEX OF FIGURES

5.2.2 INDEX OF SUPPLEMENTS

5.3 INDEX OF ABBREVIATIONS

Abbreviation	Description
µg	Microgram
µl	Microliter
µM	Micromole
ABC-transporter	ATP-binding cassette transporter
ADC	Antibody drug conjugate
ADP	Adenosine diphosphate
AGC kinases	Protein kinases A, G and C
AI	Aromatase inhibitor
ATP	Adenosine triphosphate
BCRP1	Breast cancer resistance protein 1
Bomb	Bombesin
BRCA	Breast cancer gene
cDNA	Copy desoxyribonucleic acid
CLS	Cell line service GmbH
CSC	Cancer stem cell
ctr	Control
DMEM	Dulbecco's modified Eagle's medium
DMFS	Distant metastasis free survival
DNA	Desoxyribonucleic acid
DOX	Doxycycline
DTE	Dithioerythritol
DXR	Doxorubicin
EBCTCG	Early breast cancer trialists' collaborative group
ECL	Enhanced chemiluminescence
EGFR	Epidermal growth factor receptor
EMA	European Medicines Agency
ER	Estrogen receptor
ES	Enrichment score
ESMO	European Society on Medical Oncology

FCS	Fetal calf serum
FDA	Food and Drug Administration
FDR	False discovery rate
Fig	Figure
GO	Gene ontology
GO_BP	Gene ontology biological process
GPCR	G protein-coupled receptor
GRK	G protein-coupled receptor kinase
GRK5	G protein-coupled receptor kinase 5
GRP	Gastrin releasing peptide
GRPR	Gastrin releasing peptide receptor
GSEA	Gene set enrichment analysis
Her2	Human epidermal growth factor 2
HR	Hazard ratio
KD	Knock-down
LC-MS	Liquid chromatography mass spectrometry
LFQ	Label free quantification
LPA	Lysophosphatidic acid
LTQ	Linear Trap Quadrupole
MDR1	Multidrug resistance protein 1
MEA	Molecular evolution assay
mg	Milligram
ml	Milliliter
mM	Millimole
mRCC	Metastatic renal cell carcinoma
ng	Nanogram
nl	Nanoliter
nM	Nanomole
PAGE	Polyacrylamide gel electrophoresis
PARPi	Poly(ADP-Ribose)-Polymerase
PDGFR	Platelet derived growth factor receptor
PD-L1	Programmed cell death ligand 1

PR	Progesterone receptor
qPCR	Quantitative polymerase chain reaction
R	Round
RE	Relative expression
RFS	Relapse free survival
RNA	Ribonucleic acid
RTK	Receptor tyrosine kinase
SD	Standard deviation
SDS	Sodium dodecyl sulfate
SERD	Selective estrogen receptor degrader
SERM	Selective estrogen receptor modulator
shRNA	Short-hairpin ribonucleic acid
siRNA	Small interfering ribonucleic acid
SMI	Small molecule inhibitor
TBST	TRIS-buffered saline with Tween20
TNBC	Triple-negative breast cancer
TRIS	Tris(hydroxymethyl)aminomethane
VEGFR	Vascular endothelial growth factor receptor
WHO	World Health Organization
wt	Wild type

5.4 INDEX OF GENES AND PROTEINS

Gene / protein	Description
ABHD11	Abhydrolase domain-containing protein 11
AGR3	Anterior gradient protein 3 homolog
ASS	Argininosuccinate synthase
BCAS1	Breast carcinoma-amplified sequence 1
BCRP1	Breast cancer resistance protein 1
BRCA	Breast cancer gene
CA2	Carbonic anhydrase II
CD47	Integrin associated protein
CDC42	Cell division control protein 42 homolog
CMBL	Carboxymethylenebutenolidase Homolog
CNBP	Cellular nucleic acid-binding protein
EGFR	Epidermal growth factor
ER	Estrogen receptor
FLNA	Filamin A
FLNB	Filamin B
GAPDH	Glyceraldehyde 3-phosphate dehydrogenase
GFRA1	GDNF family receptor alpha-1
GRK5	G protein-coupled receptor kinase 5
GRP	Gastrin releasing peptide
GRPR	Gastrin releasing peptide receptor
Her2	Human epidermal growth factor 2
KTN1	Kinectin
LAD1	Ladinin-1
MDR1	Multidrug resistance protein 1
NMD3	60S ribosomal export protein NMD3
PARP	Poly(ADP-Ribose) polymerase
PD-L1	Programmed cell death ligand 1
PLAU	Urokinase
PLEC	Plectin

PNPO	Pyridoxine-5'-phosphate oxidase
PR	Progesterone receptor
PRKAR1A	cAMP-dependent protein kinase type I-alpha regulatory subunit
RAC1	Ras-related C3 botulinum toxin substrate 1
ROCK1	rho-associated, coiled-coil-containing protein kinase 1
S100P	S100 calcium-binding protein P
SLC3A2	4F2 cell-surface antigen heavy chain
SLC7A5	Large neutral amino acids transporter small subunit 1
TAX1BP3	Tax1-binding protein 3
TFF1	Trefoil factor 1
TPD52L2	Tumor protein D54
TUB	Tubulin

6. PUBLICATIONS

6.1 ORIGINAL ARTICLES

6.1.1 FIRST AUTHOR PUBLICATIONS

Sommer, A.K., Falcenberg, M., Ljepoja, B., Fröhlich, T., Arnold, G.J., Wagner, E., and Roidl, A. (2019). Downregulation of GRK5 hampers the migration of breast cancer cells. Sci Rep *9*, 15548.

Sommer, A.K., Hermawan, A., Ljepoja, B., Fröhlich, T., Arnold, G.J., Wagner, E., and Roidl, A. (2018). A proteomic analysis of chemoresistance development via sequential treatment with doxorubicin reveals novel players in MCF7 breast cancer cells. Int J Mol Med *42*, 1987-1997.

Sommer, A.K., Hermawan, A., Mickler, F.M., Ljepoja, B., Knyazev, P., Bräuchle, C., Ullrich, A., Wagner, E., and Roidl, A. (2016). Salinomycin co-treatment enhances tamoxifen cytotoxicity in luminal A breast tumor cells by facilitating lysosomal degradation of receptor tyrosine kinases. Oncotarget *7*, 50461-50476.

6.1.2 CO-AUTHOR PUBLICATIONS

Ljepoja B., García-Roman J., **Sommer A.K.**, Fröhlich T., Arnold G.J., Wagner E., Roidl A. (2018) A proteomic analysis of an in vitro knock-out of miR-200c, Sci Rep. 2018 May 2;8(1):6927

Ljepoja, B., García-Roman, J., **Sommer, A.K.**, Wagner, E., Roidl, A. (2018) MiRNA-27a sensitizes breast cancer cells to treatment with Selective Estrogen Receptor Modulators, Breast. 2019 Feb; 43:31-38

6.2 POSTERS

Sommer A.K., Hermawan A., Mickler FM., Knyazev P., Bräuchle C., Ullrich A., Wagner E., Roidl A. "Tamoxifen resistance can be overcome by Salinomycin treatment", European Association for Cancer Research Conference, Munich

7. ACKNOWLEDGEMENTS

First of all, I especially thank Prof. Dr. Dipl. Ing. Ernst Wagner for giving me the chance to finish my PhD thesis in his working group. Due to his great scientific background, he offered me very valuable guidance and support.

Next, I would like to express special gratitude to Prof. Dr. Dr. h.c. Axel Ullrich, who supported me in the beginning of my PhD thesis. His advices taught me how scientific spirit can end up in clinically meaningful success.

Moreover, my special thank goes to Dr. Andreas Roidl, our team lead, who guided me with patience, passion and great scientific experience through the "labyrinth" of science. With his help I became a more mature scientist.

I also thank Dr. Mathias Falcenberg, my supervisor at the beginning of my PhD thesis, who paved my way to become a scientist with great motivation and team spirit. You are one of my most valuable mentors.

Additionally, I say thank you to Dr. Bojan Ljepoja, my lab and office mate, who supported me in scientific and students' issues. Together we were strong, also at the soccer field.

Moreover, I thank Dr. Thomas Fröhlich and Dr. Georg Arnold for the great collaboration and their guidance in proteomics.

I also would like to thank Dr. Emanuele Zanucco and Dr. Martin Bezler for their support and for teaching me a lot of necessary lab skills.

Furthermore, I say thank you to our technical assistants Wolfgang Rödl, Miriam Höhn, Melinda Kiss, Ursula Biebel and Renate Gautsch for their help and support in the lab, their guidance and patience and every kind of motivation they provided in the last years.

I also thank the two working groups of MPI and LMU. It was a great pleasure for me to be a part of these teams and enjoyed the working atmosphere. Together, we went through good and harder times, but became stronger and grew up.

Moreover, I would like to express my gratitude to the Hanns-Seidel Stiftung for my PhD fellowship and the intellectual support. As a fellow of the Hanns-Seidel Stiftung I learned a lot about politics, government, globalism, economy and many more things besides oncology. I made many new friends and experienced great support. Here, my special thank goes to Prof. Hans-Peter Niedermeier, Dr. Johannes Urban, Dr. Rudolf Pfeiffenrath and Dr. Andreas Burtscheidt.

I also say thank you to my friends who offered motivating words, hugs, smiles, food and stood by my side during the whole time of my thesis: Maria Götz, my best friend from childhood on, Vanessa Welk and Corinna Wilhelm my two lab mates during the study period, Sabrina Finsterhölzl, my best friend from high school times, "Die glorreichen Fünf" (Florian Dorn, Michael Hahn, Martin Platt and Fabian Fellersmann), my best friends of the PhD fellows at the HSS, Franziska Schmideder, my Spotzal of the HSS, Johannes Alt, Basti Hofbeck und Simona Buchner, my former flat mates and great friends.

I especially thank you, Matthias Joos, love of my life, for your great support at the end of my thesis, for your endless love and affection, for every hug, smile, distraction and motivating word. I love you forever.

Finally, a special thank goes to my family: My parents, for your unlimited love, support, encouragement and your great education. Only because of you I became the woman I am today. My "little" brother Benedikt, for all the fun we had, have and will have in the future, for your endless support and solidarity. As a team we are strong.